Miscible Displacements in Porous Media with Variation of Fluid Density and Viscosity

DISSERTATION

Approved in Fulfilment of the Requirements for
the Degree of Doctor of Natural Sciences in
the Faculty of Bio- and Geosciences of
the University of Karlsruhe

by
B.Sc., M.Sc. Chaoying Jiao
from Pixian, PR China

Karlsruhe 2001

Date of Oral Examination:	February 6, 2002
Advisor and Examiner:	Prof. Dr. H. Hötzl
Second Examiner:	Prof. Dr. G. H. Jirka

KURZFASSUNG

Sowohl theoretische als auch experimentelle Untersuchungen haben gezeigt, dass Dichte- bzw. Viskositäts- Unterschiede bei einer mischbaren Verdrängung in einem laminaren Strömungssystem im porösen Medium hydrodynamische Instabilitäten verursachen können. Dieser Vorgang ist mit anderen Stofftransportmechanismen: wie z.B. Advektion, Diffusion und Dispersion, kompliziert gekoppelt. Stabilitätsanalysen wurden von vielen Autoren auf Basis der Advektion-Dispersions-Gleichung durch Anwendung unterschiedlicher geschwindigkeitsabhängiger Dispersionsmodele durchgeführt. Bereits vorliegende Berichte über mögliche Wirkungen der Instabilität auf die Dispersion und deren Wechselwirkung können durch experimentelle Untersuchungen bewiesen werden. Ziel der vorliegenden Arbeit ist es deshalb, die Wirkung der Dichte- bzw. Viskositätsunterschiede bei Verdrängungsvorgängen auf hydrodynamische Instabilität und weiter auf Dispersionsprozesse unter streng gefassten Laborbedingungen im Feld Maßstab zu untersuchen und zu bewerten.

Eine analytische Lösung zur instabilen mischbaren Verdrängung in einer vertikalen porösen Säule wurde abgeleitet. Die Lösungen sind auch in zufriedenstellender Übereinstimmung mit experimentellen Ergebnissen aus der Literatur.

Mit Hilfe eines selbst konzipierten und aufgebauten elektrischen Messverfahrens, das im Vergleich zu der in der Literatur veröffentlichten traditionellen Beprobungsmethode, maßgebliche Vorteile hat, können Konzentrationsmessungen ohne Beeinträchtigung der Verdrängungsprozesse an beliebigem Zeitpunkt in beliebigen Zeitintervallen durchgeführt werden. Somit können die räumliche und zeitliche Entwicklung der Verdrängungsfront synchron erfasst werden.

Zur Untersuchung der direkten Abhängigkeit des Dispersionskoeffizienten von Salzkonzentrationen und der Verdrängungsgeschwindigkeiten wurde Salzwasser unterschiedlicher Konzentrationen in verschiedenen Laborversuchen durch Flüssigkeiten anderer Konzentrationen in einer entgegen der Schwerkraft gerichteten Strömung verdrängt. Die Versuche wurden in einer mit homogen Quarzsand gepackten Versuchssäule (160 cm lang, Durchmesser 20 cm) durchgeführt. Aufgrund der aus den Säulenversuchen erworbener Ergebnisse und Erfahrungen wurden vier weitere serielle Verdrängungstests in einer feldmaßstäblichen auch mit homogenem

Quarzsand gepackten Plexiglasrinne (Ausmaß: 600 cm lang, 200 cm breit und 150 cm hoch) in einer horizontalen konstanten laminaren Strömung fortgeführt:

1. Eine 35 g/l NaCl Lösung verdrängte Leitungswasser (35 g/l NaCl Lösung → Leitungswasser);
2. Die 35 g/l NaCl Lösung wurde von einer 115 g/l Glyzerin Lösung verdrängt (115 g/l Glyzerin Lösung → 35 g/l NaCL Lösung);
3. Der dritte Verdrängungsvorgang wurde umgekehrt durchgeführt (35 g/l NaCl Lösung → 115 g/l Glyzerin Lösung);
4. Zur Verdrängung der Sättigungssalzlösung wurde wieder Leitungswasser eingesetzt (Leitungswasser → 35 g/l NaCl Lösung).

Zusammenfassend zeigten die Experimentergebnisse, dass in Abhängigkeit von Dichte- bzw. Viskositätsunterschieden, Verdrängungsverhältnisse und Verdrängungsgeschwindigkeit der mischbare Verdrängungsprozess im porösen Medium stabil oder instabil sein kann. Der dispersionskoeffizient nimmt mit steigendem Viskositätsunterschied zu und die Zunahmegeschwindigkeit ist viel größer im instabilen Fall als im stabilen Fall. Im stabilen Fall nimmt der Dispersionskoeffizient mit steigendem Dichteunterschiede ab. Die Dichteunterschiede wirken im Falle der instabilen Verdrängung gerade umgekehrt. Unter den Bedingungen der durchgeführten Experimente zeigt sich, dass die Dichteunterschiede eine viel größere Modifikation der Dispersion verursachen als die Viskositätsunterschiede.

ABSTRACT

Both theoretical and experimental investigations have shown that density differences and viscosity ratio can result in hydrodynamic instability by miscible displacements in a laminar flow system in porous media. The induced flow is coupled with other solute transport processes, for example, advection, diffusion and dispersion in a complicated way. Most stability analyses in literature have been based upon the classical advection-dispersion theory and different flow-dependent dispersion models have been applied. Although possible effects of instability on dispersion have already been investigated, the interplay between instability and dispersion awaits further experimental study. The objective of the present work is therefore to examine the density and viscosity effect on instability and further the effect of instability on dispersion through field-scale experiments under strictly controlled laboratory conditions.

An analytical solution to unstable miscible displacements in a vertical porous column is derived. The results agree well with those experiment data from literature.

With a self designed and developed electrical technique, which has many significant advantages in comparison with other published traditional sampling method or qualitative (partly quantitative) visualization technology, measurement of solute concentration can be carried out at any time in any time interval without any side effect over the displacement processes. Hence the development of the displacing front in space and time can be monitored synchronously.

In order to examine the direct dependence of dispersion coefficient on fluid density and viscosity, a series of miscible displacement experiments was performed in a Plexiglas column (160 cm long with a diameter of 20 cm) filled with homogeneous quartz sand. Although solute concentration, flow velocity and displacing relationship changed from experiment to experiment, displacement direction was always the same: from the bottom of the column upward. Based on the results and experience obtained, four further displacement experiments were carried out in a large Plexiglas tank (with a dimension of 600 cm long, 200 cm wide and 150 cm high) filled also with homogeneous quartz sand in a horizontal uniform flow field:

1. A 35 g/l NaCl solution was introduced to displace tap water, which had saturated the porous medium before the experiment began (35 g/l NaCl solution → tap-water);
2. The 35 g/l NaCl solution was displaced by a 115 g/l glycerine solution (115 g/l glycerine solution → 35 g/l NaCl solution);
3. The third displacement was performed conversely (35 g/l NaCl solution →115 g/l glycerine solution);
4. To displace the saturated salt solution, tap water was applied (tap-water → 35 g/l NaCl solution).

The experimental results indicate that in stable miscible displacement, dispersion coefficient drops continually when density variations increase, while the dispersion coefficient increases with increasing viscosity ratios. In the unstable case dispersion is enhanced by an increase of both of the density and viscosity differences. And the enlargement is much stronger in the unstable case. For the conditions of these experiments (low PECLET number), it appears that density differences have more impact on dispersion than viscosity ratios.

ACKNOWLEDGEMENTS

The present dissertation was written at the Department of Applied Geology, University of Karlsruhe, Germany, under the guidance of Prof. Dr. Heinz Hötzl, to whom I wish to express my sincere thanks for his gracious hospitality, precious stimulus, grant of freedom and the wonderful topic that he has given me.

Special thanks should be given to Prof. Dr. Gerhard H. Jirka, Institute of Hydromechanics, University of Karlsruhe, for his acceptance as Co-Examiner and interests on the work.

Financial assistance in the form of a scholarship from the German Academic Exchange Service (DAAD) throughout the study is gratefully acknowledged. The investigation was partially supported by Research Grant 1980022 from the German National Research Foundation (DFG). While the first half experimental study was carried out in the Environmental Research Center (FZU) at the University of Karlsruhe, the second part was run in a large sand tank (including logistics) in the Federal Waterways Engineering and Research Institute (BAW) with the friendly allowance from Mr. BDir Armbruster.

The writer is indebted to Dr. Wasim Ali for numerous discussions and suggestions on many aspects related to the work and his invaluable assistance. The author is indebted to Dr. Renke Ohlenbusch for his hospitality and precious help. I would also like to thank my student collaborator Mr. Marcel Fulde, Mr. Robert Szabo, Miss Karina Kunoth and our institute's technician Mr. Michel D. Lambert. Special thanks are due to Mr. Marcel Fulde for his committed and independent way of working.

My appreciation and thanks should be given to Professor Dr. Dr. Kurt Czurda for his taking over references time and again.

The author wishes to acknowledge with gratitude several valuable discussions with Dipl. Geol. Roland Bäumle, Dipl. Geol. Nico Goldscheider and Dr. Klaus Schnell. Some calculations were performed using a software compiled by Dipl. Geol. Roland Bäumle.

The author wishes to thank all those who provided help and input for this dissertation in any way. A few should be mentioned here: Dr.

Mathias Eiswirt, Dipl. Geol. Roman Zorn, Dr. Reiner Haus, Dipl. Geol. Claus Heske, Dipl. Chem. Karolin Weber, Miss Daniela Meyer and Dipl. Geol. Leif Wolf from the Department of Applied Geology, University of Karlsruhe and Dr. Hanxue Qiu and Dr. Yonggang Jia from the Department of Environmental Construction, Ocean University of Qingdao, Qingdao, PR. China.

I would also like to sincerely thank my wife Song Jing and my son Boyang, without their never-ending love and support I would never bring the work to its existence.

CONTENTS

KURZFASSUNG I
ABSTRACT III
ACKNOWLEDGEMENTS V
CONTENTS VII
LIST OF FIGURES X
LIST OF TABLES XIV
NOMENCLATURE XV

1 INTRODUCTION 1

1.1 Concept and definition 1

1.2 Literature survey 2

1.3 Problem formulation and work procedure 7

2 THEORETICAL FORMULATION 11

2.1 Properties of porous media 11

2.2 Fluid properties 11

2.3 Transport mechanisms in porous media 17

2.4 Analytical description 23

2.5 Boundary and initial conditions 26

2.6 Analytical solution 29

2.7 Methods for determining dispersion coefficients 32

3 CONVECTION IN A VERTICAL POROUS COLUMN 35

3.1 Introduction 35

3.2 Analytical description 36

3.3 Similarity solution 40

3.4 Result and discussion 44
3.4.1 Descending rate of similarity flow 44
3.4.2 Descending depth of similarity flow 45
3.4.3 Rate of solute transfer 46

3.5 Summary and discussion.....48

4 EXPERIMENT IN SAND COLUMN..... 49

4.1 Introduction 49

4.2 Apparatus and procedure 54
4.2.1 Tubular Plexiglas column 54
4.2.2 Porous medium, sand packing 55
4.2.3 Measurement of concentration 55
4.2.4 Procedure 56

4.3 Result and evaluation 57
4.3.1 Tracer test 57
4.3.2 Density effect in stable miscible displacement 58
4.3.3 Density effect in unstable miscible displacement 61
4.3.4 Viscosity effect.....62

4.4 Conclusion and recommendation 64

5 EXPERIMENT IN SAND TANK..... 67

5.1 Introduction 67

5.2 Apparatus and materials.....67

5.2.1 Plexiglas tank 67
5.2.2 Porous medium, sand packing 69
5.2.3 Measurement apparatus and other accessory 73
5.2.4 Test solutions 75

5.3 Sediment and hydraulic test 76
5.3.1 Sediment test 76
5.3.2 Hydraulic test 79

5.4 Tracer test 79

5.5 Experiments of stable miscible displacement 81
5.5.1 Small viscosity difference but with significant density difference (Exp. 1: NaCl solution→Tap-water) 83
5.5.2 Small density difference but with significant viscosity difference (Exp. 2: glycerine solution→NaCl solution) 87

5.6 Experiments of unstable miscible displacement 88
5.6.1 Small density difference but with significant viscosity difference (Exp. 3: NaCl solution→glycerine solution, viscous instability) 89
5.6.2 Small viscosity difference but with significant density difference (Exp. 4: Tap water→NaCl solution, gravitational instability) 92

5.7 Results and discussion 94

6 SUMMARY AND DISCUSSION 105

7 REFERENCES 109

APPENDICES

LIST OF FIGURES

Fig. 2.1: Dependence of density and viscosity on the concentration of a NaCl solution at 20°C (Data were taken from WEAST, 1989). 12
Fig. 2.2: Dependence of density and viscosity on the concentration of a glycerine solution at 20°C (Data were taken from WEAST, 1989). 13
Fig. 2.3: Relation curve of the conductivity and concentration of NaCl solutions at 20°C. 14
Fig. 2.4: Concentration and temperature dependence of molecular diffusion coefficients for glycerine solution (after BOUHROUM, 1985). 15
Fig. 2.5: Concentration dependence of molecular diffusion coefficients for binary brine solutions (after MILLER et al., 1986), concentration in mol /l at 25°C. 16
Fig. 2.6: Dispersion mechanisms at microscopic scale. 18
Fig. 2.7: Contribution of molecular diffusion to dispersion. 20
Fig. 2.8: Heterogeneity at different scale results in scale dependent dispersion (after KINZELBACH, 1992). 21
Fig. 2.9: Longitudinal dispersivity and REVs at different scale (after DOMENICO et al., 1990). 22
Fig. 2.10: Miscible displacement in porous media with different combination of fluid density, fluid viscosity and flow rate, where b) and f) are stable displacements, while a), c), d) and e) are unstable (changed after WELTY et al., 1991). 23
Fig. 2.11: Continuous input of a tracer with concentration C_0 at the inflow boundary of a one-dimensional steady flow domain and variation of the tracer concentration. 27
Fig. 2.12: Pulse input of a tracer with concentration C_0 at the inflow boundary of a one-dimensional steady flow domain and variation of the tracer concentration. 28
Fig. 2.13: Continuous input of a tracer with concentration C_0 at an inflow point in a constant velocity flow system; Both longitudinal and transversal variation of the tracer concentration are illustrated. 29
Fig. 2.14: Pulse input of a tracer with concentration C_0 at an inflow point and variation of the tracer concentration in two dimensions in a constant velocity flow system. 29
Fig. 3.1: Scheme of the system configuration. 36
Fig. 3.2: Convection in a vertical porous column (after BEJAN, 1980). 37

Fig. 3.3: Analytical solutions compared with experiment values (a) Experiment of BACHMAT et al. (1970); (b) Experiment of WOODING (1963). 44
Fig. 4.1: Scheme of concentration contours for miscible displacements with density and viscosity differences ($\mu_2 > \mu_1$; $\rho_2 > \rho_1$) in homogeneous isotropic porous medium. (a) stable displacement; (b) Unstable displacement. 50
Fig. 4.2: Photo of the experimental set-up. 52
Fig. 4.3: Scheme of the experimental set-up. 53
Fig. 4.4: Range of dispersion coefficients based on tracer tests for various sandpacks: fine sand 200-270 mesh; medium sand 40-200 mesh. 57
Fig. 4.5: Breakthrough curves of vertically upward stable displacements with small density of the displaced fluid and a large variation of density differences. 59
Fig. 4.6: Breakthrough curves of vertically upward stable displacements with large density of the displaced fluid and variation of density differences: (a) large density of the displaced fluid and small density difference; (b) large density of the displaced fluid and large density difference. 59
Fig. 4.7: Dependency of dispersion coefficient on the RAYLEIGH (Ra) number for stable displacement. 60
Fig. 4.8: Comparison between different stable and unstable miscible displacement: (a) large density difference; (b) small density difference. 61
Fig. 4.9: Dependency of the dispersivity on RAYLEIGH (Ra) number for both stable and unstable displacement. 62
Fig. 4.10: Viscosity effect on dispersion coefficient in miscible displacement. 64
Fig. 5.1: Photo of the Plexiglas tank (by courtesy of SCHNELL, 2001). 68
Fig. 5.2: Cross section of the tank and scheme of the flow system. 68
Fig. 5.3: Plan position of electric probes and piezometers. 69
Fig. 5.4: Side view of the tank and position of the electric probes. 70
Fig. 5.5: Structure and dimensions of the electric probes. 71
Fig. 5.6: Photos: (a) Sand filling; (b) Installing electric probes and piezometers; (c) Measurement and control system. 71
Fig. 5.7: Control and measurement system. 73
Fig. 5.8: Diagrammatic plan of the electrical connection between measurement and control units. 74

Fig. 5.9: Curve of grain size distribution for sands filled in the tank....77
Fig. 5.10: Results of the DARCY test, where v = 0.123 * I and R = 0.98 are linear regression and the coefficient of regression respectively. 78
Fig. 5.11: Isolines for the relative salt concentrations (C/C_0) along central section at 0.1, 0.2, 0.3, 0.4 and 0.5 PVI each. 84
Fig. 5.12: Isolines for the relative salt concentrations (C/C_0) along central section at 0.6, 1.0, 1.4, 2.0 and 2.8 PVI each. 85
Fig. 5.13: Comparison of salt concentration breakthrough curves at locations of row 1, 3, 7, 9, 13 along the central line on the first measurement plane for the first experiment, where M = 0.9462 and $\Delta\rho$ = - 24.4 g/l....86
Fig. 5.14: Measured and simulated concentration breakthrough curves of the first experiment at effluent....87
Fig. 5.15: Glycerine concentration breakthrough curves at locations of row 1, 3, 5 and 7 along the central line on the first measurement plane for the second experiment. 88
Fig. 5.16: Measured and simulated concentration breakthrough curves of the second experiment at effluent. 89
Fig. 5.17: Measured and simulated concentration breakthrough curves at locations of row 1, 3, 5, 7, 9, 11 and 13 along the central line on the first measurement plane for the third experiment. 90
Fig. 5.18: Measured and simulated salt concentration breakthrough curves of the third experiment at effluent. 91
Fig. 5.19: Salt concentration breakthrough curves at locations of row 1, 9, 11 and 13 along the central line on the first measurement plane for the fourth experiment. 92
Fig. 5.20: Salt concentration breakthrough curves of the fourth experiment at effluent. 93
Fig. 5.21: Transversely averaged dispersivity for the first experiment. 96
Fig. 5.22: Transversely averaged dispersivity for the second experiment. 97
Fig. 5.23: Transversely averaged dispersivity for the third experiment. 98
Fig. 5.24: Transversely averaged dispersivity for the fourth experiment. 99
Fig. 5.25: Transversely averaged longitudinal dispersivity vs. distance from the displacing source. 101
Fig. 5.26: Schematic representation of density and viscosity effect on dispersion coefficient. 103

LIST OF TABLES

Tab. 3.1: Different solutions under different m values. 42
Tab. 4.1: Summary of the experimental conditions. 56
Tab. 4.2: Summary of experimental data. 63
Tab. 5.1: Properties of the test solutions. 76
Tab. 5.2: Chemical and physical properties of the packed porous medium in the tank. 77
Tab. 5.3: Results of the tracer test and relevant experiment data. 80
Tab. 5.4: Relevant parameters and calculated variables for the horizontal miscible displacements with density and viscosity differences in the sand tank. 82
Tab. 5.5: Calculated longitudinal dispersion coefficients D [cm^2/min] and dispersivity α [cm] for layer 1. 94
Tab. 5.6: Calculated longitudinal dispersion coefficients D [cm^2/min] and dispersivity α [cm] for layer 2. 95
Tab. 5.7: Calculated longitudinal dispersion coefficients D [cm^2/min] and dispersivity α [cm] for the second experiment. 96
Tab. 5.8: Calculated longitudinal dispersion coefficients D [cm^2/min] and dispersivity α [cm] for the third experiment. 98
Tab. 5.9: Calculated longitudinal dispersion coefficients D [cm^2/min] and dispersivity α [cm] for the fourth experiment. 99

NOMENCLATURE

Greek symbols

α	dispersivity [cm]
α_L	longitudinal dispersivity [cm]
α_x	longitudinal dispersivity [cm]
α_T	transversal dispersivity [cm]
β	density coefficient [-]
η	$\tau\rho\alpha\nu\sigma\iota\varepsilon\nu\tau$ variable [-]
$\Delta\mu$	viscosity difference [kg/m/s, cP]
$\Delta\rho$	density difference [kg/L]
Δt	time difference [s]
μ	dynamic viscosity [kg/m/s, cP]
θ	normalized salinity [-]
γ	electrical conductivity [mS/cm]
ρ	fluid density [kg/L]
Ψ	streamfunction [m^2/s]
τ	normalized time [-]
ζ	transient variable [-]

Latin symbols

A	area [cm^2]
B_0	regression coefficient [-]
B_1	regression coefficient [-]
B_2	regression coefficient [-]
C	concentration: volume fraction [g/L]
d_p	grain size [cm]
D	dispersion coefficient [cm^2/s]
D_x, D_y, D_z	dispersion coefficients for x, y, z directions [cm^2/s]
D_m	molecular diffusion coefficient [cm^2/s]
g	acceleration due to gravity [m/s^2]
G	solute mass [g]
H	height [m]

I	hydraulic gradient [-]
K	hydraulic conductivity[cm/s]
k	permeability [m^2]
M	viscosity ratio, mobility number [-]
m	tracer mass injected [g]
N_g	ratio between the viscous and gravitational force [-]
n	porosity [-]
Pe	PECLET number [-]
Q	flow rate [cm^3/s]
R	radius [m]
Ra	RAYLEIGH number [-]
Re	REYNOLDS number [-]
r	cylindrical coordinate axis [m]
Sc	SCHMIDT number [-]
t	time [s]
T	temperature [^oC]
U	uniformity index [-]
u	mean intrinsic velocity, longitudinal [cm/s]
V	volume [m^3]
v	DARCY velocity [cm/s]
w	mean intrinsic velocity, transverse [cm/s]
x	coordinate axis in horizontal direction [m]
y	coordinate axis in another horizontal directio [m]
z	coordinate axis against direction of gravity [m]

Abbreviations

BAW	the Federal Waterways Engineering and Research Institute of Germany (Bundesanstalt für Wasserbau)
DAAD	the German Academic Exchange Service (Deutscher Akademischer Austauschdienst
DFG	German Research Foundation (Deutsche Forschungsgemeinschaft)
DIN	German Industrial Standard (Deutsche Industrie Norm)
Fig.	Figure
FZU	the Environmental Research Centre at the University of Karlsruhe (Forschungszentrum Umwelt, Universität Karlsruhe)

INTRAVAL	an international project, which adressed the validation of models of the transport of radioactive substances through groundwater in the geosphere. The project started in 1987 on the initiative of the Swedish Nuclear Power Inspectorate with the general support of the OECD Nuclear Energy Agency
NMR	Neclear Magnetic Resonance
OECD	Organisation for Economic Co-operation and development
PVI	Poren Volume Injected
REV	Representative Elementary Volume
Tab.	Table

1 INTRODUCTION

In this introductory chapter a few important concepts and definitions concerning miscible fluid displacements in porous media are presented. Then relevant investigations in a large amount of literature are surveyed. After that, a problem formulation, and a work procedure will be outlined.

1.1 Concept and definition

Miscible displacements in porous media are of special importance in a large number of fields, which include, but are not limited to, geophysics (geophysical fluid mechanics), hydrology, hydrogeology and environmental sciences (solute transport in aquifers), petroleum and chemical engineering (enhanced oil recovery), and some other fields of both natural science and several branches of technology. Since a few pioneering works were done over a century ago, they have resulted in a considerable interest and research. Particularly, growing concern about groundwater contamination and applications in petroleum engineering (enhanced oil recovery) have led to increased attention to the subject of miscible displacements in association with hydrodynamic instability due to density and viscosity differences between the miscible fluids.

To study miscible displacement processes in porous media, it is necessary to understand the terms “miscible displacement” and “porous media”. Following those definitions, fluid properties will be outlined.

HOLM (1986) defines ***miscible displacements*** as a physical condition between two or more fluids that will permit them to mix in all portions without the existence of an interface”. Consequently, there does not exist any interfacial tension.

A ***porous medium*** is a material of a solid matrix with pores. The solid matrix is either deformable or non-deformable. The pores may be connected or disconnected. As our concern is fluid flow through the porous medium, only the interconnected pores are of interest. The interconnected pore space is called effective pore space.

Soils and rocks are examples of natural porous media. Generally, the distribution and shape of pores in a natural porous medium is random. Flow pattern inside individual pores is therefore irregular. However, if the characteristics of porous medium and subsequently flow variables are defined as an appropriate mean over a sufficiently large representative elementary volume (REV, for more detail, see in BEAR, 1972), the irregularity is evened. It is assumed that the result is independent of the size of the representative elementary volume. The definition for REV makes it possible to describe fluid flow in porous medium by employing continuum approach.

By employing the definition of REV, an actual porous medium is represented by a fictitious continuum where values of any parameters and variables, e.g., porosity, permeability, velocity, solute concentration and pressure that are defined on the REV, are independent of the dimension of the REV. The values assigned to a point in the continuum are averaged ones, taken over the REV centered at the point.

Having defined porous medium and identified its characteristic properties, we turn our attention to its counterpart: fluids.

Fluid with passive solute. One or more fluid phases may be present within the interconnected pores. Due to the mixing of miscible fluids (e.g., fresh water and salt water), dissolution and precipitation of substances, adsorption, radioactive decay, biochemical and chemical reactions or changing of physical conditions (e.g., pressure and temperature), a single fluid phase may experience composition and property variations. This study will not focus on multiphase flow, chemical reaction, radioactive decay, or adsorption. It focuses on the flow of a single fluid phase (i.e., aqueous solution) with possible variation in density and viscosity due to concentration differences. Unlike an ideal tracer, which is inactive to the ambient fluid and solid matrix and does not affect fluid properties, passive solutes may, due to concentration variations, change the fluid's density and viscosity. Salt, glycerine and a few fluorescent dyes are typical passive solute.

1.2 Literature Survey

Tracer dispersion. Since early 1960s dispersion of an ideal tracer in porous media has been studied extensively, notable among are de

JOSSELIN DE JONG (1960), SCHEIDEGGER (1960), BEAR (1961 a&b, 1972, 1979), ELRICK et al. (1966), FRIED et al. (1975), FREEZE et al. (1979), DE MARSILY (1986), GÜVEN et al. (1986) and DOMENICO et al. (1990).

For miscible displacements of a passive solute in porous media, it is conventionally assumed that the transport phenomena are determined by the relative importance of two hydrodynamic processes: dispersion and advection, if they are actually separable. Due to the complexity a rigorous pore level mathematical description does not exist (YORTSOS, 1990; MANNHARDT et al., 1994). Based on a continuum theory, an advection-dispersion equation on a macroscopic scale was established (see BEAR, 1972). In this most commonly used theory, the "lumped" dispersion coefficient (MANNHARDT et al., 1994) is the key parameter, which is a second order tensor that depends not only on local variations of the velocity field but also on large scale characteristics of the medium (SCHWARTZ, 1977; PICKENS et al., 1981; MACFARLANE et al., 1983; SUDICKY et al., 1983, 1986; DOMENICO et al., 1984; CALA et al., 1986; DAGAN, 1986; FREYBERG et al., 1986; MOLTYANER, 1988; KNOPMAN et al., 1991; LEBLANC et al., 1991; BOGGS et al., 1992; GARABEDIAN et al., 1991 and HU et al., 1995).

In their excellent reviews, OGATA (1970), SPOSITO (1979) and MANNHARDT et al. (1994) gave fundamental mathematical descriptions and provided a large number of analytical solutions to various models.

Instead of the continuum theory, many researchers (e.g., SCHEIDEGGER, 1954; FREEZE, 1975; GUTJAHR et al., 1978; DELHOMME, 1979; GELHAR et al., 1979, 1986&1993; BARRY et al., 1990 and WELTY et al., 1991) have used statistical approach in interpreting fluid flow and the dispersion phenomena in porous media.

KOCH et al. (1986, 1987 a&b, 1988, 1989 a&b) presented a non-local theory for tracer dispersion and tried to verify their result through the integration of both laboratory and field scale experiments obtained from literature.

Depending on a variety of influence factors, miscible displacement in porous media can be greatly modified, beyond the mechanisms of advection and dispersion for tracer, by the onset and growth of two types of hydrodynamic instability (QUINTARD, 1987): RAYLEIGH-BENARD instability induced by density variations in the gravity field (gravitational

instability) and SAFFMAN-TAYLOR instabilities induced by the viscosity difference (viscous instability).

Density effect. Neglecting the viscosity dependence on concentration, tremendous work have been done on gravitational instability, notable among which are WOODING (1963), KRUPP and ELRICK (1969), BACHMAT et al. (1970), ROSE et al.,(1971), SCHINCARIOL and SCHWARTZ (1990), DANE et al. (1991), HAYWORTH et al. (1991), KOCH et al. (1992), OOSTROM et al. (1992a&b), ISTOK and HUMPHREY (1995), and OPHORI (1998). During their field investigations of groundwater contamination, KIMMEL and BRAIDS (1980), FRIND (1982), MACFARLANE et al. (1983), SUDICKY et al. (1983), VAN der MOLLEN et al. (1988) and LEBLANC et al. (1991) both observed downward movement of dense plume, which was attributed to density effect. The density effect was also cited by FREYBERG (1986), BOGGS et al. (1992) as a possible explanation for observed unexpected sinking of tracer plumes.

Viscous instability. Some researchers, however, concentrate their attention upon viscous instability, for example, in SAFFMAN et al. (1958); HICKERNELL et al. (1986); TAN et al. (1986, 1988); YORTSOS (1987, 1990); BACRI et al. (1987, 1991, 1992); ZIMMERMAN et al. (1991); MANICKAM et al. (1993). Both kinds of instability have been included in the study of HELLER (1965); SCHOWALTER (1965); WOODING (1969); CHANG et al. (1986, 1988a, 1988b, 1989); BACRI et al. (1992); QUINTARD et al. (1987); ASIF et al. (1990); CHRISTIE et al. (1990); BUES et al. (1991); MANICKAM et al. (1994, 1995); ROGERSON (1993a, b); TCHELEPI et al. (1993); SIMMONS and NARAYAN (1997). These researches have produced tremendous important information in understanding the nature of viscous instabilities and their relationships to the nature of porous media and fluids.

Dispersion effect on instability. For such a still more complex flow configuration, a proper form of the dispersion tensor is generally not known (PETITJEANS and MAXWORTHY, 1996). Employing the same conventional convection-dispersion formalism but different dispersion model, the effect of dispersion on the stability of miscible displacement was investigated theoretically by TAN et al. (1986) and CHANG et al. (1986). Their results suggested that disturbances with wave numbers larger than a finite cutoff are stable, while instability is promoted by larger mobility constant, a higher injection velocity, and sharper base states. Considering the changes in longitudinal dispersion YORTSOS et al. (1988) found that for steep profiles and for disturbances of small

wavelength, a strongly destabilizing effect arises, which is in contrast to the stabilizing contribution of transverse dispersion. Similar effects were also reported by MANICKAM et al. (1995). However, such effects await further rigorous, experimental or numerical studies.

Instability effect on dispersion. Reversely, the onset and development of instabilities cause the variation of flow velocity inevitably, which, in turn, results in additional dispersion.

The effect of instability on dispersion was recently investigated by BOUHROUM (1985), RIGORD et al. (1990), GUILLOT et al. (1991), BACRI et al. (1992), LEROY et al. (1992), TCHELEPI et al. (1993), MOSER (1995) and JIAO (2000). Using an acoustic technique, BACRI et al. (1992) carried out a three-dimensional (3-D) experiment to study the growth of viscous fingering within porous media. Based on their stability analysis, a new instability parameter was presented and it was validated by their experimental data.

Another point of interest for miscible displacements concerns the density and viscosity effects on dispersion in stable cases, which have partially considered in MOSER (1995), BOUHROUM (1985) and JIAO (2000).

Experimental investigations. Both sand column and HELE-SHAW cell (flow container consisting of two parallel plates spaced a few millimeter apart, the space is then filled with sand or glass beads) have long been used as suitable laboratory models for investigating miscible fluid displacements in porous media.

Experiment in sand column. Experimental studies in sand column by WOODING (1963), BACHMAT and ELRICK (1970), BIGGAR and NIELSEN (1964), KRUPP and ELRICK (1969), ROSE and PASSIOURA (1971) found that the occurrence of instabilities was related to the density differences and the average pore water velocities. Recent experimental studies were conducted by BOUHROUM (1985) and MOSER(1995). Also in a sand column, but their objective was to check the validity of the classical advection-dispersion equation for the transport phenomena when density and/or viscosity effects were considered.

In order to provide sets of data for validation of transport models, the INTRAVAL project carried out a series of experiments in a column (rather HELE-SHAW cell) packed with fine glass beads. Some other flow

container experiments concerning the subject were reported by LIST (1965), MULQUEEN and KIRKHAM (1972), PASCHKE and HOOPES (1984), SCHINCARIOL and SCHWARTZ (1990), OOSTROM et al. (1992 a&b), ISTOK and HUMPHREY (1995), LENHARD et al. (1995), OSWALD et al. (1996).

Experimental techniques. Past investigations have employed a variety of experimental techniques. Not only were the tracers in great difference, included among were NaCl, $CaCl_2$, KBr, NaI, KCl, $MgCl_2$, $NaNO_3$ or $^{18}O_2$, experimental set-up was also quite different, with its scale ranging from 10 mm to several meters. Traditionally both flow visualization and fluid sampling techniques were employed. Although both techniques are very useful, it is obvious, however, that the former method cannot provide quantitative results. Due to the introduction of sampling devices inside the porous media and because of the removal of volumetric fluid samples, the traditional sampling techniques may interfere with flow and transport. What is more, to analyse a large number of fluid samples is not economic (OOSTROM et al., 1992 a).

Electrical method were used by BEAR (1961) to measure solute concentrations in porous media. The advantage of using electric measurements in-situ is that there is no need to extract volumetric samples, which could disturb the flow pattern significantly, and the results are obtained faster and more economically than by chemical determinations. Similar method has been also employed by BUES et al. (1991), INTRAVAL (1992) and MOSER (1995).

Other nonintrusive techniques such as the dual-energy (662-KeV ^{137}Cs and 60-KeV ^{241}Am) gamma radiation technique and the magnetic resonance imaging (MRI) technology were reported to obtain ideal quantitative observations (see in OOSTROM et al., 1992; OSWALD et al., 1996; GUILLOT et al., 1991; LEBON et al., 1997). Due to its high expensive and limitation for large size (dimension) of physical models, MRI or NMR (Nuclear Magnetic Resonance) has not yet been a standard tool in measuring fluid flow in porous media. However, that it provides high resolution in tracing fluid particles and its non-intrusive character would certainly attract much more attention to further develop the measurement technology, to improve analysis method and last but not the least to reduce the expense in the future.

Numerical models. In the past three decades progress has been also made in numerical methods to simulate miscible fluids displacements with both density and viscosity variations in porous media. The process

is severely non-linear. Different numerical approaches (CFEST, FAST, NAMMU, SICK 100, SWIFT, SUTRA, HST3D, METROPOL, TOUGH2 and FEFLOW) have managed to handle the severe non-linearity in their own ad hoc ways. Beside these commercial (customary) software package, KOCH and ZHANG (1992), LIU and DANE (1997), FAN and KAHAWITA (1994), SCHINCARIOL et al. (1994) and OSWALD et al. (1996) developed each an numerical approach.

Related works. The following related studies should be also appreciated : circulation of fluids around salt domes by HERBERT et al. (1988), RANGANATHAN et al. (1988) and EVANS et al. (1991); salt water upconing beneath a pumping well by REILLY and GOODMAN (1987), the circulation of high salinity thermal brines by WILLIAMS (1997); flow and solute transport through a leeve separating fluids with different densities by BROOKER and TOWNLEY (1994); the storage of thermal energy by BUSCHECK et al. (1983); circular convection during subsurface injection of liquid waste by HICKEY (1989); salt-leaching of soils due to irrigation by MULQUEEN and KIRKHAM (1972); brine transport in relation with the disposal of high-level radioactive waste in salt formations by HASSANIZADEH et al. (1988); saline water generated in lakes OSTERCAMP et al. (1987) and WOOD et al. (1987); mixing in inland and coastal waters by FISCHER et al. (1979); convection in porous media by BEJAN et al. (1980) and buoyancy-induced flows and transport by GEBHART et al. (1988).

1.3 Problem formulation and work procedure

Although a lot of work on miscible fluid displacements has been reported, the effects of dispersion on flow instability have not been completely understood, considering that the dispersion effect is anisotropic and flow dependent. Most of the theoretical and numerical investigations have not been experimentally verified. Another point of concern for miscible fluid displacements is density and viscosity effect to dispersion in both stable and unstable flow conditions at field scale, which will be a primary goal of the present investigation. Contrary to miscible displacement with tracer, experiments with dense solute are scarce. Most of them deal with a pseudo small-scale two-dimensional (2-D) geometry with qualitative visualization or sampling technique, which, due to the sampling of certain fluid volume, might disturb the flow regime significantly. In the present study, apart from a theoretical

derivation of free convection (gravitational instability) in a vertical porous column, experiments have been carried out using a non-intrusive electrical measuring technique. In a large vertical sand column and in a large sand tank, a large number of electrodes were introduced to monitor solute concentration within the porous media without inducing any significant disturbances to the flow being studied. In the sand column, experiments were performed with a wide range of density and viscosity differences and flow rates. In the sand tank, due to its large volume, only two density differences and two viscosity ratios under almost the same ambient flow conditions were considered.

Objective. Objectives of the present investigation are outlined as follows.

- Analyze and evaluate the formation and development of gravitational instability in a vertical porous column with impermeable walls.
- Check the validity of the classical theoretical formulation in describing miscible displacements of fluids with density and viscosity differences in porous media at field scale.
- Investigate density and viscosity effect on dispersion coefficient in stable cases.
- Determine effects of instability (both gravitational and viscous instability) to macrodispersion at field scale.

Work procedure. Chapter 2 provides theoretical background for the investigation. Based on a brief description of properties of porous media and fluids and a detail examination of the miscible displacement mechanisms, the derivation of the conventional advection-dispersion equation will be briefly introduced. Relevant initial and boundary conditions are discussed subsequently. Finally, two analytical solutions with simple boundary and initial conditions in homogeneous porous media are given. Analytical solutions to the formulation and development of gravitational instability in a vertical porous column with impermeable walls are derived in chapter 3. The results are in satisfactory agreement with experimental data from literature.

In chapter 4, a series of experiments on both stable and unstable miscible fluid displacements with both density and viscosity differences in a vertical sand column are performed. When it is possible, results have been compared with those from literature.

The study put emphasis on miscible displacements with fluids of different fluid density and viscosity in a large-scale sand-tank. The experimental apparatus, procedures and results are described in chapter 5.

Chapter 6 evaluates the whole investigation; results are discussed; conclusions are drawn and suggestions for further research are made.

2 THEORETICAL FORMULATION

2.1 Properties of porous media

The two most important parameters that characterize a porous medium are porosity and permeability. Total ***porosity*** of a porous medium is defined as the fraction of the total volume of the medium that is occupied by pores. It is a measure of the pore space and hence an indication of the fluid storage capacity of the medium. Qualitatively, ***permeability*** may be defined as the ease with which fluids can move through a porous medium under the influence of a driving pressure. Quantitatively, it is measured by the flow rate in REV.

Permeability of a porous medium usually varies in space. They may also vary in the directions of measurement at any given point. The first property is termed ***heterogeneity*** and the second ***anisotropy***. A porous medium is said to be homogeneous if its permeability is the same at all its points. Otherwise, the domain is said to be heterogeneous. If, however, the permeability at a considered point is independent of direction, the medium is said to be isotropic at that point. If the permeability varies with the direction at a point in a porous medium, the porous medium is anisotropic.

2.2 Fluid properties

To study fluid flow in porous medium, fluid properties as density, viscosity, electrical conductivity, heat capacity, thermal conductivity and surface tension may need to be considered. These properties change with temperature, salinity and pressure. In the present investigation only salinity dependence of density, viscosity and electrical conductivity are of concern.

Consider an aqueous solution of volume V containing a certain solute with mass G. The solute's concentration is conventionally defined as:

$$C = \frac{G}{V} \tag{2.1}$$

Clearly the unit of concentration is kg/m^3 or g/l (g/cm^3). Sometimes concentrations can be expressed also as mass fractions, which are the mass of the solute divided by the mass of the solution. The dimensionless unit is often noted as ppt, ppb, ppm etc. When chemical reactions are of interest, mole fraction (mole concentration) would be a good alternative description. The three concentration descriptions can be easily switched from one to the other.

In this investigation, tap water, NaCl and glycerine solution were applied, where solute concentration is defined as mass per unit volume (kg/m^3). Depending on solute concentration, the solution has different density and viscosity.

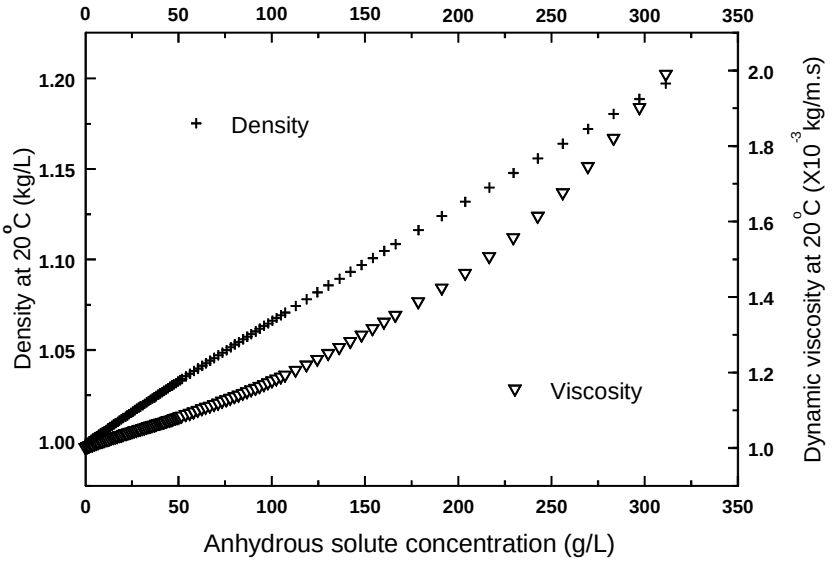

Fig. 2.1: **Dependence of density and viscosity on the concentration of a NaCl solution at 20°C (Data were taken from WEAST, 1989).**

Dependence of density and viscosity on the solute concentration of a NaCl and glycerine solution is illustrated in Fig. 2.1 and Fig 2.2 respectively. Using regression method, the dependence can be formulated quantitatively. Comparing Fig. 2.1 with Fig. 2.2, it is clear to

see that both density and viscosity of a salt solution and glycerine solution increase with their concentrations. While the salt solution is significant for its density variations, the glycerine solution is characterised by its viscosity. A suitable combination of the two solutions can produce a large variety of density and viscosity differences.

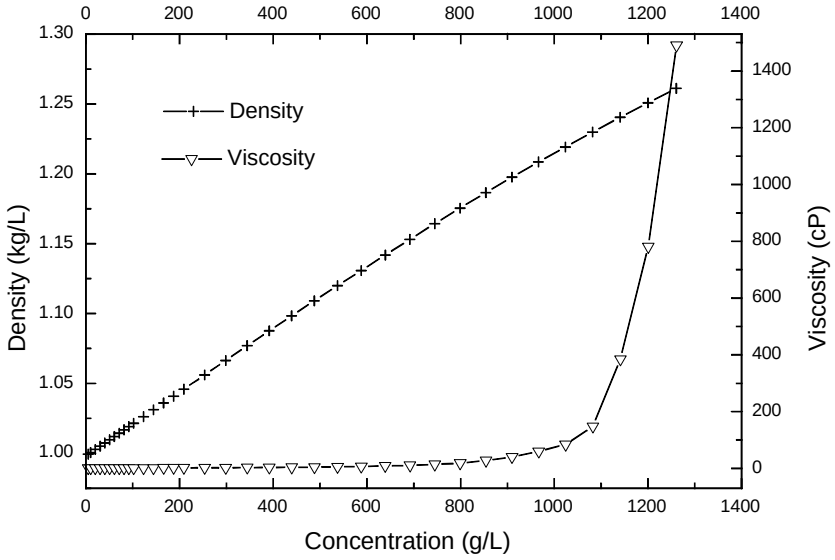

Fig. 2.2: **Dependence of density and viscosity on the concentration of a glycerine solution at 20°C (Data were taken from WEAST, 1989).**

For the solution of NaCl at 20°C and 1 atm (1×10^5 Pa), for example, $\rho(C)$ can be approximated by :

$$\rho(C) = \rho_{H_2O} + B_0 \cdot C \tag{2.2}$$

where $\rho_{H_2O} = 0.99834$ kg/L, $B_0 = 7.0153E-4$, C is salt concentration in g/L,

or more precisely,

$$\rho(C) = 0.99834 + 7.0153E-4 \times C - 2.35969E-7 \times C^2, \qquad (2.3)$$

and equation (2.4) is a good approximation for $\mu(C)$,

$$\mu(C) = \mu_{H_2O}(B_0 + B_1 \cdot C + B_2 \cdot C^2), \qquad (2.4)$$

where B_0 = 1.00585, B_1 = 0.00122, B_2 = 4.98456E-6.

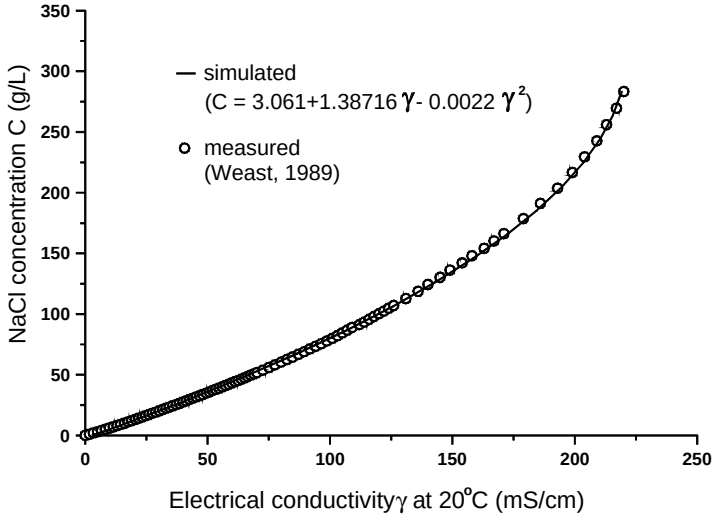

Fig. 2.3: **Relation curve of the conductivity and concentration of NaCl solution at 20°C.**

Because such a large volume of solution is needed for the experiment, it is unwise and impossible to measure the solute concentration directly. It is not possible to do so even outside the porous medium. By measuring conductivity, the solute concentration can be indirectly determined (see Fig. 2.3). The solute concentration outside the porous medium was determined with (by) a conductivity meter LF 191 (SER. No. 88100075, WTW, 8120 Weilheim, Germany). Although there are conversion formulae between solute concentration and measured conductivity in literature (c.f., HOLZBECHER, 1998), they cannot be used directly. Fig. 2.3 illustrates that the relationship between salt

concentration and electrical conductance can be satisfactorily expressed by a parabola.

$$C = 3.061 + 1.38716\gamma - 0.0022\gamma^2 \tag{2.5}$$

where C is salt concentration (g/L) and γ the electrical conductivity (mS/cm).

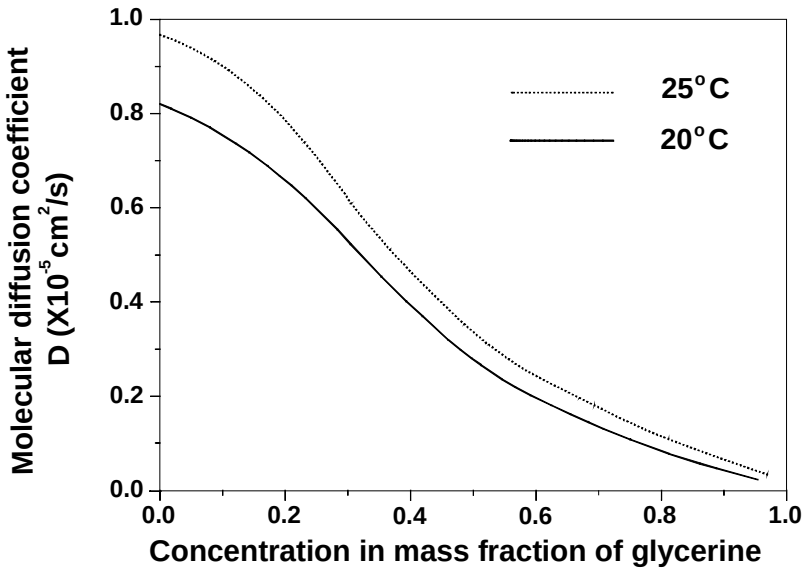

Fig. 2.4: **Concentration and temperature dependence of molecular diffusion coefficients for glycerine solution (after BOUHROUM, 1985).**

From Fig. 2.4 we see that molecular diffusion coefficients of glycerine solution are dependent on both concentration and temperature of the solution. Some researchers assigned the value at (C_1 – C_0)/2 to the molecular diffusion coefficient. This method is easy and direct. However, in the case of large variations of solute concentrations it could result in great error. Some others took the dependent function $D(C)$ into account, thus a mean diffusion coefficient can be given:

$$D(C) = \frac{\int_{C_0}^{C_1} D(C)dC}{C_1 - C_0} \tag{2.6}$$

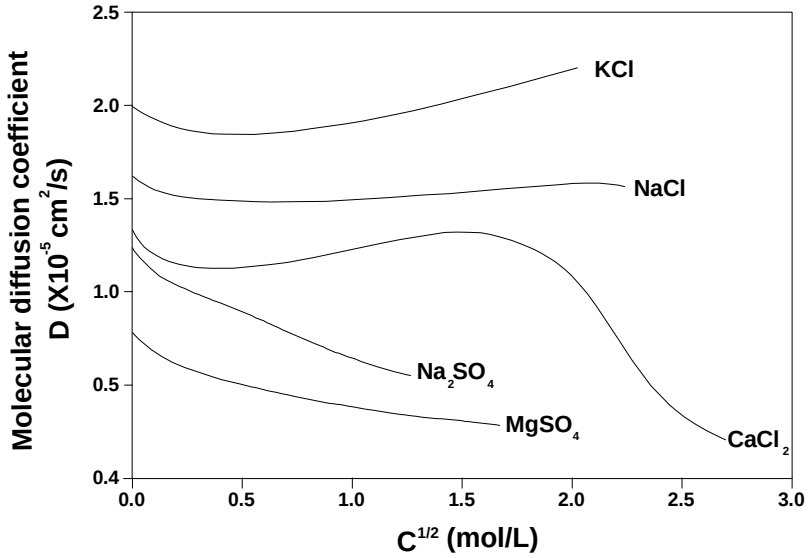

Fig. 2.5: **Concentration dependence of molecular diffusion coefficients for binary brine solutions (after MILLER et al., 1986), concentration in mol /L at 25°C.**

Fig. 2.5 indicates the concentration dependence of molecular diffusion coefficients D_m of some aqueous electrolyte solutions at 25°C. It shows that some D_m increase, some decrease and some others vary in a still complex way as concentration increases.

In the present study, molecular diffusion coefficient for NaCl solution is considered to be constant at 1.5×10^{-5} cm^2/s. For glycerine solution, a linear function of $D(C)$ is applied and the second averaging process is used.

2.3 Transport mechanisms in porous media

When two miscible fluids interacts with each other in porous media, initially there is a sharp interface, which changes into a transition zone as the differences of physical properties between the two fluids tend to be levelled with time. This macroscopic effect results from several physicochemical processes, including advection, molecular diffusion, dispersion and instability or induced convection, which will be discussed in detail in the present section.

Mechanisms. Essential mechanisms that determine miscible fluids displacement in porous media include the following:

Advection. Transport by the bulk motion of the flowing fluids. This means, solutes are carried at an average rate equaling the average linear velocity of the fluids. The flow may be a ***forced convection***, a result of an imposed hydraulic gradient; or an ***induced convection*** because of certain density or viscosity gradients. Depending on the relative magnitude of these two forces, some of these mixed systems may be characterized by the development of hydrodynamic instabilities.

Molecular diffusion. The scattering of solute particles due to random molecular motions. Although it causes particles to move in all directions in space, the scattering intensity in each direction is not the same, depending on the magnitude and direction of concentration gradient. As a result, particles are transferred from zones of high concentration to those of low concentration. Molecular diffusion takes place at any flow situations, even in a still fluid. The transport process obeys Fick's first and second Laws.

Mechanical dispersion. Because of the variations in the microscopic velocity within each channel and from one channel to another, solutes spread gradually and occupy an ever-increasing portion of the flow domain, beyond the region that which is expected to occupy according to the average flow rate. Microscopically, there is no mixing; however, if continuum approach is employed to describe concentration distribution, an apparent spreading arises at the macroscopic scale. TAYLOR's (1953) investigation into dispersion of a passive tracer flowing slowly through a tube suggested that, this flow-dependent dispersion is Fickian. Therefore, ***mechanical dispersion*** is also called ***TAYLOR dispersion***. Even in a homogeneous porous medium, there exists

mechanical dispersion as well. In a natural system, permeability may exhibit variations over a range of scales from the size of individual grains or pores to the size of the whole system. Such a heterogeneity in permeability induces the same level of fluctuation in flow rates, which in turn, cause additional dispersion inevitably to those caused by the above microscopic processes.

Hydrodynamic dispersion. Spreading of solute beyond the scope of *advection*. The scattering phenomenon is, in fact, a result of the coupling between ***mechanical dispersion*** and ***molecular diffusion***. Athough the magnitude of molecular diffusion is much smaller than that of the mechanical dispersion, its importance on the overall dispersion should not be neglected. Unlike mechanical dispersion, molecular diffusion does take place also in the absence of motion.

Because molecular diffusion depends on time, its effects on the overall dispersion will be more significant at low flow velocities. On the other hand, molecular diffusion plays a very important role in the so called "hold-up" and "boundary-layer" dispersion, which, besides heterogeneity, contributes to non-local dispersion at high PECLET numbers ($Pe = u.d_p/D$) as well (for detail, see in KOCH et al., 1987a).

Secondly, molecular diffusion accounts to a great extent for lateral dispersion. Thirdly, it is molecular diffusion that makes the dispersion phenomenon in purely laminar flow irreversible.

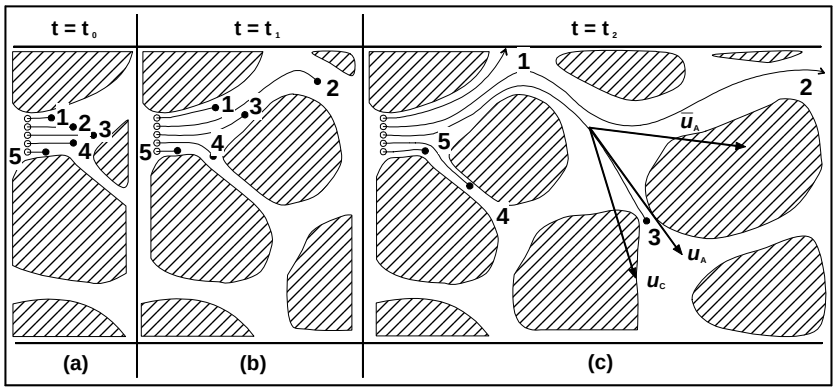

Fig. 2.6: **Dispersion mechanisms at microscopic scale.**

Similar to the consequence of heterogeneity of porous media, variations of fluid properties, such as viscosity and densities are known to produce gravitational instability (RAYLEIGH-BENARD instability, gravity override) and viscous instability (TAYLOR-SAFFMAN instability, fingering, viscous instability) respectively, in which the injected fluid (displacing fluid) does not displace the resident fluid with a uniform front, but in a very irregular lob-shaped (finger) flow pattern.

Generally, dispersion is caused by the interplay of two velocity differences (Fig. 2.6):

- Difference between the microscopic fluid velocity (u_A) and the macroscopic ($\overline{u}_A$) fluid velocity.

- Discrepancy between the microscopic fluid velocity (u_A) and the microscopic velocity of tracer components (u_C).

The first difference resulted from the microscopic heterogeneity. Variability in velocity at the microscopic scale develops due to the following three mechanisms:

- Fluid particles (1, 2, 3, 4 and 5 in Fig. 2.6a) travel at different velocities at different points along a cross section of a single pore channel because of the roughness of the pore surfaces and the viscous fluid (Fig. 2.6a).

- Discrepancies in pore dimensions (including dead-end pore) cause some fluid particles (particle 2 and 3 in Fig. 2.6b) to move faster than the other (particle 4 in Fig. 2.6b).

- Variations in pore geometry (including tortuosity, branching and fingering) along the flow paths result in fluctuations of the microscopic flow velocity with respect to the macroscopic average flow velocity (Fig.2.6c).

Obviously, the macroscopic average velocity is generally different, both in direction and in magnitude, from the real microscopic fluid velocity at each point within the REV . At some points, the difference may be quite large, for example, Fig. 2.6c illustrates that particle 1 is flowing at time

t_2 in a completely different direction. It is self-evident that the fluid flow in pore channels is a tracer carrier. Therefore, the difference between the two fluid velocities causes inevitably spreading of tracer particles beyond the scope with respect to the macroscopic average flow.

Due to the branching in Fig. 2.6 (b) and (c), spreading occurs both in the direction of bulk flow (longitudinal dispersion) and in directions perpendicular to the flow (transverse dispersion). Not only branching, other microscopic variations of pore channels such as tortuosity, interfingering and dead end contribute to the velocity difference at microscopic scale as well.

The second velocity discrepancy exists at microscopic scale (Fig. 2.6). Because of molecular diffusion (due to concentration gradients), which occurs during the fluid flow and does not depend upon the fluid flow, a tracer particle moves generally in a different velocity (u_C) as the carrying fluid does.

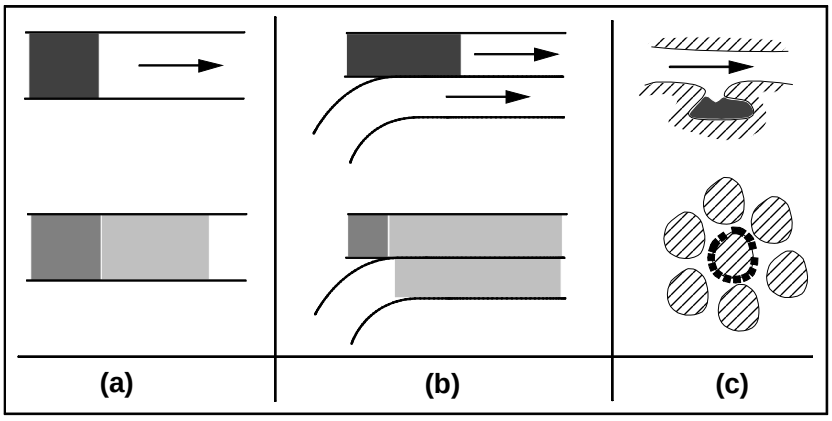

Fig. 2.7: **Contribution of molecular diffusion to dispersion.**

Molecular diffusion alone contributes to dispersion also in three different ways:

- In individual pore channels, concentration gradients, which are approximately in the same direction as that of the mean stream, tend to disappear gradually. This effect promotes

longitudinal dispersion and is important only at low fluid velocity (or when the concentration gradients are extremely high (Fig. 2.7a).

- Between two adjacent pore channels (channel branching and fingering) tracer mass is also transported in the direction of decreasing concentration. This effect accounts to a great extent for transverse dispersion (Fig. 2.7b).

- "Holdup" dispersion and "boundary layer" dispersion (KOCH et al., 1987a). Due to the so called "holdup" effect, where tracer components are absorbed by the solid phase or are constrained within dead-end pores or closed streamlines, or because of the "boundary layer" effect on fluid-solid surfaces, the fluid velocity within these regions goes to zero. Thus molecular diffusion provides the only possibility for tracer to spread. As a result, a part of the tracer is left far behind the scope with respect to the macroscopic average fluid velocity at high PECLET number (Fig. 2.7c).

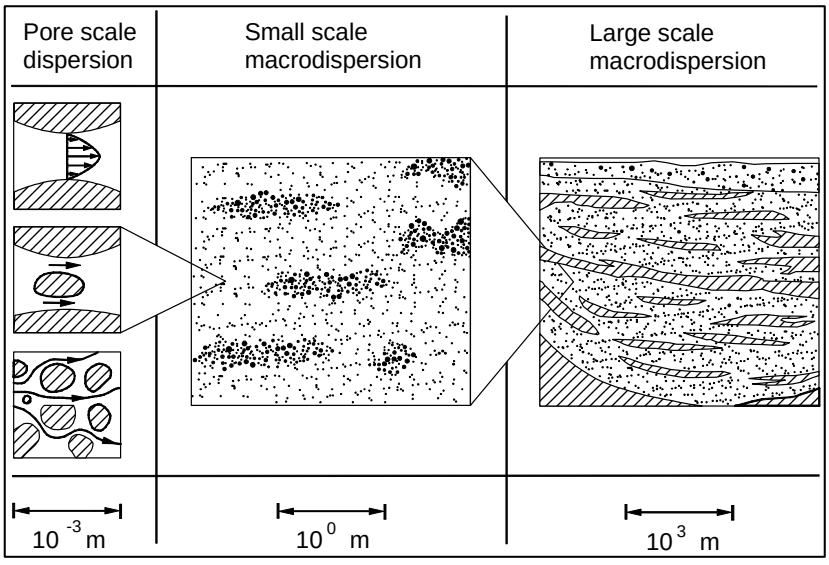

Fig. 2.8: **Heterogeneity at different scale results in scale dependent dispersion (after KINZELBACH, 1992).**

Having discussed pore-scale dispersion (local dispersion), we now turn our attention to macrodispersion (non-local dispersion), which is largely dependent upon macroscopic heterogeneity of the medium to a great extent. Owing to this heterogeneity dependence, values of macroscopic dispersivity may vary from centimetre (cm) scale to thousands of meter (Fig. 2.8 from KINZELBACH, 1992, p35; OHLENBUSCH, 2001, p15). However, DOMENICO et al. (1990) argued that longitudinal dispersivity values might exceed 10m, but not too much more than that value. Defining REV at different scales, they gave a concise explanation for the spatially varying dispersivity (Fig. 2.9, DOMENICO et al., 1990, p375).

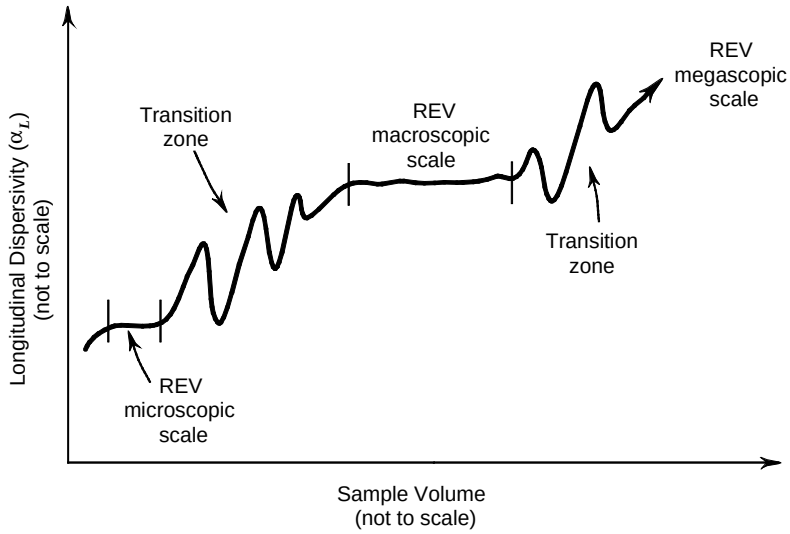

Fig. 2.9: **Longitudinal dispersivity and REVs at different scale (after DOMENICO et al., 1990).**

Dependending on the fluid combination and displacement relationship, miscible displacements in porous media can be either stable or unstable. Six possible flow configurations are shown in Fig. 2.10. U indicates the flow direction, which is a result of an imposed hydraulic gradient. The socalled “gravitational instability” might be produced for the upward flow in Fig. 2.10 a). The density difference in Fig. 2.10 c) may also lead to gravitational instability. The increase of viscosity along the flow direction in Fig. 2.10 a), d) & e) may cause the so called “viscous instability”. In other cases, the density and viscosity

differences have either neutral or stabilizing effect on the flow. Because both the density and viscosity differences in Fig. 2.10 a) act to produce instability, the flow is always unstable. As they both have a stabilizing effect on the flow in Fig. 2.10 b). the flow is always stable. The most complecated case is shown in Fig. 2.10 c) and d) where the density and viscosity contrasts have opposite effects. It is generally believed that in horizontal cases (Fig. 2.10 e) and f)), only viscosity ratio ($M = \mu_{displaced}/\mu_{displacing}>1$) is the trigger for instability. However, as will be shown in Chapter 5, density effect should not be neglected in horizontal miscible displacements in a homogeneous sand tank.

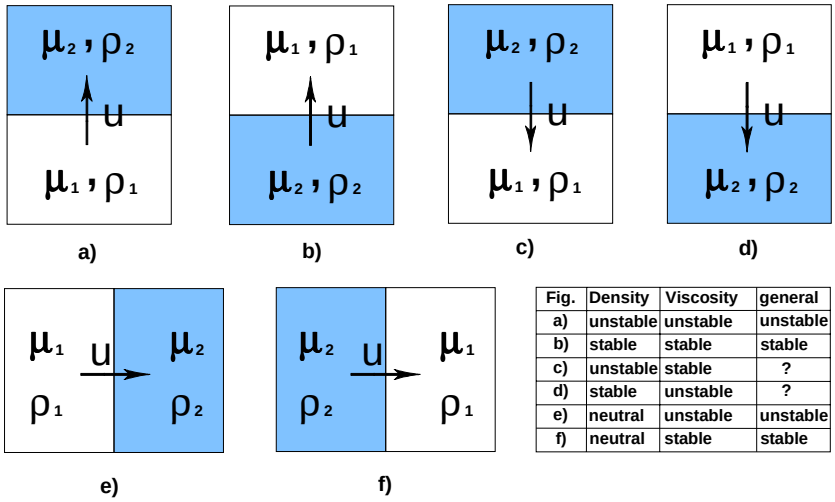

Fig.	Density	Viscosity	general
a)	unstable	unstable	unstable
b)	stable	stable	stable
c)	unstable	stable	?
d)	stable	unstable	?
e)	neutral	unstable	unstable
f)	neutral	stable	stable

Fig. 2.10: **Miscible displacement in porous media with different combination of fluid density ($\rho_2>\rho_1$), fluid viscosity ($\mu_2>\mu_1$) and flow rate (u), where b) and f) are stable displacements, while a) and e) are unstable. Due to the contrary effect of viscosity and density in c) and d), the general flow state must be determined specifically. (changed after WELTY et al., 1991).**

2.4 Analytical description

The complete analytical description (theoretical derivation) for miscible fluid displacements in a saturated porous medium has been described

in numerous classical works (e.g., BEAR, 1972; FRIED, 1975; FREEZE and CHERRY, 1979; NIELD and BEJAN, 1992; KINZELBACH, 1995; HOLZBECHER, 1998). Due to space limit, a brief description of the most important concepts and methods are presented here and thereafter a set of differential equations is derived.

Equation of Continuity

Based on the REV concept (abbreviation of Representative Elementary Volume, for detail, see BEAR, 1972), a continuum model could be deduced. In this continuum model, a macroscopic variable is defined as an appropriate mean value over the sufficiently large REV. It is assumed that the averaging result is independent of the size of the REV, which is much larger than a single pore space or grain size, but considerably smaller than the total macroscopic domain.

Two fluid velocities need to be distinguished: real average velocity $\vec{u}$ (or simply real velocity) and filtration velocity $\vec{v}$ (seepage velocity or DARCY velocity). While the real velocity is the result of an average taken over the fluid volume only, the average process for filtration velocity is taken over the whole volume of the REV (incorporating both solid and fluid material). The two velocities are related by the DUPUIT-FORCHHEIMER relationship $\vec{v} = n\vec{u}$, where n is effective porosity.

Consider a unit volume of porous media in a Cartesian reference frame. According to the law of conservation of mass, the rate of fluid mass flow into the unit volume is equal to the rate of fluid mass flow out of the same unit volume. Translating the mass conservation law into mathematical equation, we get the equation of continuity:

$$\frac{\partial}{\partial t}(n\rho) = -\nabla \cdot (\rho\vec{v}) \tag{2.7}$$

where ρ is the fluid density and ∇ is a mathematical operator, which is defined by the following vectors:

$\nabla = (\frac{\partial}{\partial x}, \frac{\partial}{\partial y})$ in 2D, $\nabla = (\frac{\partial}{\partial x}, \frac{\partial}{\partial y}, \frac{\partial}{\partial z})$ in 3D

Description of Solute Transportation

For solute transport in porous medium, besides advection, there occurs dispersion simultaneously. Aiding the term of dispersion and changing our attention from the carrier to the solute itself, equation (2.7) becomes:

$$\frac{\partial}{\partial t}(n\rho C) = -\nabla \cdot (\rho \vec{v} C) - \nabla \cdot \vec{J} \tag{2.8}$$

where C is the solute concentration, t is the time and $\vec{J}$ is the solute dispersive mass flux.

Generalised Fick's Law

Analogue to Fick's law the dispersion flux of a solute is proportional to the concentration gradient:

$$\vec{\mathrm{J}} = -n\rho \vec{D} \nabla C \tag{2.9}$$

where $\vec{D}$ is the dispersion tensor.

DARCY'S Law

The filtration velocity is related to the imposed pressure gradient and to the vector of the external forces by an experimental law, referred to as DARCY's law:

$$\vec{v} = -\frac{\vec{\mathrm{k}}}{\mu}(\nabla \vec{p} - \rho \vec{g}) \tag{2.10}$$

where $\vec{k}$ is the permeability tensor, μ is the fluid viscosity, $\vec{g}$ is the gravitational acceleration vector.

Because the equation is based on the momentum balance it is also called the momentum equation.

Assumption and Simplification

For simplification, one can neglect the density variations with concentration if concentration differences are small in the physical system. According to HOLZBECHER (1998), both OBERBECK and BOUSSINESQ proved that the neglect of density variations does not result in any change even in the analytical description. However, as the density difference in the term of $\rho\vec{g}$ in DARCY's equation is the source of driving force for natural convection, its variation with concentration differences should not be neglected. This simplified approach is known as OBERBECK-BOUSSINESQ assumption.

With this approximation and assuming that the fluid and the porous medium are incompressible, the equation of continuity (2.6) and the mass conservation of a solute (2.7) reduce to:

$$\nabla \cdot \vec{v} = 0 \tag{2.11}$$

$$n\rho \frac{\partial C}{\partial t} = -\rho \nabla \cdot (\vec{v} C) - \nabla \cdot \vec{J} \tag{2.12}$$

Substitute Eq. (2.8) and Eq. (2.10) into Eq. (2.11) and let Eq. (2.11) be divided by ρ, we get:

$$n \frac{\partial C}{\partial t} = -\vec{v} \cdot \nabla C + n \nabla \cdot (\vec{D} \cdot \nabla C) \tag{2.13}$$

2.5 Boundary and initial conditions

The continuity equation (2.11) and mass balance equation (2.13), coupled with the momentum balance equation (2.10) and state equation (2.3) & (2.4) constitute a complete system in describing the physical processes of miscible fluid displacements in porous medium. However, for a given configuration of a flow system, the initial and boundary conditions are needed in order to get particular solutions to the previous general equations. There are many kinds of combinations of boundary and initial conditions. However, except under some flow circumstances in homogeneous porous medium with simple boundary

and initial conditions, there are no analytical solutions even for the ideal tracer problem. In the present study, only two kinds of simple combinations in a one- and two-dimensional case each are considered.

Plane step-input. The plane step-input is understood that, in one-dimensional semi-infinite porous medium over a defined plane, say $x = 0$, the concentration is to be maintained at a known and feasible value C_o, which is different from those of the fluid flowing in a steady-state flow domain on a continuous basis. Fig. 2.11 illustrates how the tracer concentration varies in time and space. This is an example of one-dimensional transport involving advection and dispersion.

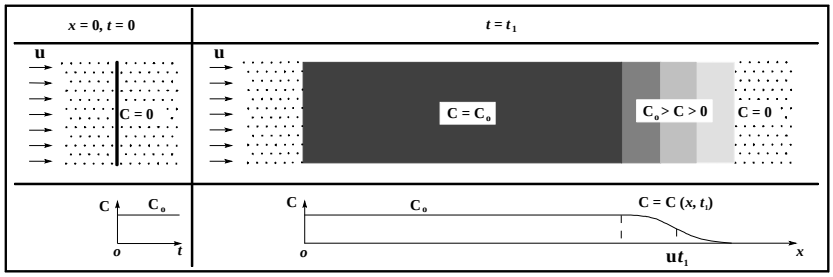

Fig. 2.11: **Continuous input of a tracer with concentration C_o at the inflow boundary of a one-dimensional steady flow domain and variation of the tracer concentration.**

The step input boundary and initial conditions are described in equation (2.14), (2.15) and (2.16) respectively.

Boundary condition:

$$C(0,t) = C_0 \text{ ; for } t \geq 0 \tag{2.14}$$

$$\lim_{x \to \infty} C(x,t) = 0 \text{ ; for } t \geq 0 \tag{2.15}$$

Initial condition:

$$C(x,0) = 0 \text{ ; for } x \geq 0 \tag{2.16}$$

Plane Dirac-input. When tracer input across the cross section is not continuous, but instantly, variation of tracer concentration in space and time is shown in Fig. 2.12.

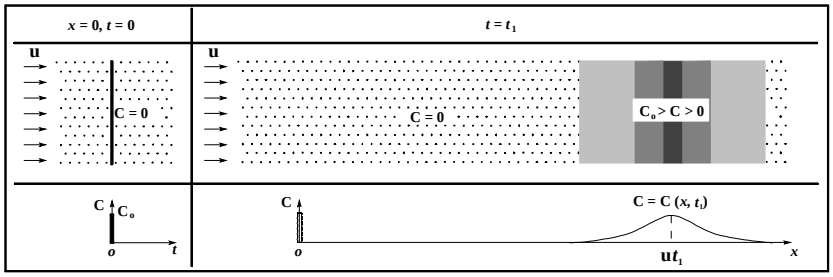

Fig. 2.12: **Pulse input of a tracer with concentration C_o at the inflow boundary of a one-dimensional steady flow domain and variation of the tracer concentration.**

Mathematical description of the Dirac-input is:

$$C(0,t) = \frac{G}{n \cdot u \cdot A} \cdot \delta(t) \quad \text{or} \quad C(0,t) = \frac{G}{Q} \cdot \delta(t) \tag{2.17}$$

where C is the tracer concentration, δ(t) is the Dirac delta-function G is the mass injected, u is the mean velocity of the flow, A is the area of the cross section perpendicular to the flow direction, n is the porosity.

$$C(\infty,t) = 0 \,; \text{ for } \; t \geq 0 \tag{2.18}$$

Initial condition:

$$C(x,0) = 0 \,; \text{ for } \; x \geq 0 \tag{2.19}$$

Point step input & point Dirac input. When tracer input is not across a whole cross section, but at an injection point, the two kind of initial conditions are shown in Fig. 2.13 (point step input) and Fig. 2.14 (point Dirac input) respectively.

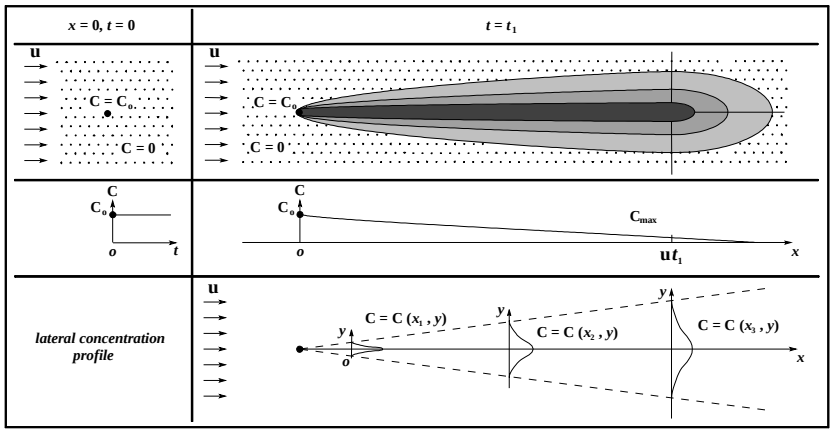

Fig. 2.13: **Continuous input of a tracer with concentration C_o at an inflow point in a constant velocity flow system; Both longitudinal and transversal variation of the tracer concentration are illustrated.**

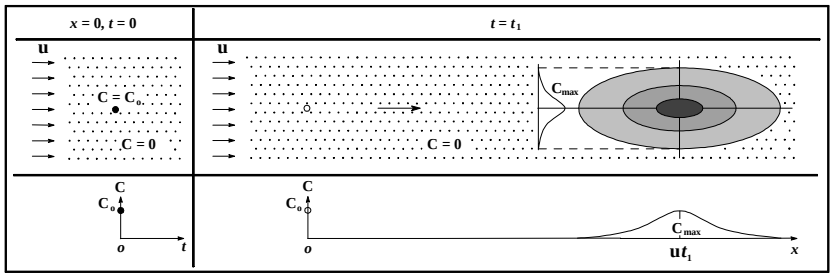

Fig. 2.14: **Pulse input of a tracer with concentration C_o at an inflow point and variation of the tracer concentration in two dimensions in a constant velocity flow system.**

2.6 Analytical solution

Difficulties in knowing the details of transport processes of a nonpassive solute prohibit us to have a precise description at microscopic scale, however following the classical advection-dispersion

formulism and in analogue to the case of a passive solute (tracer), miscible fluid displacement with density and viscosity differences can be simulated through some macroscopic average quantities such as average concentration and thereafter dispersion coefficient. Some analytical solutions that closely relate to the present investigation are to be given in this section.

1-D with pulse-input

1-D advection-dispersion equation is:

$$D_x \frac{\partial^2 C}{\partial x^2} - u \cdot \frac{\partial C}{\partial x} = \frac{\partial C}{\partial t} \tag{2.20}$$

For the 1-D advection-dispersion equation with boundary conditions of pulse-input (Dirac-input, equation (2.17), (2.18) & (2.19)) under the assumption of:

- Homogeneous, isotropic porous medium
- Steady state flow

Analytical solution is:

$$C(x,t) = \frac{m}{Q} \cdot \frac{x}{\sqrt{4\pi D_x t^3}} \cdot \exp\left(- \frac{(x-ut)^2}{4D_x t} \right). \tag{2.21}$$

where C is the tracer concentration (g/L), t is the time (s), m is the mass injected (g), Q is the flow rate (cm^3/s), u is the mean velocity of the flow (cm/s), D_x is the longitudinal dispersion coefficient (cm^2/s).

1-D with step-input

For the 1-D advection-dispersion equation with conditions depicted in equation (2.14), (2.15) & (2.16) under the same assumption, analytical solution is (OGATA, 1970):

$$\frac{C}{C_0} = \frac{1}{2} erfc\left(\frac{x-ut}{2\sqrt{D_x t}} \right) + \frac{1}{2} \exp\left(\frac{ux}{D_x} \right) erfc\left(\frac{x+ut}{2\sqrt{D_x t}} \right). \tag{2.22}$$

The second term in the solution is generally small, so that only the first term is to be put into practical usage:

$$\frac{C}{C_0} = \frac{1}{2} erfc\left(\frac{x-ut}{2\sqrt{D_x t}}\right), \tag{2.23}$$

where C_0 is the constant tracer concentration at inlet plane, u is the mean velocity of the flow, D_x is the longitudinal dispersion coefficient, and *erfc (z)* is known as the complementary error function.

2-D with pulse-input

Similarly, for 2-D advection-dispersion equation with boundary conditions of pulse-input under the assumption of:

- Homogeneous, isotropic porous medium
- Steady state flow
- The flow direction is parallel to x axis
- Two dimensional flow when $x > \frac{1}{2} \cdot \frac{H^2}{\alpha_x}$

Analytical solution is given:

$$C(x,y,t) = \frac{G}{n \cdot H} \cdot \frac{x}{4\pi\ v \cdot t^2 \sqrt{D_x \cdot D}_y} \cdot \exp\left(-\frac{(x-ut)^2}{4D_x t} - \frac{y^2}{4D_y \cdot t}\right) \tag{2.24}$$

where C is the tracer concentration (g/L), t is the time (s), G is the mass injected (g), u is the mean velocity of the flow (cm/s), H is the thickness of the porous medium (cm), α_x is the longitudinal dispersivity, n is the porosity, D_x and D_y are the dispersion coefficients for two orthogonal directions x and y.

3-D with pulse-input

For a point impulse injection (Dirac input) carried out in an infinite medium at the beginning of the coordinate system under the assumption of:

- Homogeneous, isotropic porous medium
- Steady state flow
- The flow direction is parallel to x axis
- Ideal tracer (passive solute)

The concentration of the input tracer at time t and point (x, y, z) is:

$$C(x,y,z;t) = \frac{G}{n} \cdot \frac{x}{\sqrt{4\pi D_x t}} \cdot \exp\left(-\frac{(x-ut)^2}{4D_x t}\right) \cdot \frac{1}{\sqrt{4\pi D_y t}} \cdot \exp\left(-\frac{y^2}{4D_y \cdot t}\right) \cdot \frac{1}{\sqrt{4\pi D_z t}} \cdot \exp\left(-\frac{z^2}{4D_z t}\right) \tag{2.25}$$

where $C(x,y,z;t)$ is the tracer concentration; G is the mass injected; u is the mean flow velocity; D_x, D_y, D_z are the dispersion coefficients for three orthogonal directions.

2.7 Methods for determining dispersion coefficients

This section discusses the use of the advection-dispersion equation as a tool in experimental determinations of the magnitude of the dispersion coefficients. Analytical solutions to the equation for the most common used boundary and initial conditions have been given in the last section. Dispersion coefficient can be determined by performing a least-squares fit or using a linear regression fit (straight-line correlation) of the analytical solutions to measured concentrations, if concentration measurements have been carried out at some distance from the injection position without disturbing the flow.

Method of least-squares fit

The least-squares fit requires an estimated initial value for the dispersion coefficient. It is actually an iteration process. The process will not stop until the expression (2.26) reaches the minimum value.

$$Minimum \sum \left[C(x,y,z)_{measured} - C(x,y,z)_{simulated} \right]^2 \tag{2.26}$$

Method of linear regression

The complementary error function in equation (2.23) is defined and related to the error function:

$$erfc\ z = 1 - erf\ z = \frac{2}{\sqrt{\pi}} \int_z^{\infty} e^{-t^2} dt \tag{2.27}$$

The error function is defined:

$$erf\ x = \frac{2}{\sqrt{\pi}} \int_0^{x} e^{-t^2} dt \tag{2.28}$$

It may be also expressed in another way (series):

$$erf\ x = \frac{2}{\sqrt{\pi}} \left(x - \frac{x^3}{3} + \frac{1}{2!}\frac{x^5}{5} - \frac{1}{3!}\frac{x^7}{7} + \cdots \right) \tag{2.29}$$

The error function has the following property:

$$erf\ x = -erf\ (-x) \tag{2.30}$$

Equation (2.23) can be rewritten:

$$erf \left(\frac{x - ut}{2\sqrt{D_x t}} \right) = 1 - 2 \cdot \frac{C}{C_0} \tag{2.31}$$

The error function is related to the Normal Probability function $f(t)$ in the following way:

$$\int_0^x f(t)dt = \frac{1}{2} erf\left(\frac{x}{\sqrt{2}}\right) \tag{2.32}$$

Combining equation (2.31) with equation (2.32), we have:

$$\int_0^{\sqrt{2}\cdot\frac{(x-ut)}{2\sqrt{D_x t}}} f(t)dt = \frac{1}{2}\cdot\left(1-2\cdot\frac{C}{C_0}\right) \tag{2.33}$$

Following OGATA (1970), the other method of determining dispersion coefficient is to examine the slope of a straight line plotted on rectangular coordinates that associate two middle variables (ζ, η) with a given value of C/C_0, where $\zeta = \frac{x-ut}{2\sqrt{Dt}}$ and $\eta = \frac{x-ut}{2}\cdot\sqrt{\frac{1}{utx}}$. $\sqrt{2}\,\zeta$ is related to $\frac{1}{2}\cdot\left(1-2\cdot\frac{C}{C_0}\right)$ in equation (2.33). From the tables of the normal probability function in Appendix III, $\sqrt{2}\,\zeta$ can be determined. The other middle variable η can be directly calculated. The average slope is $\eta/\zeta = \sqrt{\frac{D}{ux}}$, the value of D can thus be calculated.

3 CONVECTION IN A VERTICAL POROUS COLUMN

3.1 Introduction

Unstable density gradients arising from differences in dissolved solute exist in a wide variety of fields. The gradient can induce convection currents and thus induce the hydrodynamic instability.

Vertical flow due to density differences was cited as a possible explanation for observed unexpected sinking of the tracer plume by BOGGS et al. (1992), LEBLANC et al. (1991) FREYBERG (1986), SUDICKY et al. (1983). Based on their experiments conducted in a large-scale physical aquifer model containing a homogeneous and isotropic sand pack, ISTOK and HUMPHREY (1995) concluded that the vertical flow due to density differences must be considered when interpreting tracer tests conducted with anion concentrations as low as 50 mg/l!

In laboratory, density effects have been studied in columns and flow containers. WOODING (1963) and BACHMAT et al. (1970) performed experiments in a vertical porous column, which was connected to an open reservoir with an aqueous solution denser than water.

Column displacement studies with salt solutions were also carried out by BIGGAR and NIELSEN (1964), KRUPP and ELRICK (1969), and ROSE et al., (1971). They found that the occurrence of instabilities was related to the density differences and the average pore water velocities.

It will be the object of the chapter to analyse the mechanism of free convection and the formation and development of hydrodynamic instability in a long vertical column with impermeable walls. Section 3.2 gives an analytical description for the problem. Following BEJAN'S analysis, an approximate analytical solution is derived in section 3.3. Section 3.4 outlines the vertical penetration distance and the rate of vertical transportation of the dense solute in the upper reservoir is calculated. The results are compared with the experimental results of WOODING (1963) and BACHMAT et al. (1970).

3.2 Analytical description

Suppose that a long vertical column (radius R; height L) is filled with a homogeneous, isotropic porous material (porosity n, permeability k) saturated with a static aqueous solution of density ρ_o (concentration C_o); viscosity μ and closed at the bottom, while the top of the tube is connected to an open reservoir (radius R_1) containing the same aqueous solution but with a higher concentration C_1 and thus a higher density $\rho_1 > \rho_o$. The system is at a constant uniform temperature. This is a classical experiment on hydrodynamic instability (c.f. WOODING, 1963; BACHMAT et al., 1970). The configuration is shown in Fig. 3.1.

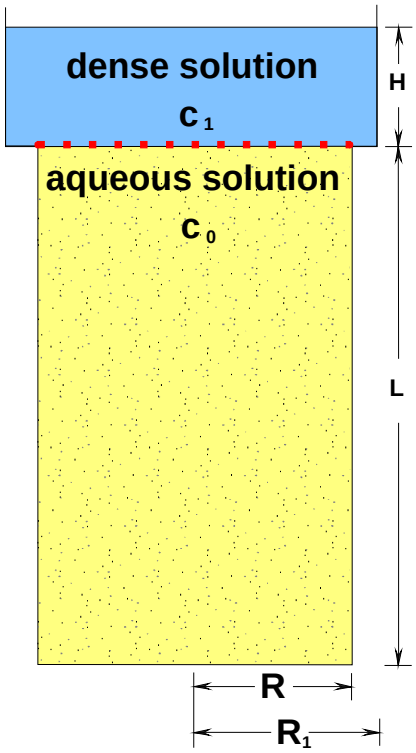

Fig. 3.1: **Scheme of the system configuration.**

For such a problem we need to answer four questions:

- When happens natural convection?
- How fast descends the dense solute?
- If the bottom of the column is closed, how deep can the descending dense flow arrive?
- How much is the rate of solute-transfer?

It is easy to get an answer for the first question. In fact, fluid motion sets in as soon as the smallest concentration difference $\Delta C = C_1 - C_0$ is imposed between the upper permeable horizontal boundary and the fluid in the column (NIELD et al., 1992). The configurations of the isodensity surfaces vary in shape and rate in a much different manner from those predicted by ordinary molecular diffusion alone (BACHMAT and ELRICK, 1970).

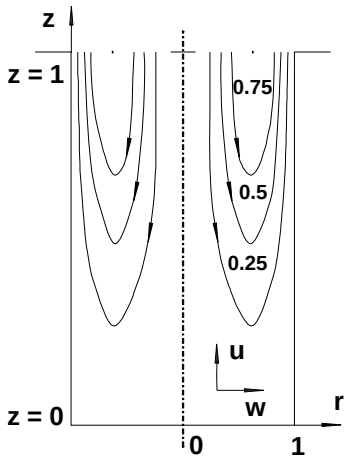

Fig. 3.2: **Streamline and schematic of the vertical porous column (after BEJAN, 1980).**

In the cylindrical coordinate system the streamfunction ψ can be defined by (HOLZBECHER, 1998):

$$u = \frac{1}{2\pi r}\frac{\partial \psi}{\partial r}, \quad w = -\frac{1}{2\pi r}\frac{\partial \psi}{\partial z} \tag{3.1}$$

where u and w are the vertical and horizontal flow velocity respectively. The continuity equation (2.11) becomes (HOLZBECHER, 1998):

$$\frac{\partial u}{\partial z}+\frac{1}{r}\frac{\partial}{\partial r}(rw)=0 \tag{3.2}$$

According to DARCY'S Law, the momentum equation (2.10) in the cylindrical coordinate system is written as:

$$u=-\frac{k}{n\cdot\mu}\left(\frac{\partial p}{\partial z}+\rho g\right),\quad w=-\frac{k}{n\cdot\mu}\frac{\partial p}{\partial r} \tag{3.3}$$

Eliminating p from the above two equations, we have:

$$\frac{\partial u}{\partial r}-\frac{\partial w}{\partial z}=-g\cdot\frac{k}{\mu}\cdot\frac{\partial \rho}{\partial r} \tag{3.4}$$

The transport equation (2.13) becomes:

$$\frac{1}{r}\cdot\frac{\partial}{\partial r}\left(D_r\cdot r\cdot\frac{\partial C}{\partial r}\right)+\frac{\partial}{\partial z}\left(D_z\cdot\frac{\partial C}{\partial z}\right)-u\frac{\partial C}{\partial z}-w\frac{\partial C}{\partial r}=\frac{\partial C}{\partial t} \tag{3.5}$$

where D_r and D_z are the transversal and longitudinal dispersion coefficients.

The equation of state is:

$$\rho=\rho_{H_2O}+\beta\cdot C\text{, or }\rho=\rho_o+\beta(C-C_o) \tag{3.6}$$

where $\beta=d\rho/dC$ is the density coefficient of the solution in the concentration range of $C_o<C<C_1$ Let z, r, u, w, C and t be substituted by the following dimensionless variables:

$$z \to \frac{z}{L}, \quad r \to \frac{r}{R}, \quad u \to \frac{u \cdot R^2}{D_z \cdot L}, \quad w \to \frac{w \cdot R}{D_z} \tag{3.7}$$

$$\theta \to \frac{k \cdot g \cdot \beta \cdot L \cdot (C_o - C)}{n \cdot D_z \cdot \mu} \left(\frac{R}{L} \right)^2 \tag{3.8}$$

$$\tau \to \frac{t \cdot D_z}{R^2} \tag{3.9}$$

where C_o is the solute concentration in the porous material of the column.

The dimensionless continuity equation and equations of momentum and mass conservation are (BEJAN, 1980; HOLTZBECHER, 1998)

$$\frac{\partial u}{\partial z} + \frac{w}{r} + \frac{\partial w}{\partial r} = 0 \tag{3.10}$$

$$\frac{\partial u}{\partial r} - \left(\frac{R}{L} \right)^2 \frac{\partial w}{\partial z} = \frac{\partial \theta}{\partial r} \tag{3.11}$$

$$u \frac{\partial \theta}{\partial z} + w \frac{\partial \theta}{\partial r} = \frac{D_r}{D_z} \left(\frac{\partial^2 \theta}{\partial r^2} + \frac{1}{r} \frac{\partial \theta}{\partial r} \right) + \left(\frac{R}{L} \right)^2 \frac{\partial^2 \theta}{\partial z^2} - \frac{\partial \theta}{\partial \tau} \tag{3.12}$$

Generally $\frac{R}{L} << 1$ so the terms with $\left(\frac{R}{L} \right)^2$ in equations (3.11) and (3.12) can be omitted. If the flow is assumed to be in a quasi steady-state equation (3.12) can be further simplified:

$$u \frac{\partial \theta}{\partial z} + w \frac{\partial \theta}{\partial r} = \frac{D_r}{D_z} \left(\frac{\partial^2 \theta}{\partial r^2} + \frac{1}{r} \frac{\partial \theta}{\partial r} \right) \tag{3.13}$$

The appropriate boundary conditions are

$$r = 1 \quad : \quad w = 0, \quad \theta = 0 \tag{3.14}$$

$$z = 0 \quad : \quad u = 0, \quad \theta = 0 \tag{3.15}$$

3.3 Similarity solution

Because of nonlinearity in equations (3.10), (3.11) and (3.13) without the $(R/L)^2$ terms, there does not exist exact analytical solutions for u, w and C. Analogous to heat-transfer analysis by BEJAN (1980), however, it is possible to seek a similarity solution, considering that both u and θ are proportional to z while w is a function only of radial position.

$$\begin{aligned}
&\frac{d}{dz}\left(\int_0^1 r \cdot u \cdot \theta \cdot dr\right) = \int_0^1 r \cdot \left(u \cdot \frac{\partial \theta}{\partial z} + \theta \frac{\partial u}{\partial z}\right) \cdot dr \\
&= \frac{D_r}{D_z}\int_0^1 \left(r \cdot \frac{\partial^2 \theta}{\partial r^2} + \frac{\partial \theta}{\partial r}\right) \cdot dr + \int_0^1 r \cdot \left(\theta \cdot \frac{\partial u}{\partial z} - w \frac{\partial \theta}{\partial r}\right) \cdot dr \\
&= \frac{D_r}{D_z} \cdot r \cdot \frac{\partial \theta}{\partial r}\Big|_{r=0}^{r=1} - \int_0^1 \left[w \cdot \theta + r \cdot \left(\theta \cdot \frac{\partial w}{\partial r} + w \cdot \frac{\partial \theta}{\partial r}\right)\right] \cdot dr \\
&= \frac{D_r}{D_z}\left(\frac{\partial \theta}{\partial r}\right)_{r=1} - w \cdot \theta \cdot r\Big|_{r=0}^{r=1} = \frac{D_r}{D_z}\left(\frac{\partial \theta}{\partial r}\right)_{r=1}
\end{aligned} \tag{3.16}$$

Equation (3.13) must hold at the boundary $r = 0$ and $r = 1$ as well

$$\left(u \frac{\partial \theta}{\partial z} + w \frac{\partial \theta}{\partial r}\right)_{r=0,r=1} = \frac{D_r}{D_z}\left(\frac{\partial^2 \theta}{\partial r^2} + \frac{1}{r}\frac{\partial \theta}{\partial r}\right)_{r=0,r=1} \tag{3.17}$$

From the continuity equation we see that $(w/r)_{r=0}$ must be a finite function. According to the theory of similarity that both u and θ are

proportional to z while w is a function only of radial position, we may let $w = r \cdot f(r)$. Equation (3.17a) changes into:

$$\left(u \frac{\partial \theta}{\partial z} \right)_{r=0} = \frac{D_r}{D_z} \left(\frac{\partial^2 \theta}{\partial r^2} + \frac{1}{r} \frac{\partial \theta}{\partial r} \right)_{r=0} \tag{3.18}$$

Similarly, equation (3.17b) changes into:

$$\frac{D_r}{D_z} \left(\frac{\partial^2 \theta}{\partial r^2} + \frac{1}{r} \frac{\partial \theta}{\partial r} \right)_{r=1} = \left(u \frac{\partial \theta}{\partial z} + w \frac{\partial \theta}{\partial r} \right)_{r=1} = 0 \tag{3.19}$$

It is clear that polynomial functions are good approximation for concentration and vertical velocity.

$$\theta = z \cdot (a_o + a_2 r^2 + a_4 r^4 + a_6 r^6) \tag{3.20}$$

$$u = z \cdot (b_o + a_2 r^2 + a_4 r^4 + a_6 r^6) \tag{3.21}$$

These approximations satisfy the momentum equation (61) identically. Substituting them into equations (3.10), (3.14b), (3.16), (3.18) and (3.19) respectively, we get

$$12 b_o + 6 a_2 + 4 a_4 + 3 a_6 = 0 \tag{3.22}$$

$$a_o + a_2 + a_4 + a_6 = 0 \tag{3.23}$$

$$\begin{aligned} &\frac{a_o b_o}{2} + \frac{a_o a_2 + a_2 b_o}{4} + \frac{a_o a_4 + a_2^2 + a_4 b_o}{6} + \frac{a_o a_6 + 2 a_2 a_4 + a_6 b_o}{8} \\ &+ \frac{a_4^2 + 2 a_2 a_6}{10} + \frac{a_4 a_6}{6} + \frac{a_6^2}{14} = (a_2 + 2 a_4 + 3 a_6) \frac{D_r}{D_z} \end{aligned} \tag{3.24}$$

$$a_2 = \frac{a_o b_o}{4} \cdot \frac{D_z}{D_r} \tag{3.25}$$

$$a_2 + 4a_4 + 9a_6 = 0 \tag{3.26}$$

Let $m = \frac{D_z}{D_r}$, from the equation (3.22), (3.23), (3.25) and (3.26) we have:

$$\begin{aligned} b_o &= \frac{96a_o}{240 + 7ma_o};\ a_2 = \frac{24ma_o^2}{240 + 7ma_o} \\ a_4 &= \frac{-51ma_o^2 - 432a_o}{240 + 7ma_o};\ a_6 = \frac{20ma_o^2 + 192a_o}{240 + 7ma_o} \end{aligned} \tag{3.27}$$

Substitute equation (3.27a, b, c&d) into (3.24) we get:

$$32.7m^3a_o^4 + 2370m^2a_o^3 + 64396.8ma_o^2 + 483840a_o = 0 \tag{3.28}$$

The first solution of this equation $a_o^{(1)} = 0$ should obviously be rejected. If $m = 1$, this means if $D_z = D_r$, we have:

$$32.7a_o^3 + 2370a_o^2 + 64396.8a_o + 483840 = 0 \tag{3.29}$$

The only real solution of the equation is $a_o = -11.81$. Subsequently we get $b_o = -7.206$, $a_2 = 21.27$, $a_4 = -12.781$, $a_6 = 3.317$. Similarly we can get all the solutions when m has other values:

$$a_o^{(m)} = \frac{a_o}{m},\ b_o^{(m)} = \frac{b_o}{m},\ a_2^{(m)} = \frac{a_2}{m},\ a_4^{(m)} = \frac{a_4}{m},\ a_6^{(m)} = \frac{a_6}{m} \tag{3.30}$$

Substituting them into equations (3.20) and (3.21), we have:

$$\theta = \frac{D_r}{D_z} \cdot z \cdot (-11.81 + 21.278r^2 - 12.786r^4 + 3.319r^6) \tag{3.31}$$

$$u = \frac{D_r}{D_z} \cdot z \cdot (-7.207 + 21.278r^2 - 12.786r^4 + 3.319r^6) \qquad (3.32)$$

Combining equation (3.32) with (3.10) yields:

$$w = \frac{D_r}{D_z}(3.603r - 5.32r^3 + 2.131r^5 - 0.415r^7) \qquad (3.33)$$

Tab. 3.1: **Different solutions for different *m* values.**

M	a_o	a_2	a_4	a_6	b_o
1	-11.810377	21.278183	-12.786413	3.3186078	-7.2066056
2	-5.9051876	10.639087	-6.3932009	1.6593019	-3.6033018
3	-3.9367919	7.0927251	-4.2621347	1.1062015	-2.4022013
4	-2.9525940	5.3195444	-3.1966017	0.8296514	-1.8016511
5	-2.3620751	4.2556347	-2.5572804	0.6637208	-1.4413207
6	-1.9683960	3.5463629	-2.1310678	0.5531009	-1.2011007
7	-1.6871969	3.0397408	-1.8266310	0.4740870	-1.0295152
8	-1.4762970	2.6597720	-1.5983007	0.4148256	-0.9008255
9	-1.3122640	2.3642418	-1.4207117	0.3687340	-0.8007338
10	-1.1810376	2.1278177	-1.2786407	0.3318605	-0.7206604
11	-1.0736707	1.9343802	-1.1624011	0.3016916	-0.6551460
12	-0.9841979	1.7731811	-1.0655335	0.2765503	-0.6005503
13	-0.908490	1.6367826	-0.9835694	0.2552772	-0.5543541
14	-0.8435983	1.5198700	-0.9133146	0.2370432	-0.5147574
15	-0.7873576	1.4185414	-0.8524226	0.2212388	-0.4804395
16	-0.7381485	1.3298860	-0.7991503	0.2074128	-0.4504128
17	-0.6947279	1.2516572	-0.7521412	0.1952120	-0.4239179
18	-0.6561321	1.1821215	-0.7103566	0.1843672	-0.4003670
19	-0.6215988	1.1199043	-0.6729691	0.1746635	-0.3792950
20	-0.5905206	1.0639170	-0.6393302	0.1659337	-0.3603319

This solution satisfies equation (3.14a) automatically. Restoring the variables in equations (3.32) and (3.33) into original dimensional ones

and substituting one of the equations into the definition equation of streamfunctions in (3.1a&b), we have:

$$\psi = \frac{2\pi \cdot n \cdot D_r}{R^8} \cdot z \cdot (-3.603R^6 r^2 + 5.32R^4 r^4 - 2.131R^2 r^6 + 0.415r^8) \qquad (3.34)$$

Streamlines Ψ = 0.25, 0.5, 0.75 are shown in Fig. 3.2. Some of the results under different *m* values are listed in Table 3.1.

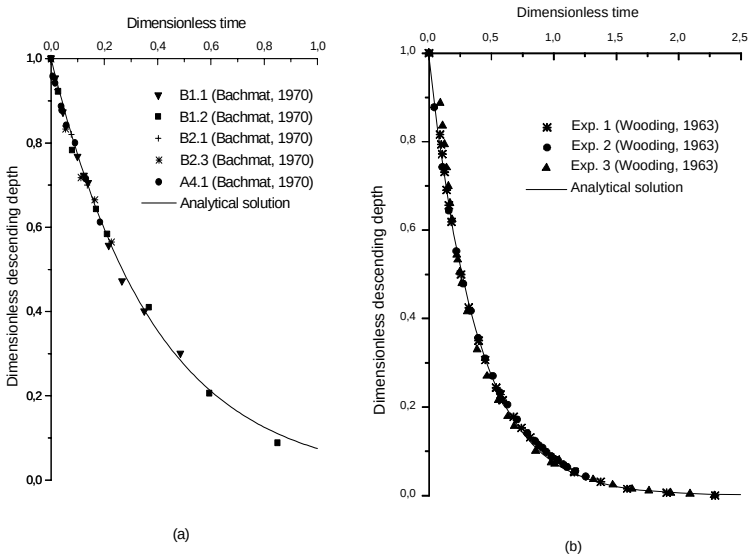

Fig. 3.3: **Analytical solutions compared with experiment results; (a) Experiment of BACHMAT et al. (1970); (b) Experiment of WOODING (1963).**

3.4 Result and discussion

3.4.1 Descending rate of similarity flow

Let's consider the descent of the dense solute along the centerline of the column. From equation (3.21) we have:

$$u = b_o z = \frac{dz}{d\tau} \quad \text{and} \quad \tau = 0, \quad z = 1 \tag{3.35}$$

This normal differential equation can be simply integrated.

$$z = e^{b_o \tau} \tag{3.36}$$

Theoretical and experimental results are shown in Fig. 3.3. It is clear to see that the theoretical results of equation $z = e^{b_o \tau}$ are in good agreement with the experiment data of WOODING (1963) and BACHMAT et al. (1970).

3.4.2 Descending depth of similarity flow

If we assume that the centerline concentration at the mouth of the column equals the solute concentration in the upper reservoir. Equation (3.8) may be written in another way:

$$\theta = -Ra_L \left(\frac{R}{L} \right)^2 \quad \text{at } z = 1, \quad r = 0 \tag{3.37}$$

where Ra_L is the RAYLEIGH number based on the height of the column:

$$Ra_L = \frac{k \cdot g \cdot \beta \cdot L \cdot (C - C_0)}{n \cdot D_z \cdot \mu} \tag{3.38}$$

Combining equation (3.37) with equation (3.20) and (3.7a) yields:

$$\frac{z}{L} = 0.0847 Ra_L \left(\frac{R}{L} \right)^2 \tag{3.39}$$

Here z is the physical length of the similarity regime. From equation (3.37) and equation (3.39) we see that the depth of similarity regime is proportional to the concentration difference driving the flow.

Equation (3.39) tells us also that the similarity regime will exist as long as $z \leq L$. Or we may express it in another way, as long as $Ra_L\left(\frac{R}{L}\right)^2 \leq 11.81$, the free convection has the pattern of similarity regime. Otherwise, the concentration and velocity fields depart from the similarity regime. It should be noted that the critical value 11.81 could only be regarded as approximate (BEJAN, 1980), because the terms with $\left(\frac{R}{L}\right)^2$ in equations (3.11) and (3.12) are omitted.

3.4.3 Rate of solute-transfer

With the beginning of free convection in the column in Fig. 3.2, solute is carried downward at a rate:

$$q = 2\pi\int_0^R C(r,z,t)\cdot r\cdot u(r,z,t)\cdot dr\ ,\ \ z = L\ . \tag{3.40}$$

Substituting equations (3.7a, b&c) and (3.8) into (3.40), the rate of solute-transfer can be expressed as:

$$q = 2\pi\int_0^1\left(C_o - \frac{n\cdot D_z\cdot\mu}{k\cdot g\cdot\beta\cdot L}\left(\frac{L}{R}\right)^2\theta\right)\cdot\frac{n\cdot D_z\cdot L}{R^2}u\cdot R^2\cdot r\cdot dr \tag{3.41}$$

at $z = 1$

$$q = 2\pi\cdot C_o\cdot n\cdot D_z\cdot L\int_0^1 urdr - \frac{2\pi\cdot n\cdot D_z\cdot L\cdot\left[C(r,z,t)-C_0\right]}{Ra_L\left(\frac{R}{L}\right)^2}\int_0^1\theta\cdot u\cdot r\cdot dr\ ,\qquad z = 1 \tag{3.42}$$

The mass conservation condition means:

$$\int_0^1 urdr = 0 \tag{3.43}$$

Equations (3.16), (3.20), (3.21) and (3.43) were substituted in equation (3.42) to yield:

$$q = 0.255n \cdot D_z \cdot L \cdot Ra_L \left(\frac{R}{L}\right)^2 \cdot \left[C(r,z,t) - C_0\right] \tag{3.44}$$

Let C_o be zero and $C(r, z, t)$ be simplified as C. Combining equation (3.44) with equation (3.38) yields:

$$q = 0.255 \cdot \frac{R^2 \cdot k \cdot g \cdot \beta}{\mu} C^2 \tag{3.45}$$

As a result the solute concentration in the upper reservoir drops continuously and the RAYLEIGH number decreases. The dropping rate will, however, be still less. Assuming that the solute concentration is the same everywhere inside the upper reservoir and it equals the centerline concentration at the upper end of the column, we have:

$$q = -\frac{dC}{dt} \cdot \pi \cdot R_1^2 \cdot H \tag{3.46}$$

where R_1 is the radius and H is the height of the dense solute in the upper reservoir. Combining equation (3.46) with (3.45) yields:

$$\frac{C_1}{C} - 1 = 0.255 \cdot \frac{R^2 \cdot k \cdot g \cdot \beta}{\pi \cdot R_1^2 \cdot H \cdot \mu} C_1 \cdot t \tag{3.47}$$

The result can be compared with the expression of BACHMAT et al. (1970):

$$\frac{C_1}{C} - 1 = A \cdot \frac{k \cdot g \cdot \beta}{\mu_o H} C_1 \cdot t \tag{3.48}$$

where A is a nondimensional relative variance of the macroscopic concentration distribution in the considered horizontal plane $z = L$. And equation (3.48) has been successfully proved by their experimental results.

3.5 Summary and discussion

Whenever a dense solute is introduced over a porous material saturated with a less dense static one, a vertical convection is induced. Solute is then transported downward through a coupling process of convection, hydrodynamic dispersion and molecular diffusion.

Through a proper simplification, an analytical similarity solution has been obtained. Based on the similarity solution, descending rate, descending depth and rate of solute transfer have been examined. The theory of similarity regime described in this paper has been found to give good approximation to experimental results from literature. However, since a half quantitative visual technique was used in both experiments, only the averaged leading edge was measured. And in both cases, hydrodynamic dispersion and changes in viscosity with changes in solute concentration were neglected. These might have hidden some shortcomings of the present theoretical simulation.

Some use has been made of this experimental configuration for the determination of diffusion coefficient (AL-NAAFA et al., 1994). After vertical convective movement stops completely, the system reaches a pseudo-steady state under an adverse density gradient. From that stage on, the only mechanisms that result in solute transport is molecular diffusion. The diffusion coefficient is related to the vertical gradient of solute concentrations, which can be measured directly. Moreover, this experimental method might help us in better understanding the hydrodynamic instability itself and its interaction with hydrodynamic dispersion. It is recommended that variations of both fluid density and viscosity with changes in solute concentration should be considered in future experimental studies.

4 EXPERIMENT IN SAND COLUMN

In order to investigate density and viscosity effect on dispersion coefficient, a series of different experimental investigations were designed and carried out (from concept to realization). The main purpose was to monitor concentration distribution under controlled flow conditions in artificial physical models (sand column, 1-D; sand tank, 2-D and 3-D).

Medium quartz sand was used to fill in a Plexiglas column. Because of its non-conductivity, the medium quartz sand is a suitable porous medium for carrying out the present miscible displacement experiment, where a self designed and developed electrical measurement technique was applied to determine solute concentrations. The hydraulic boundary condition was therefore set to be as simply as possible, in order to focus on the investigation of hydrodynamic instability and its effect on solute transport. NaCl, glycerine solution and Karlsruhe tap water were used.

4.1 Introduction

The theoretical analyses in chapter 3 have shown that if a dense solution is brought into contact with an underlying vertical porous column, which is initially saturated with a static less dense miscible solution and sealed at the bottom, the density difference may cause a convective motion of the dense solution. Under some specific simplifications an analytical solution has been derived. In that analysis, the dispersion coefficient is assumed to be approximated by a constant. Essentially, however, besides the dependence on local variations of the velocity field and on porous medium characteristics, it generally depends on the concentration and the type of dissolved compounds as well (OGATA, 1970). Therefore, investigating the macroscopic dispersion coefficient can help one to understand the microscopic structure of a porous medium, the interaction between the solid matrix and fluid and the effects of fluid property on solute transportation process through the porous medium.

Dispersion coefficients for porous media are usually measured in laboratory displacement experiments, where a tracer is injected into a

tubular column filled with unconsolidated sand or glass beads. Measurement of tracer concentrations is generally made at the column outlet by means of an electric probe or through chemical methods. Measurements within sand columns using either electrical or chemical methods have been also reported.

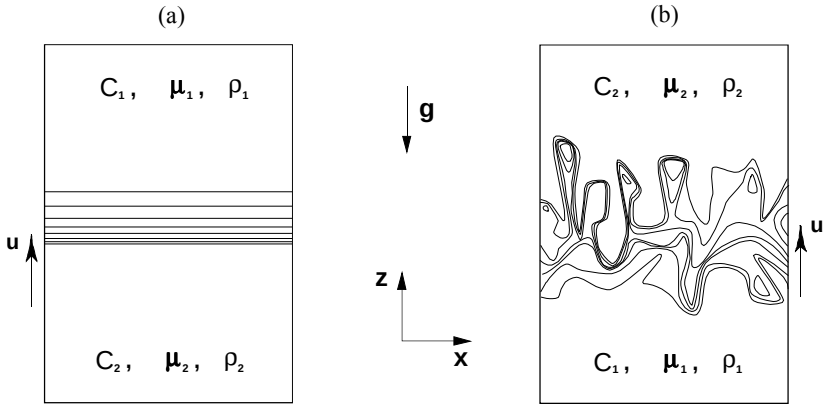

Fig. 4.1: **Scheme of concentration contours for miscible displacements with density and viscosity differences ($\mu_2 > \mu_1$; $\rho_2 > \rho_1$) in a homogeneous isotropic medium (a) Stable displacement; (b) Unstable displacement.**

The subject of miscible displacement in porous media has drawn much attention from a variety of research areas and from engineering practice. Some of the mixing processes are characterized by significant density and viscosity differences, and depending on the density and viscosity differences and displacing direction, the system may be either stable (Fig. 4.1 a) or unstable (Fig. 4.1 b). In accordance with its underlying process, the unstable displacement can be further classified into two types of instabilities, namely: RAYLEIGH-BENARD instability induced by density variations in the gravity field (gravitational instability) and SAFFMAN-TAYLOR instability induced by viscosity differences (viscous instability) (QUINTARD et al., 1987).

Neglecting the viscosity dependence on concentration, tremendous work has been done on gravitational instability, notable among which are WOODING (1963), KRUPP and ELRICK (1969), BACHMAT et al. (1970),

ROSE et al. (1971), SCHINCARIOL and SCHWARTZ (1990), DANE et al. (1991), HAYWORTH et al. (1991), KOCH et al. (1992), OOSTROM et al. (1992a&b), ISTOK and HUMPHREY (1995), and OPHORI (1998). Some researchers, however, concentrate their attention upon viscous instability, e.g., SAFFMAN et al. (1958), HICKERNELL et al. (1986), TAN et al. (1986, 1988), YORTSOS (1987), BACRI et al. (1987, 1991), ZIMMERMAN et al. (1991) and MANICKAM et al. (1993). Both kinds of instability have been included in the study of, Heller (1965), SCHOWALTER (1965), WOODING (1969), CHANG et al. (1986, 1988a, 1988b, 1989), ASIF et al. (1990), CHRISTIE et al. (1990), BUES et al. (1991), MANICKAM et al. (1994, 1995), ROGERSON (1993a, b), SIMMONS and NARAYAN (1997). These works have demonstrated that the formulation and development of the hydrodynamic instability can exert great influence on the flow patterns, causing a quite different spreading and distribution of the denser flow components (Fig. 4.1 b). Not only are the density and viscosity effects very important and of great interest for unstable miscible displacements but they are also non-trivial for stable miscible displacements (BOUHROUM, 1985; MOSER, 1995).

Using a small sand pack model, BOUHROUM (1985) investigated density and viscosity effects on hydrodynamic dispersion through a series of stable miscible displacement experiments at small Pe number. In a small glass cylinder with the length of 22 cm and internal diameter of 6 cm, GUILLOT et al. (1991) studied the density effects on dispersion qualitatively by using NMR (Nuclear Magnetic Resonance) imaging technology. The density effects associated with very small density differences were reported by LEROY et al. (1992). MOSER (1995) performed stable miscible displacement experiments in a big vertical porous column using fluids with density differences and demonstrated a strong density effect on dispersion coefficients. The effect of viscous instability on dispersion was recently studied by BACRI et al. (1992) in their first 3D experiment. Similar to the experiment of BACRI et al. (1992), TCHELEPI et al. (1993) simulated how dispersion and viscous instability interact as the viscosity ratio M varies in miscible displacements. In spite of these related studies, density and viscosity effects on hydrodynamic dispersion have not been adequately considered up to date. Experimental investigation on these effects with a variety of density and viscosity differences for both stable and unstable displacements is of practical importance for environmental problems as well as of interest from a more classical fluid - dynamical point of view.

Objective, scope and procedure

Stable and unstable miscible displacement experiments were performed in a large homogeneous and isotropic vertical sand column in order to investigate the dependence of the dispersion coefficient on density and viscosity differences (at relatively large PECLET number, $Pe = u.d_p/D$, where u is the mean intrinsic velocity, d_p is the mean particle diameter, D is the dispersion coefficient). Essential points thereby are to monitor the development of the displacing front in time and space under different controlled laboratory conditions. Section 4.3 gives a detailed description of the experimental apparatus and materials applied. Using the conventional convection-dispersion theory and the measured data the dispersion coefficient is evaluated in section 4.4. Results for a variety of stable miscible displacement are compared with the results from literature.

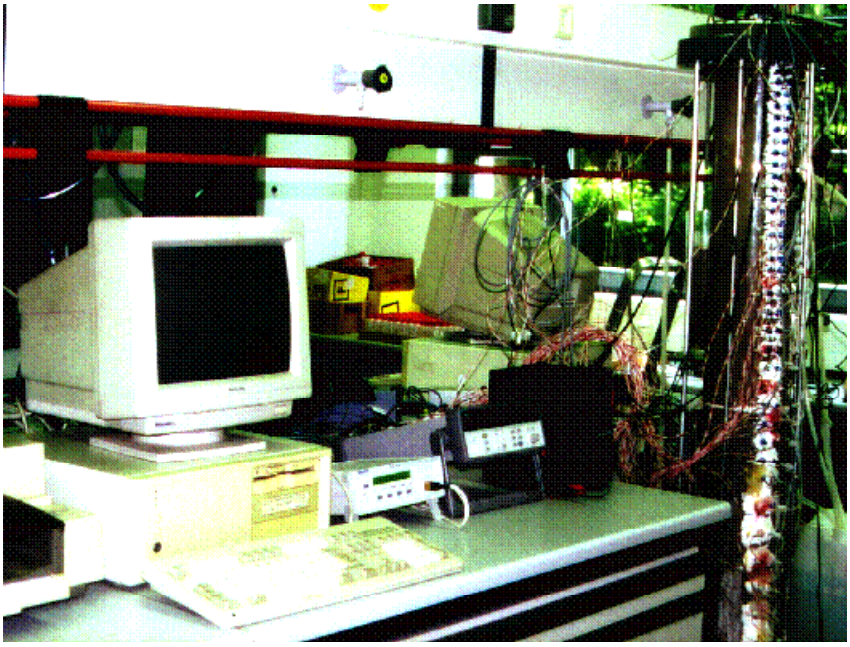

Fig. 4.2: **Photo of the experimental set-up.**

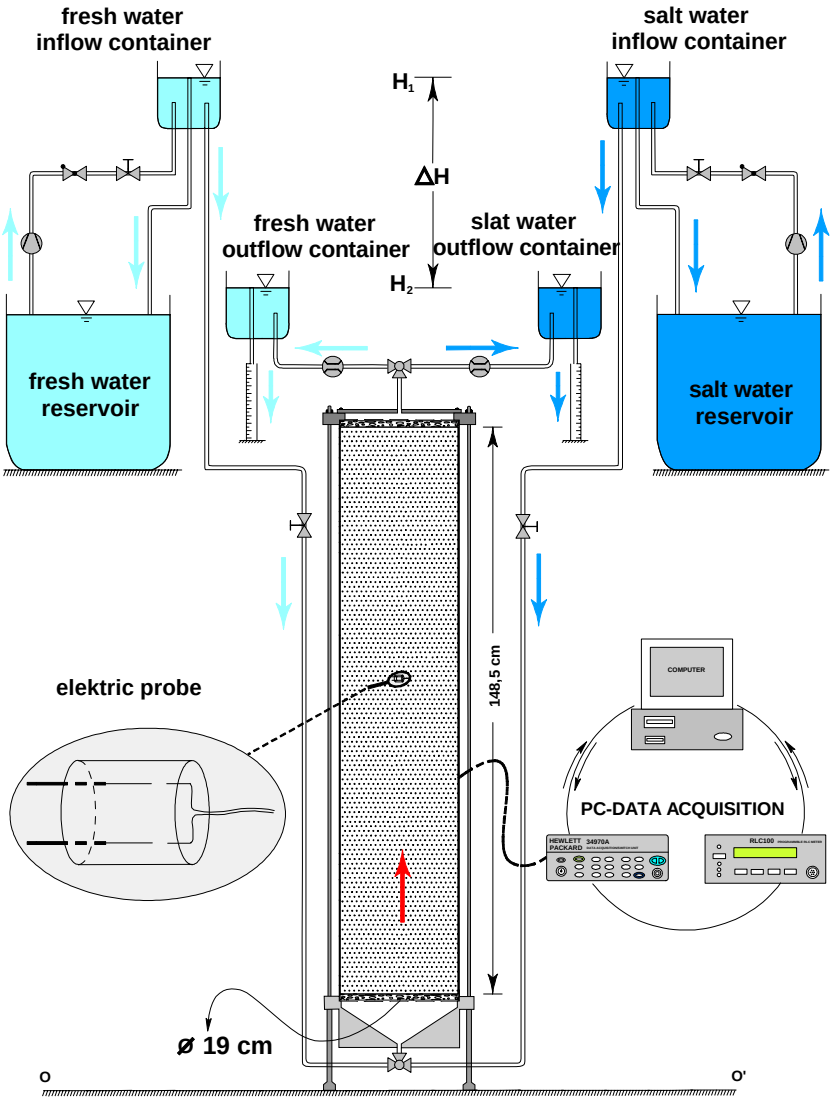

Fig. 4.3: **Scheme of the experimental set-up.**

4.2 Apparatus and procedure

In a large tubular Plexiglas column, riddled commercial spherical quartz sand was packed. Special attention was given to achieve a homogeneous and isotropic porous medium. A non-intrusive in-place electrical measurement technique is briefly introduced here; an extensive description of the method is in the next chapter. Through a series of sediment and hydraulic tests, the packed porous medium was characterized. Thereby the whole experimental system was coordinated and relevant necessary adjustment was made.

4.2.1 Tubular Plexiglas column

In order to minimize system error, the experiments were conducted in a vertical Plexiglas tubular column with the length of 1550 mm and internal diameter of 190 mm. The column was supported and fixed by a steel framework. The framework had four leveling feet in order to level the base of the column. Figure 4.2 and Figure 4.3 show the general appearance of the column and accessories. The column consisted of three parts: a lower conical reservoir, the sand column with a net length of 1485 mm, and an upper cylindrical reservoir. Perforated plastic plates combined with textile cloth separated the reservoirs from the column interior, prevented fine grain of the packed sand from washout and guaranteed sufficient filtration stability. The lower reservoir provided a homogeneous flow condition and a uniform abrupt front over the column's cross section when a displacing fluid was introduced from below into the sand column. As electrical methods were to be used, except electric probes, only non-conductive materials were applied.

The column was closed except one inlet/outlet hole at the top and bottom each. Through a 3-way valve each of the holes was connected to two separate flow circuits: fresh-water and salt-water. Each circuit consisted of a main reservoir, a pump, a constant-head inflow reservoir and a constant-head outflow reservoir. A unidirectional or fluctuating displacing flow could be produced at any desired rate both upward and downward by means of adjusting the level of the constant-head reservoirs.

4.2.2 Porous medium, sand packing

The column was packed with riddled commercial quartz sands (Heinz Weisenburger Corporation, Karlsruhe, Germany) in diameters from 0.4 to 0.6 mm, which are non-conductive and non-adsorptive. To characterize the packed sands, a test of corn grain size analysis and a test of sediment density and porosity were carried out. The sand consisted of spherical grains having a uniformity index ($U = d_{60} / d_{10}$) of 1.1 and an effective grain size (mean particle diameter) of 0.5 mm. The intrinsic permeability and porosity of the packed porous medium in the column was determined to be 1.57×10^{-10} m^2 and 0.35 respectively. To avoid possible hydraulic disturbances, displacing fluids were introduced from the bottom of the column and flow was directed upward throughout the experiments.

To achieve a homogeneous and isotropic sand pack, special packing technique was used, where the sands were filled into the column by means of a PVC pipe while the column was vibrating. After having placed the sands in a satisfactory manner; the porous medium was consolidated using three wetting/drainage cycles. As the uniformity index of the sands is 1.1, the volume of the sand pack did not change practically through the three cycles of consolidation. Subsequently the air in the column was evacuated by a vacuum pump. Thereafter, the column was filled with distilled water and kept saturated.

4.2.3 Measurement of concentration

The electrodes used were made of two insulated platinum wires 0.5 mm in diameter. The two wires were fixed parallel to each other at a distance of 3 mm apart (for more detail, see in Chapter 5). Twenty-seven such electrodes were inserted into the centre of the sand column, accompanying the sand packing. Intervals were 2.5 cm in the upper part of the column, increasing through 4 cm in the central part to 6.0 cm near the lower end of the column.

Through a HP 34970A Data Acquisition/Switch system all the electrodes were connected to a RLC-100 meter. A computer controlled both of the instruments. Fluids used in the displacing tests were salt solutions at a concentration from 0.0 to 190 g/L and a few glycerine solutions. The dependence of density and viscosity upon concentrations of NaCl and glycerine solutions is shown in Fig. 2.1 and

Fig. 2.2 respectively. Calibration curves relating conductivity to volumetric concentration were used to convert conductivity measurements to local concentration measurements. The relationship between the conductivity and concentration of NaCl solutions at 20^{o}C is shown in Fig. 2.3. It can be seen that except a small top and bottom segment the solid simulated curve is in good agreement with the measured values. Owing to the shape and scale of the electrodes, 27 locations were sampled in less than 1 minute without any obvious disturbance of the flow field. Thus, the concentration distribution along the central line of the column can be determined at any instant by simultaneous readings. The concentrations reported are estimated to be accurate to within 2%. The resulting concentration breakthrough curves provide detail information on the concentration distribution in the transition zone.

Tab. 4.1: **Summary of the experimental conditions.**

Parameter	Dimension	Value
Range of grain size	[mm]	0.4~0.6
Effective grain size	[mm]	0.5
Uniformity index	[-]	1.1
Volume of packed sand	[l]	42.1
One pore volume	[l]	14.7
Porosity	[-]	0.35
Sediment density	[g/cm^3]	2.638
Permeability	[m^2]	1.57×10^{-10}

4.2.4 Procedure

In order to further characterize the hydraulic nature of the packed porous medium and thereby test and adjust the whole flow and measurement system, DARCY tests and tracer tests were carried out at first. Results of the hydraulic test and the above sediment tests are compiled in Table 4.1. Displacement experiments under stable and unstable conditions were performed for a wide range of density and viscosity differences and displacing rate. In stable displacements, a dense solute displaced a less dense one, and in the unstable displacement, the reverse was true. After the concentration in outflow had reached the level of the displacing solution, the experiment continued and changed into a classical DARCY test. To avoid possible

hydraulic disturbances, upward displacements are taken throughout the study.

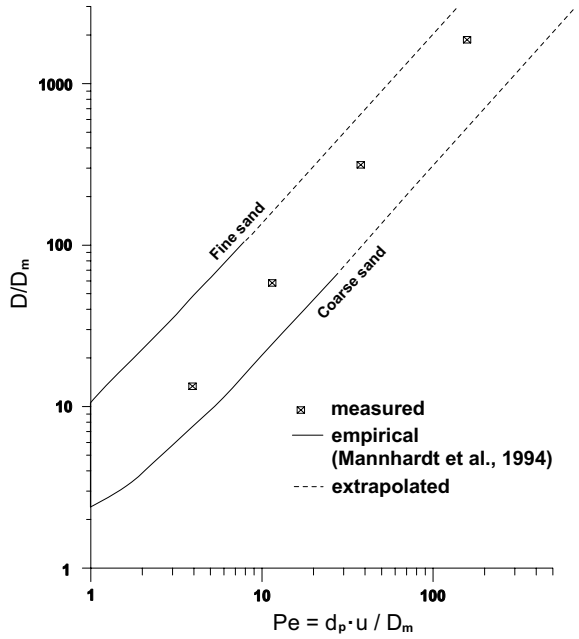

Fig. 4.4: **Range of dispersion coefficients based on tracer test for various sand packs: fine sand 200-270 mesh, medium sand 40-200 mesh.**

4.3 Result and evaluation

4.3.1 Tracer test

In order to characterise the packed porous medium and calibrate the whole measurement system, very dilute NaCl solution was brought from the bottom of the column to displace pure water with different displacing velocities. Conductivity was measured both within the porous medium and at effluent. Concentration was then calculated through the relationship shown in Fig. 2.3. Dispersion coefficient was determined by performing the least-squares fit introduced in section 2.7.

Results of the tracer tests are presented in the form of normalized dispersion coefficient D/D_m versus molecular PECLET number Pe diagrams on a log-log scale (see Fig. 4.4), where D is the observed dispersion coefficient, D_m the molecular diffusion coefficient, Pe the PECLET number, u the flow velocity and d_p the average diameter of the packed sand. In the figure the solid curves are empirical curves given first by BLACKWELL (1962) and latter cited by MANNHARDT et al. (1994). The dashed line is an extrapolation of the empirical curves. It is shown that all the measured dispersion coefficients in the form of D/D_m fall within the range of the empirical and extrapolated curves. The dispersion coefficient increases linearly in the limit of the experiment PECLET number.

Having discussed miscible displacements of passive solutes, we turn our attention to the non-passive case, where density and viscosity of the miscible fluids is a function of the solute concentration. The density effects in stable and unstable miscible displacements and the viscosity effects in both kinds of displacements are to be investigated in section 4.3.2, 4.3.3 and 4.3.4 respectively.

4.3.2 Density effect in stable miscible displacement

During the experiments attention was drawn on the dependency of dispersion coefficients on the density of the miscible fluids and the density differences between them. Three different density combinations (viscosity ratio was kept at about 1) are used in this study. For the first group of experiment the porous column was at first saturated with less dense fluid and then displaced by much denser solution. The density differences varied slightly from experiment to experiment (Fig. 4.5). At the beginning of the second group of experiment dense solution was introduced to the column and a denser one was then used to displace it. While the density of the displaced fluid was large, the density difference was small (Fig. 4.6a). During the third group of experiment both the density of the displaced solution and the density difference were large (Fig. 4.6b).

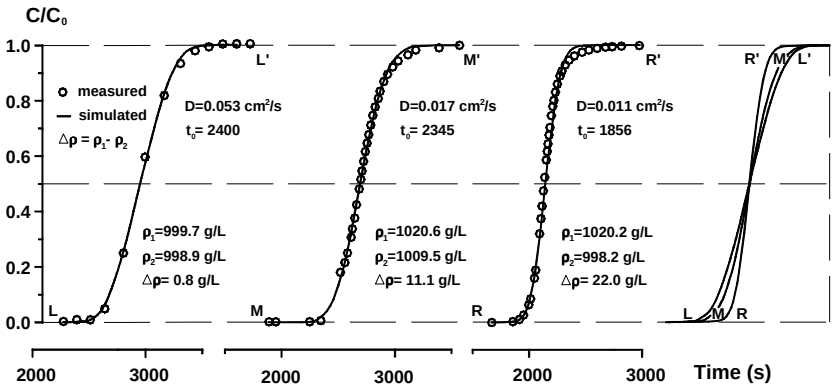

Fig. 4.5: **Breakthrough curves of vertically upward stable displacements with small density of the displaced fluid and a large variation of density differences.**

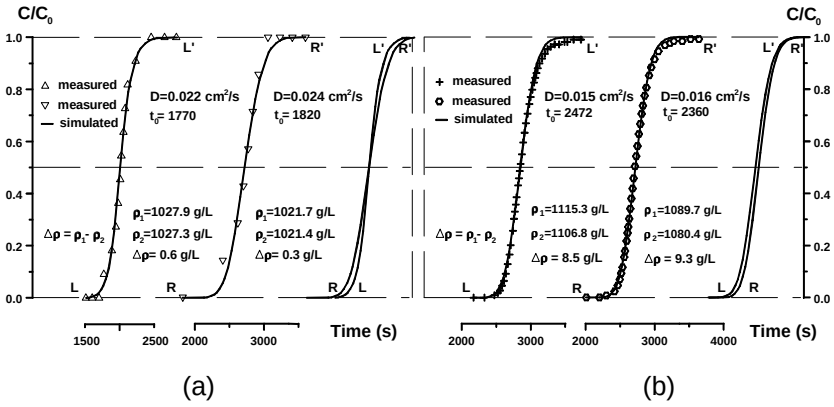

Fig. 4.6: **Breakthrough curves of vertically upward stable displacements with large density of the displaced fluid and variation of density differences: (a) large density of the displaced fluid and small density difference; (b) large density of the displaced fluid and large density difference.**

Concentration breakthrough curves together with the input parameters and the analytical solutions are shown in Fig. 4.5 and Fig. 4.6. The

concentration breakthrough curves in these two figures become steeper when density differences increase from experiment to experiment. As a result, the dispersion coefficient reduces steadily (see Fig. 4.7). Both the density of the displaced fluid (ρ_2) and the density difference ($\Delta\rho$) are small in Fig. 4.6 (a), while they are high in Fig. 4.6 (b). The same magnitude of density difference in Fig. 4.6 (a) or Fig. 4.6 (b) result in the same magnitude of dispersion coefficient, though the density of the displaced fluid (ρ_2) varies from case to case. It could be concluded that dispersion coefficient is not sensitive to the density of the displaced fluid but to the density differences. It is also remarkable that all the measured breakthrough curves in Fig. 4.5 and 4.6 are almost the same as analytical solutions. The result shows that miscible displacement of fluids with significant density differences can be satisfactorily described by the classical advection-dispersion equation. The initial breakthrough times (t_0) are related to density differences: The larger the density difference, the shorter the initial breakthrough time (Fig. 4.5 and Fig. 4.6).

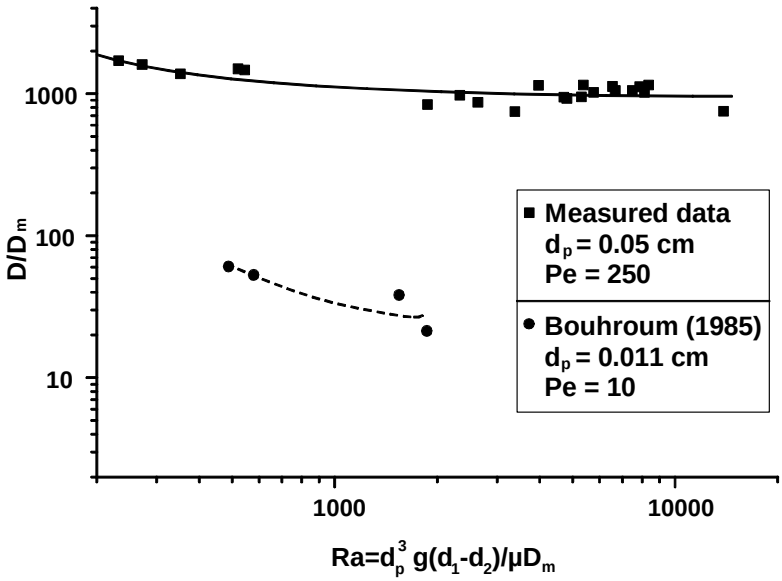

Fig. 4.7: **Dependency of dispersion coefficient on the RAYLEIGH (Ra) number for stable displacement.**

4.3.3 Density effect in unstable miscible displacement

Not only stable displacements, but also unstable displacements were carried out. Their results are in Fig. 4.8 and Fig. 4.9. Concentration breakthrough curves, analytical solutions, densities of the displaced fluid and density differences, and measured dispersion coefficients are presented in Fig. 4.8, while Fig. 4.9 describes the dependency of measured dispersivities on density differences relative to Ra.

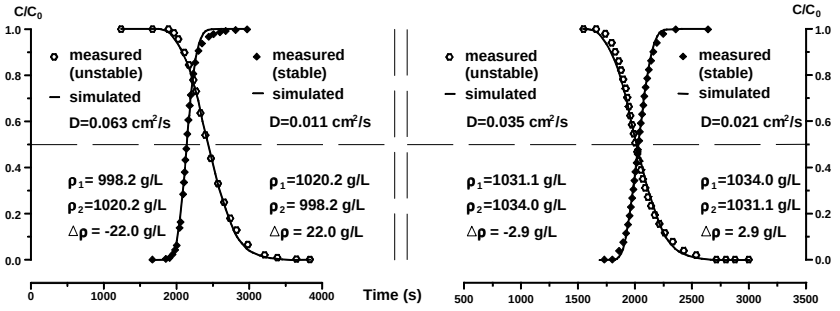

(a) (b)

Fig. 4.8: **Comparison between different stable and unstable miscible displacement: (a) large density difference; (b) small density difference.**

Similar to stable displacements, measured concentration breakthrough curves of unstable displacements can be also satisfactorily simulated by the classical advection-dispersion formulation. Due to the occurrence of natural convection at the displacing front, the concentration breakthrough curves of unstable displacements is not symmetric and there exists a tailing effect (see Fig. 4.8), where it took longer for the solute concentration at certain cross section to reach the concentration of the displacing fluid. Except for one experiment with two miscible fluids of 41.9 and 42.7 g/L, where small density difference and large initial density made it difficult to differentiate the displacing and displaced fluids, this tailing effect was observed in all experiments. As a result, the displacing process is prolonged. The dispersion is, however, increased (see Fig. 4.9). Upon examining Fig. 4.8 and Fig. 4.9, we see that both the measured dispersion coefficient and dispersivity increase with the increase of the density differences for

unstable displacements, whereas the contrary is true for stable displacements. Limited by the measurement technique, effect of very small density differences on dispersion in both stable and unstable displacements (- 400 < Ra < 270) could not be quantitatively investigated.

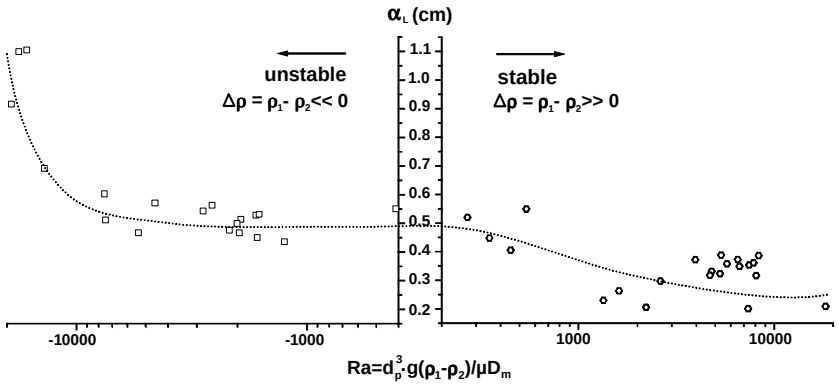

Fig. 4.9: **Dependency of the dispersivity on RAYLEIGH (Ra) number for both stable and unstable displacement.**

4.3.4 Viscosity effect

Having discussed miscible fluid displacement with density differences, let us see what happens in the case of unequal viscosities. If the viscosity of the displacing fluid is greater, the displacement will differ only very little from the equal viscosity case. It is a stable displacement. However, if the displacement is carried out reversely, the interface between the two fluids may be unstable and the resulting instabilities develop into “viscous fingering” or “channeling”. Examples of viscous fingering can be seen in Fig. 2.10 a), d) & e) and Fig. 4.1 (b). Such an instability may alter completely the displacement process.

Results from the last section indicate that it is the density differences, not the absolute density of the displacing fluid that affects dispersion coefficient. This and the fact that, generally, both the density and viscosity of salt and glycerine solution increase with their concentration (cf. Fig.2.1 and Fig. 2.2) make it possible to examine viscosity effect

alone by using different combinations of salt and glycerine solution, which have the same absolute density but significant viscosity differences.

Tab. 4.2: **Summary of the experiment data for miscible displacement with viscosity differences.**

Experiment	$\Delta\rho$ (g/L)	M (-)	u(cm/s)	D_L (cm^2/s)
1	-0.45	0.24	0.0732	0.043
2	-0.2	0.61	0.0700	0.046
3	-0.5	0.79	0.0690	0.047
4	-0.2	1.0	0.0625	0.053
5	-1.0	1.22	0.0684	0.058
6	-0.4	1.64	0.0614	0.0742

Similar to those tests for density differences, both stable (Experiment 1, 2, 3 & 4) and unstable displacement (Experiment 5 & 6) under viscosity differences were performed. Applied fluid pairs and their properties are compiled in Tab. 4.2. To avoid possible effect of gravitational instability, the injected displacing fluid had always slightly higher density than that of the displaced one, which means that the density difference had always stabilising effect here.

Using the simulation methods discussed in section 2.7, dispersion coefficients were calculated and summarized and drawn in Tab. 4.2 and Fig. 4.10 respectively, where cited data from literature are also indicated.

Fig. 4.10 shows the normalized longitudinal dispersion coefficient for a variety of viscosity ratios M obtained from the simulation of measured concentration breakthrough curves. The strong increase of dispersion coefficients in the unstable case for the limestone in Fig. 4.10 is, besides the viscosity effect, attributed to the effect of heterogeneity (BACRI et al., 1992). It could be seen that the dispersion coefficient increases with viscosity differences and in the unstable case the rate of increase is much greater than in the stable case.

Generally, the increase rate due to viscosity ratios (M) is quite smaller than that due to density differences when a solute concentration increases (see Fig. 2.1 and Fig. 2.2). Examining Fig. 4.7, Fig. 4.9 and

Fig. 4.10 together, we see that effects on dispersion caused by viscosity variations are smaller than those by density differences.

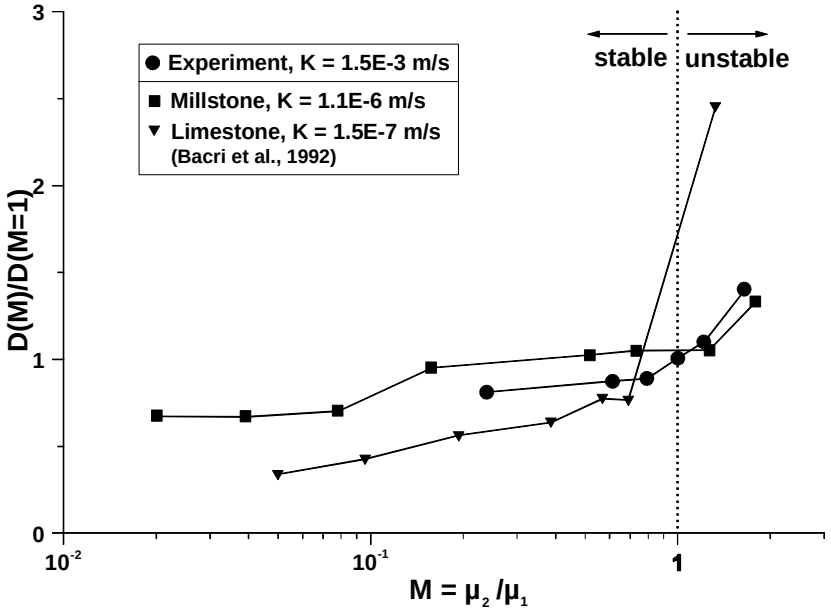

Fig. 4.10: **Viscosity effect on dispersion coefficient in miscible displacement.**

4.4 Conclusion and recommendation

Due to the large density differences in seawater intrusion and depending on geometric conditions, both stable and unstable displacements may occur at the displacing front. Similar processes could also appear in connection with the injection of freshwater or less dense wastewater into saline groundwater aquifers. Therefore, the result of this study should be considered to evaluate the stability of the interface and the spreading of saltwater front.

Based upon this 1-D experimental study of both stable and unstable miscible displacements in a large, homogeneous, isotropic vertical

porous media with fluid pairs having a large variety of density and viscosity differences, the following conclusions can be drawn:

a) The classical advection-dispersion formulation is valid in describing both stable and unstable displacements with dense solute and large density differences (Fig. 4.4, Fig. 4.5 and Fig. 4.6). For a given porous medium and flow condition, the dispersion coefficient is, however, not a constant.

b) Dependency of dispersion coefficient on density and viscosity differences is given in Fig. 4.7, Fig. 4.9 and Fig. 4.10 respectively. In the stable case, dispersion coefficient drops continually when density variations increase, whereas the dispersion coefficient increases with viscosity ratios steadily.

c) In the case of unstable displacements dispersion is enhanced by the increase of both the density and viscosity differences. As only homogeneous sand packing was applied in the present investigation, the density and viscosity effects could be strongly modified by heterogeneity and anisotropy.

Following the 1-D experiments of miscible displacements in the vertical column, 3-D experiments at still larger scale with four fluid combinations were performed, where the principal flow direction is perpendicular to the gravity force. They will be discussed in detail in the next chapter.

5 EXPERIMENT IN SAND TANK

5.1 Introduction

Miscible displacements of fluids with significant density and viscosity differences and their effect on dispersion coefficient have been investigated in a large sand column. However, the effect of a three dimensional flow situation and in still larger scale await further examination. Similar to the one-dimensional experiment in the sand column, essential points are to monitor the development of the displacing front in time and space under different controlled laboratory conditions in the following experimental investigation in a large scale sand tank.

Section 5.2 give a detail description of the experimental apparatus and materials applied. Through a series of sediment and hydraulic tests, the packed porous medium was characterised in section 5.3. To examine properties of the packed porous medium further and provide a base for the following miscible displacements with significant density or viscosity differences, a tracer test was carried out in section 5.4. A detailed description of the miscible displacements with significant density differences or viscosity contrast or both is given in section 5.5 and 5.6 respectively. Experimental data is analysed and evaluated in section 5.7, where a short discussion is given in the end.

5.2 Apparatus and materials

5.2.1 Plexiglas tank

For the planned experiment a physical model with internal dimensions of 600 cm (length) $\times$ 200 cm (width) $\times$ 150 cm (depth) is available. The tank is constructed of Plexiglas and is supported by a steel and concrete framework (Fig. 5.1). A cross section of the tank and schematic of the flow system is given in Fig. 5.2.

To guarantee a homogeneous flow, two coarse filters consisting of customary gravel (16~32 mm) with dimensions of 30 cm (length, thickness) $\times$ 200 cm (width) $\times$ 150 cm (depth) are installed at each end

of the tank. Two other more fine filter composing of smaller graded customary gravel WQ2 and WQ4 with dimensions of 10 cm (length, thickness) $\times$ 200 cm (width) $\times$ 150 cm (depth) serve as separation layer between the coarse filters and the tank interior. Parallel to the sand packing, both kinds of filters are set into their due position. This arrangement prevents fine sand particles from being washout and in the same time guarantees sufficient filtration stability as well.

Fig. 5.1: **Photo of the Plexiglas tank (by courtesy of SCHNELL 2001).**

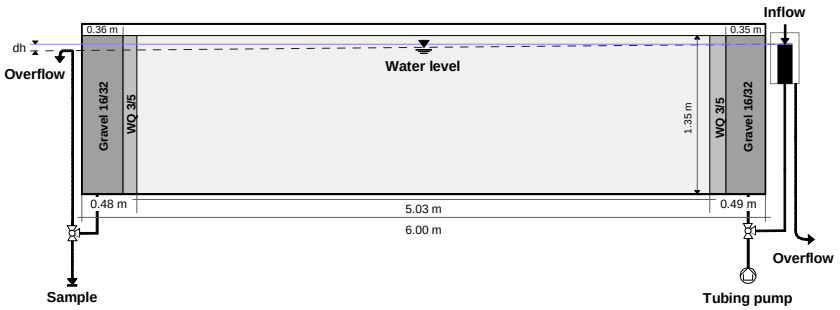

Fig. 5.2: **Cross section of the tank and scheme of the flow system.**

Three holes were drilled and tapped at each end of the base of the tank, which are connected to water supply or outlet through valved ports (Fig. 5.2).

5.2.2 Porous medium, sand packing

In order to give prominence to the complex horizontal displacement process and the interaction between dispersion and hydrodynamic instability, a homogeneous porous medium is used to simplify ambient hydraulic conditions. The huge Plexiglas tank was packed with 25 tons of riddled granular quartz sand in diameter of 0.3 mm to 0.8 mm from Weisenburg Corporation (Karlsruhe, Germany). Mean particle diameter and uniformity index was analyzed to be 0.64 mm and 2.2 respectively (see in section 5.2.3).

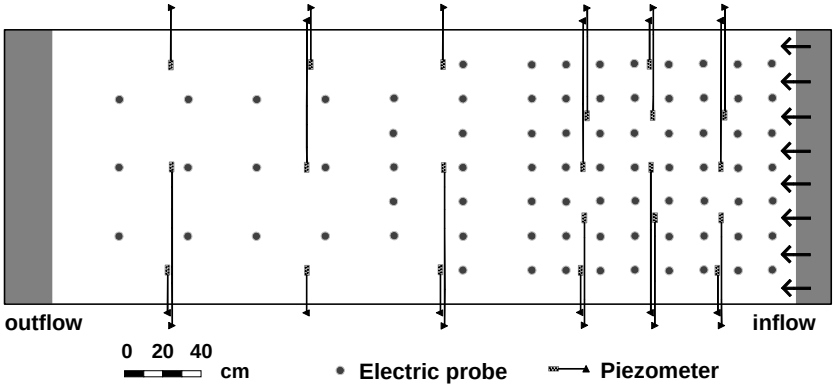

Fig. 5.3: P**lan position of electric probes and piezometers.**

The sand packing was performed in a wet situation in layers of 10 cm each (Fig. 5.6 a). After filling a layer, the layer was evenly impacted for three times with a 10-kg-square-steel-plate. Then 4 sand samples were taken using a soil sampling tube. The sediment density was determined to be 1.55 g/cm^3 and it is evenly distributed. Before the next layer of sand was dumped into the tank, the impacted sand surface was roughed through a rake. When the sand packing reached a prescribed level for the instalment of piezometers and electrical probes, further 10 cm layer of sand was dumped into the tank.

For the sake of extracting water samples, five layers of piezometers were installed, whose positions are shown in Fig. 5.3. Each layer consists of 24 pieces. They are made of PE-tubes of 6 mm in diameter and 2 mm of wall thickness. An end of the tubes was perforated up to 2 cm long all around and clothed with fine textiles to prohibit fine sand particles from entering the tubes. They were set into position horizontally and fixed to an internal broadside of the tank through a plastic connecting tube, which joins another vertical plastic tube on the outside of the tank (see Fig. 5.1). Beside the function of monitoring water head and taking tracer samples, the piezometers can be applied to check concentration distribution in emergency cases. Note that generally no water sample should be taken during a miscible displacement experiment. All the piezometers worked perfectly.

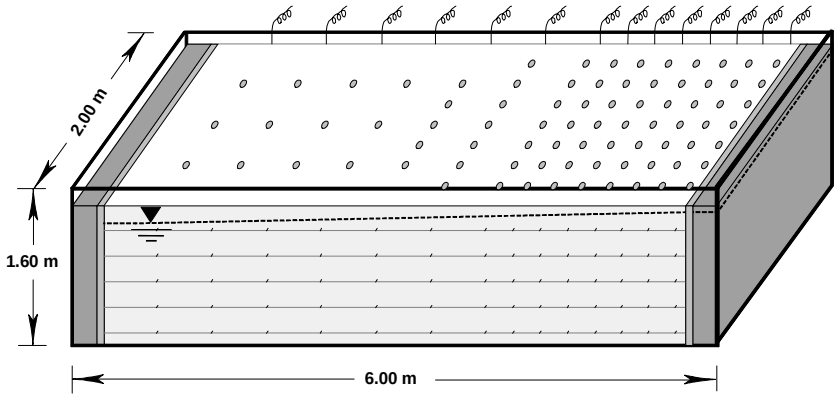

Fig. 5.4: **Side view of the tank and position of the electric probes.**

To monitor concentration distribution within the porous medium, five layers of totally 400 electrical probes were installed, which were displayed parallel to and within the same layer of the piezometers (see Fif. 5.3, Fig. 5.4 and Fig. 5.6 b). Structure and dimensions of the electric probes are sketched in Fig. 5.5. The electrical probe is constructed of two parallel short fine platinum wires, which are, in turn, connected to two customary thin insulated wires. The connection (splice) is fixed and insulated in a thin epoxy-glass tube. Similar to the instalment of piezometers, electrical probes were positioned horizontally. After they had reached a broadside of the tank, they were

turned vertically and moved out of the tank along the internal broadside.

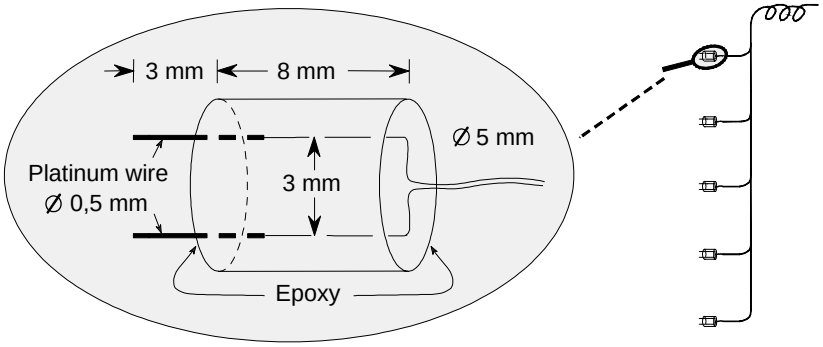

Fig. 5.5: **Structure and dimensions of the electric probes.**

The packed porous medium was consolidated through 4 saturation/drainage cycles for up to three months.

Fig. 5.6: **Photos: (a) Sand filling; (b) Installing electric probes and piezometers; (c) Measurement and control system.**

5.2.3 Measurement apparatus and other accessory

Salt concentration has been proven to be measured very easily and is therefore used in the present experimental study. Because of its electrolytic characteristic, in-situ measurement of the salt concentration can be obtained by means of an electric probe. The requirement is that measurements be taken at some distance from the solute source, at a location in a manner, which does not disturb the flow. For the sake of creating significant viscosity differences, tap-water and glycerine solution were also used to displace or to be displaced by the salt solution.

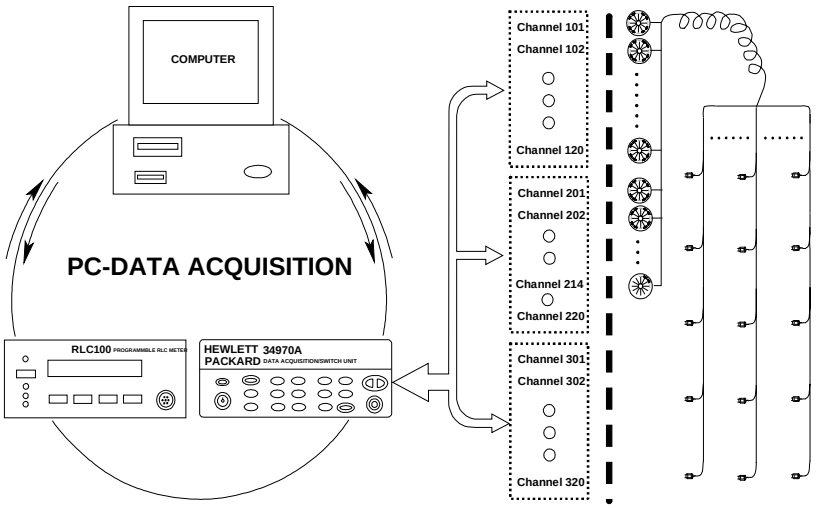

Fig. 5.7: **Control and measurement system.**

An electrical technique was used to measure the space and time dependence of concentration during stable and unstable miscible displacements. Using the electric monitoring technique, electrical resistance at the 400 measurement positions was measured directly. Thanks to the control unit (computer and HP 34970A in Fig. 5.6 c) of the system, measurement can be carried out automatically at any given time interval. Solute concentration at a particular position was determined from calibration curves, which relate variations in electric

resistance to solute concentration. The concentrations reported are estimated to be accurate to within 2% with a spatial resolution of 3 mm. The resulting breakthrough curves at the 400 electric probes provide detail information on the concentration distribution in the development of the displacing front.

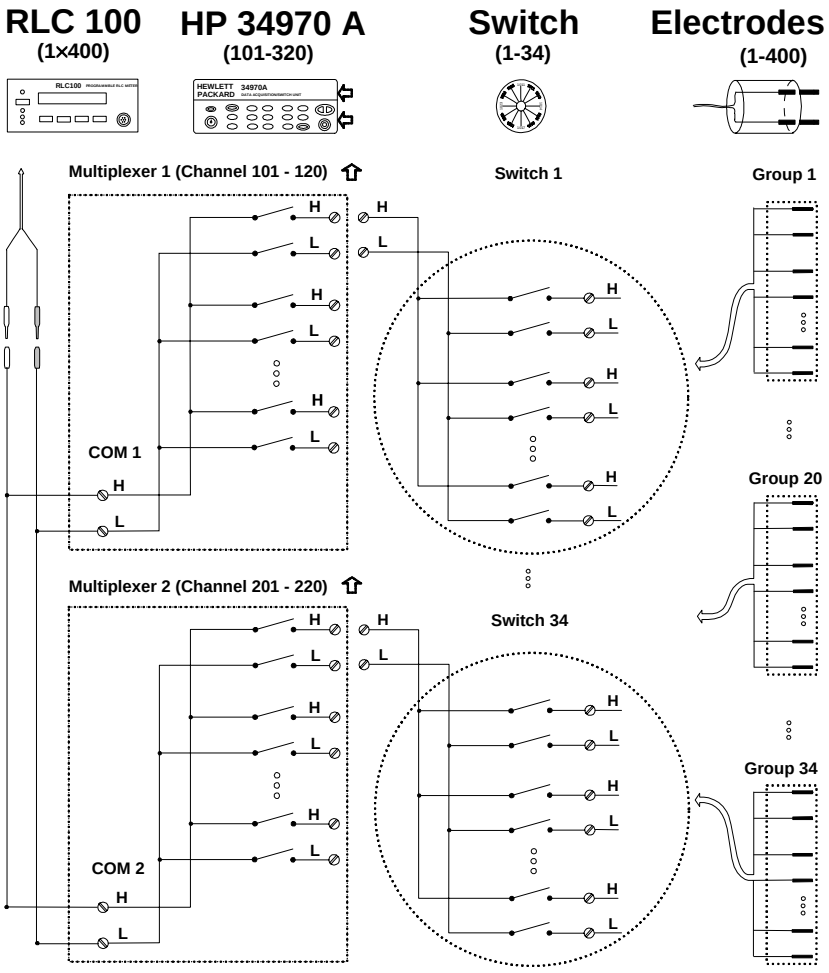

Fig. 5.8: **Diagrammatic plan of the electrical connection between measurement and control units.**

Fig. 5.7 and Fig. 5.8 give a schematic description of the principal measurement apparatus, which is also shown in Fig. 5.6 c. Section 5.2.2 has described the instalment of the 400 electrical probes within the tank. Outside the tank, wires of the probes are coded, combined in bundles and connected to 35 switches (with 12 channels each) mounted on a switchboard (Fig. 5.6 and Fig. 5.7). The switchboard is, in turn, connected to a HP 34970A data acquisition and switch system (Hewlett-Packard Company), which, similar to the central measurement instrument RLC 100 Meter (GRUNDIG Professional Electronics Corporation, Fürth, Germany), is controlled by a computer. The arrangement makes it possible that solute concentrations at each measurement point can be examined at any time in any time steps automatically.

A conductometer LF 198 (WTW Corporation, Germany) is applied to determine solute concentrations outside the tank that is at the inlet and outlet. Before the instrument was put into use, a calibration curve had been produced (see Fig. 2.3).

Due to the huge amount of water required, tap water was used as the basic fluid and solvent in the same time. Besides the conductometer, a large plastic water vat, three plastic can and an electrical plastic mixer were also applied for preparing experimental solutions. It had been planned to use a constant water head system (standpipe/overflow system) for all experiments, however, significant density and/or viscosity differences result in fluctuation of the flow rate continually, though, seemingly, the imposed hydraulic pressure (water head difference between inlet and outlet) does not change at all. Therefore, an eight channel peristaltic tubing pump BVK MS/CA8-6 (ISMATEC Corporation, Germany) was used, in combination with both the coarse and the fine gravel filters to control the flow of water into the sand tank and to create a constant horizontal flow field with no vertical gradients.

5.2.4 Test solutions

Test solutions were prepared by dissolving specified amount of NaCl and glycerine in a known amount of tap water with an electric mixer.

To avoid experimental error induced by differences in fluid temperatures, elaborate precautions were taken to insure that the

injected fluid and the connoted solution in the sand pack had the identical temperature. After a test solution had been prepared, instead of using it immediately, it was kept in a large plastic can until its temperature had reached the room temperature. The sand tank was stored in a temperature-controlled laboratory, which had a constant temperature of 20±0.5^{o}C.

Characteristics of the test solutions, including density and viscosity dependence on solute concentration are described in Tab. 5.1, Fig. 2.1, Fig. 2.2 and Fig. 2.3.

Drinking water of Karlsruhe city was used because large volume of water was required to saturate and flush solute from the porous media after each experiment. The mean pH value of the drinking water was 7.36 and had measured chloride and sodium concentrations of 25 and 11.3 mg/L respectively (SCHNELL, 2001). Electrical conductivity of the drinking water was measured to be 683 µs/cm.

Tab. 5.1: **Properties of the test solutions.**

Parameter	Dimension	Tap water	NaCl solution	Glycerine solution
Concentra.	[g/L]	-	35	115
Density	[kg/L]	0.9982	1.0226	1.0244
Viscosity	[cP]	1.002	1.059	1.336
E. conduct.	[ms/cm]	0.683	56.15	0.479
M. diffusion	[cm^2/s]	-	1.484E-5	8E-6

5.3 Sediment and hydraulic test

5.3.1 Sediment test

To characterize material and hydraulic properties of the packed porous medium, including porosity n and hydraulic conductivity K, grain size analysis was carried out according to DIN 18123 (a German Industrial Standard).

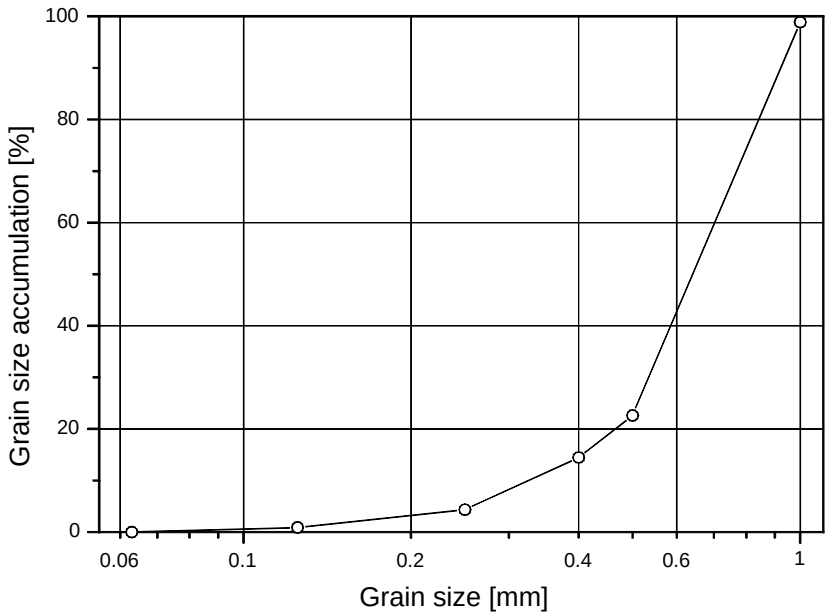

Fig. 5.9: **Curve of grain size distribution for sands filled in the tank.**

Tab. 5.2: **Chemical and physical properties of the packed porous medium in the tank.**

Parameter	Dimension	Value
SiO_2	[w%]	92.2
Al_2O_3	[w%]	2.5
Fe_2O_3	[w%]	0.5
CaO+MgO	[w%]	1.2
Na_2O	[w%]	0.2
K_2O	[w%]	2.0
Sand volume	[m^3]	15
Porosity *n*	[-]	0.35
Grain density	[g/cm^3]	2.65
Hydraulic conductivity *K*	[cm/s]	0.12

From the grain size distribution in Fig. 5.9, it is clear that this porous medium consists mainly of medium sand. No clay is shown in the inclusion. According to HAZEN's empirical formula for disturbed loose grain sediment, hydraulic conductivity was calculated to be 0.12 cm/s.

In a graduated cylinder, sand probes were saturated with tap water for 24 hours. Then the probes were dried at 105 ^{o}C for another 24 hours. In this way, the grain density and effective porosity were determined to be 2.65 g/cm^3 and 0.35 respectively.

Tab. 5.2 compiles the chemical composition specified by the supplier and the investigated hydraulic or material parameters by the above discussed methods.

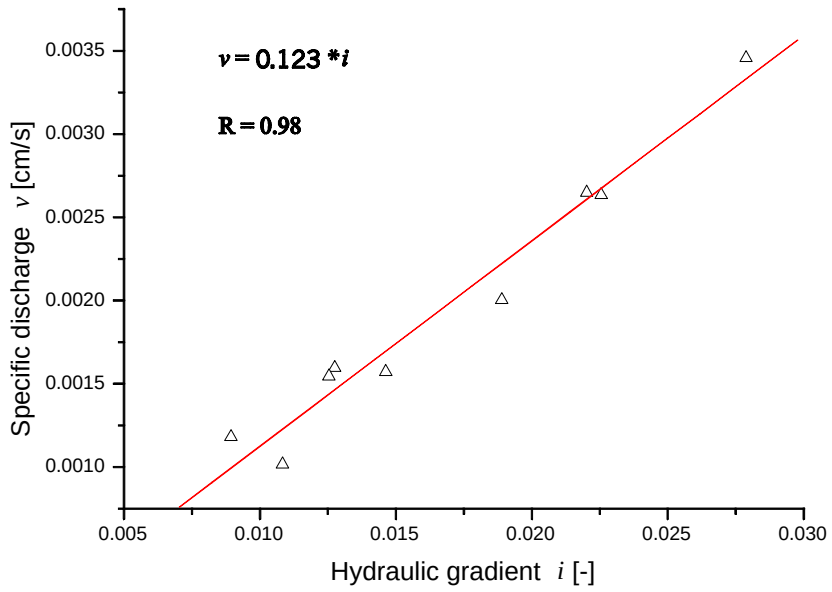

Fig. 5.10: **Results of the DARCY test, where v = 0.123 * I and R = 0.98 are linear regression and coefficient of regression respectively.**

5.3.2 Hydraulic test

After the tank had been filled with the Weisenburg medium sand, three months of consolidation phase followed. During and after this consolidation stage, Karlsruhe drinking water was applied to perform a DARCY test. Thereafter a tracer with a fluorescent dye Uranin was followed. Thereby the whole electric measurement system and the water supply-drainage system were further characterized and adapted accordingly.

5.4 Tracer test

Before the described experiment began, salt solution with different concentrations and Karlsruhe drinking water had been used to saturate the porous medium and flowed thoroughly through it for more than four months. During this period of time, the whole measurement system was tested, adapted and regulated.

To characterise the packed porous medium, a tracer test, besides the above discussed DARCY test, was conducted, where 1000 mg fluorescent dye (Uranin) was introduced to the tank as quickly as possible through a plastic tube. An overflow column controls water height at the inflow and outflow sides of the tank, in order to produce a uniform flow field. Tap water was used. The lower end of the tube located exactly at the point of 85 cm above the bottom of the tank, 45 cm away from the inflow point and 100 cm to both side of the tank. The tracer was dissolved in 500 ml tap water. After the solution was injected to the ambient running tap water through the plastic tube, 2-liter tap water was used to rinse the tube.

The most suitable test concentration for Uranin is greater than 0.005 µg/L, while smaller than 5 µg/L. A pore volume of the packed sand tank is $16.8\ m^3 \times 0.35 = 5.88\ m^3$. Even when the tracer is thoroughly mixed with its ambient fluid, 1000 mg tracer is sufficient for characterizing the packed porous medium.

DARCY velocity is 0.0026642 cm/s. Real velocity is 0.007612 cm/s. To get a nice breakthrough curve, past experience suggested that it would be best to take 20 out of total 70 samples before the peak arrives. It

had been planned to take 15~20 ml water samples from each of the following sample spots: Piezometer P423, P433, P443, P453, P463, P431, P432, P434, P533, P333, P233, P133 and from outflow (Fig. 5.3). However, after a few times of sampling, it was discovered that even such a small amount of water sample (if samples were taken simultaneously at the 12 Piezometers, the total volume of sampled water is about 0.003 %~0.004 % of a pore volume) could affect the whole flow regime significantly. Thereafter, sampling was done alternatively and each sample volume was reduced to about 10 ml.

The whole test continued for 60 hours and a total of 1000 samples were taken and analyzed on a PERKIN ELMER Spectrofluorimeter. Except at the sample spots along the central flow line: P423, P433, P443, P453, P463 and at the outflow, no tracer was detected. Distribution of these spots are shown in Fig. 5.3.

Based on the simulation method given in section 2.7, longitudinal dispersion coefficients and dispersivities were determined. Results of the tracer test and relevant variables and parameters are compiled in Tab. 5.3.

Tab. 5.3: **Results of the tracer test and relevant experiment data.**

Sample	Position	v	u	n	D_L	α_L
		(cm/min)	(cm/min)	(-)	(cm^2/min)	(cm)
P423	(85, 0,0)	0.16	0.60	0.27	1.01	1.68
P433	(135,0,0)	0.16	0.44	0.36	1.90	4.32
P443	(235,0,0)	0.16	0.32	0.5	2.68	8.38
P453	(335,0,0)	0.16	0.33	0.49	1.50	4.55
P463	(435,0,0)	0.16	0.34	0.47	2.45	7.21
Outflow	(555,0,0)	0.16	0.44	0.36	5.64	12.8

Due to variation of flow rate near the outflow, the calculated longitudinal dispersion coefficient is enlarged to a great extent. Because large amount of water was abstracted, a drawdown cone was formed for a short time. Transport ahead of the sample point P433 was accelerated, while between P433 and outflow it was slowed down. Extra mixing was introduced by the sampling scheme. In spite of this drawback, the results are generally acceptable. In conclusion, the effective porosity and the longitudinal dispersivity of the packed porous medium in the

tank is 0.35 and 6.5 cm respectively. The latter is much greater than those shown in Fig. 4.9.

5.5 Experiments of stable miscible displacement

Theoretical investigations into the stability of miscible displacement in porous media by TAN et al. (1985), YORTSOS et al. (1988) and many others have demonstrated that: when a more viscous fluid is used to displace another less viscous miscible fluid, the displacement is stable. However, if the displacing fluid is less viscous than the displaced one, instability can occur and greatly modify the mixing process. Density differences have been considered when vertical miscible displacements are of interest, where displacing more dense fluid upwardly by a less dense can result in gravitational instability and thus greatly modifies the mixing process (BOUHROUM, 1985; MOSER, 1995; BUES et al., 1992). In case of horizontal miscible displacements, however, except CHRISTIE et al. (1990), the effect of density differences on the horizontal bulk flow has generally been neglected.

A series of horizontal miscible displacement experiments were conducted in the large homogeneous sand tank using fluid pair with different density and viscosity. The test conditions were designed to create a horizontal flow field with no vertical gradients. After an initial period of pumping with a test solution (for example, tap water) to establish the wanted flow field in the sand pack, the inlet feed line was switched to the displacing fluid. The injection continued until measured solute concentrations at outflow had reached the same value as those of the injected fluid.

Because of the packed 400 electric probes (see Fig. 5.5), miscible displacement processes could be monitored at a pre-designed time-interval without extraction of any amount of fluid samples. The order of sample collection for each experiment was identical, namely, along the displacing direction from right to left (see Fig. 5.3 & Fig. 5.4) and from bottom to top. Flow rate, temperature and solute concentration were measured simultaneously both within the sand pack and at the effluent.

Following the completion of each experiment, the sand pack was saturated throughout with the displacing fluid, which has a constant

solute concentration. This fluid, in turn, was going to be displaced by another test solution in the next test.

To characterize miscible displacement in porous media, CHRISTIE et al. (1990) defined a dimensionless number N_g, which is a ratio between the viscous force and gravitational force:

$$N_g = \frac{v \cdot \Delta\mu}{\Delta\rho \cdot g \cdot k} \frac{H}{L} \tag{5.1}$$

where H and L are the height and length of the saturated sand pack respectively, v is the DARCY velocity, $\Delta\mu$ = $\mu_{displaced}$ - $\mu_{displacing}$ is the viscosity difference, $\Delta\rho$ = $\rho_{displaced}$ - $\rho_{displacing}$ is the density difference, g is the gravitational acceleration and k is the permeability (1.26 E -10 m^2 in the present case).

The dimensionless number indicates that density effects play a dominate role at low flow rates, while the displacement is dominated by viscosity effect at high flow rates. Overall four displacement experiments were carried out in the sand tank, among which experiment one and two are stable, while experiment three and four are unstable. Relevant parameters and calculated variables are compiled in Tab. 5.4.

Tab. 5.4: **Relevant parameters and calculated variables for the horizontal miscible displacements with density and viscosity differences in the sand tank.**

Exp.	Duration	PVI	v (cm/s)	$\Delta\rho$ (g/L)	$\Delta\mu$(cP)	M	Ng
1	36 days	2.76	1.871E-4	-24.4	-.0570	0.9462	7.6E-4
2	13 days	1.25	2.368E-4	-1.8	-.277	0.7927	6.2E-2
3	15 days	1.46	2.408E-4	1.8	.277	1.262	6.5E-2
4	8 days	.884	2.635E-4	24.4	.0571	1.057	1.1E-3

The present section handles two stable miscible displacements (Exp. 1 and Exp. 2): the first experiment with small viscosity differences but significant density differences, whereas the second with small density differences but significant viscosity differences.

5.5.1 Small viscosity differences but with significant density difference (Exp. 1: NaCl solution→Tap-water)

To begin with the present experiment, the porous medium was saturated with tap water. After an initial measurement had been carried out, the connoted tap water (ρ = 998.2 g/l, μ = 1.002 cP) was displaced by a 35 g/l NaCl solution (ρ = 1022.6 g/l, μ = 1.059 cP) at a constant pumping rate of 4.5 ml/s. The pair of fluids are chosen so that they have approximately the same viscosity ($M = \mu_{\text{tap- water}} / \mu_{\text{NaCl solution}}$ = 0.9462), whereas their density difference is quite significant ($\Delta\rho = \rho_{\text{tap-water}} - \rho_{\text{NaCl solution}}$ = -24.4 g/l).

During the experiment, NaCl concentration at each measurement point within the porous medium was taken at a prescribed time interval, which had been determined according to the result of the sediment, hydraulic and tracer tests.

Measured solute concentrations at 0.1, 0.2, 0.3, 0.4, 0.5, 0.6, 1.0, 1.4, 2.0, 2.8 PVI (pore volume injected) are compiled in two tabulated diagrams Fig. 5.11 and Fig. 5.12, where the displacing fluid was advancing from the right. Due to the density differences, a slope interface is required to achieve an equilibrium state. Dashed lines in Fig. 5.11 and Fig. 5.12 outline a gravity tongue composed of the dense displacing fluid. Note that the lower side of the gravity tongue moves more quickly than its upper counterpart. When the tip of the lowest layer of displacing fluid has reached the outlet (Fig. 5.1, Fig. 5.2 and Fig. 5.11) at 0.5 PVI, the fluid particles of the dense solution at a height of 85 cm above the bottom of the sand pack have just begun their journey. From then on, the longer the displacement is continued, the slower is the change of the shape and position of the displacing front (dashed line). The flow regime slowly reached a quasi-steady state.

By performing the least squares fit discussed in section 2.7, measured concentration breakthrough curves were simulated. Thereby longitudinal dispersivity was determined. For comparison, both measured and simulated salt concentration breakthrough curves at 5 selected locations along the central line on the first measurement plane are shown in Fig. 5.13. It is clear that the simulation produces reasonable accuracy for development of the transition zone in the three dimensional porous medium.

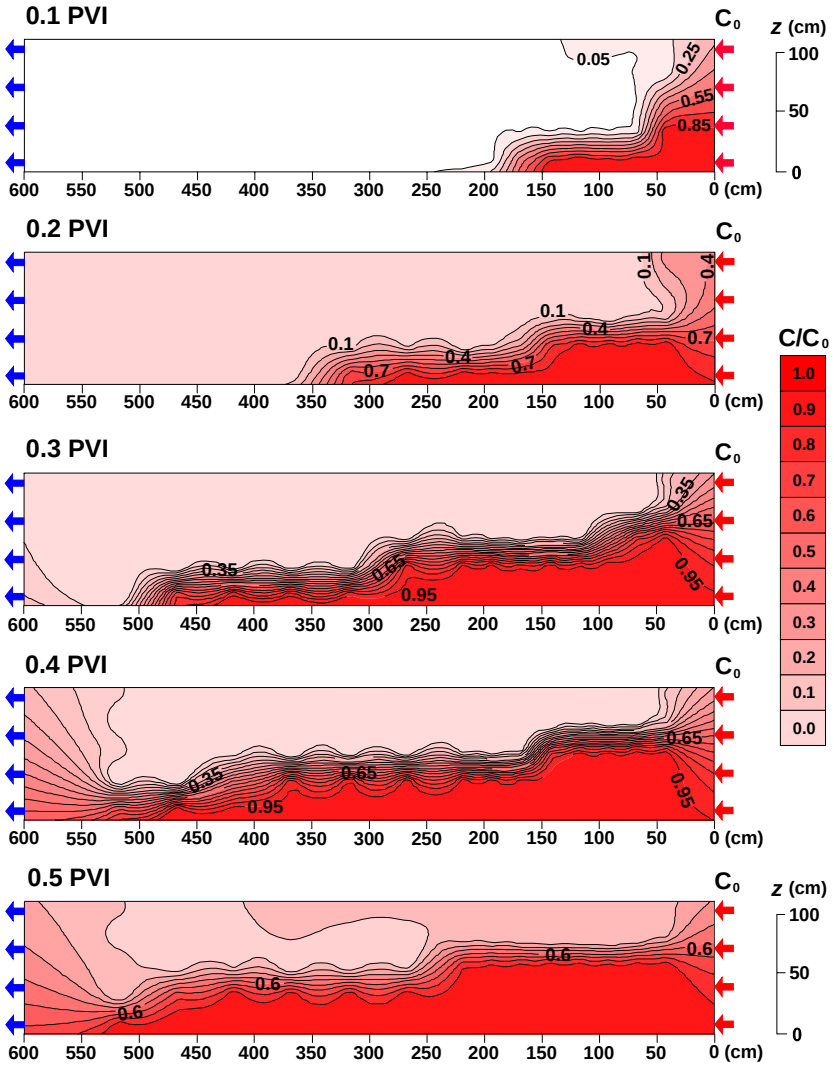

Fig. 5.11: **Isolines for the relative salt concentrations (C/C_0) along central section at 0.1, 0.2, 0.3, 0.4 and 0.5 PVI each.**

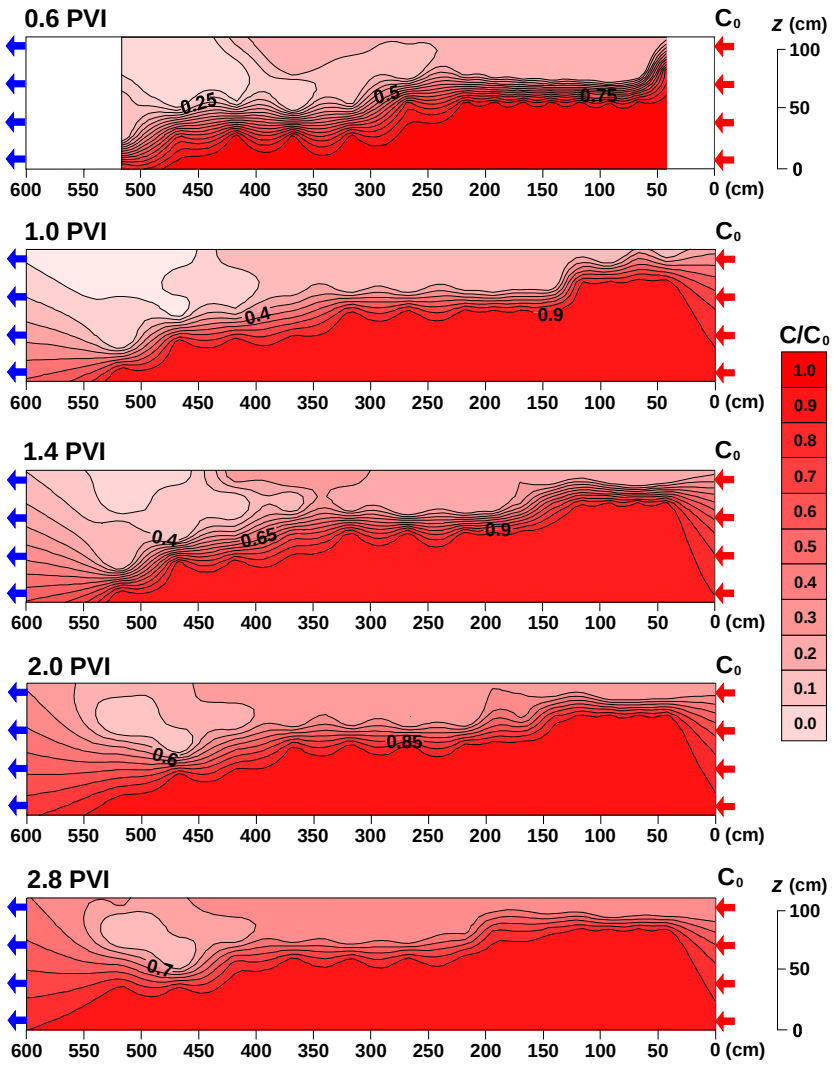

Fig. 5.12: **Isolines for the relative salt concentrations (C/C_0) along central section at 0.6, 1.0, 1.4, 2.0 and 2.8 PVI each.**

All concentration breakthrough curves measured within the gravity tongue have the same characteristic as those shown in Fig. 5.13. The

concentration distribution in Fig. 5.11 and Fig. 5.12 indicates that the connoted fluid above the second measurement plane (35 cm above the bottom of the packed sand) has not been completely displaced even at 2.8 PVI. Electrical probes outside the gravity tongue could not give enough samples for a complete breakthrough curve.

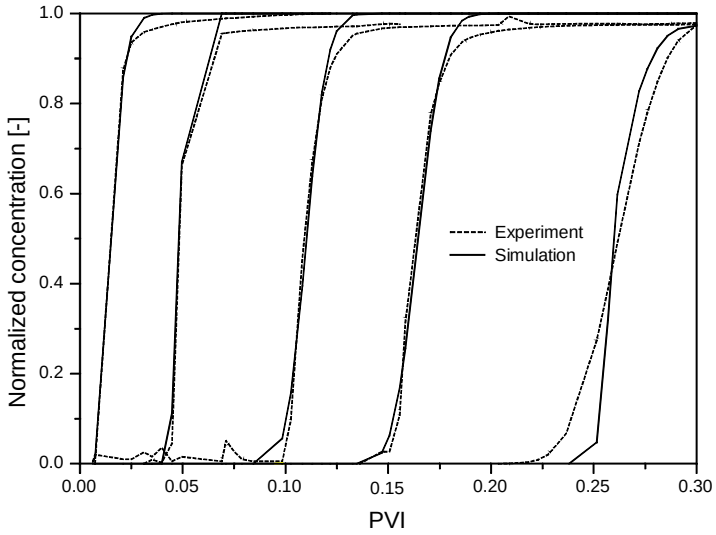

Fig. 5.13: **Comparison of salt concentration breakthrough curves at locations of row 1, 3, 7, 9, 13 along the central line on the first measurement plane for the first experiment, where M = 0.9462 and $\Delta\rho$ = -24.4 g/L.**

At the outflow, both the flow rate and NaCl concentration were measured as well. The measured salt concentrations, which are a function of time (breakthrough curves) as shown in Fig. 5.14, are in good agreement with simulation. Fig. 5.13 and Fig. 5.14 show that this kind of stable miscible displacement in homogeneous sand pack is dispersive. Computed average dispersivities are to be discussed in this section latter.

5.5.2 Small density differences but with significant viscosity difference (Exp. 2: glycerine solution→NaCl solution)

After the first displacement experiment had been finished, the porous medium was saturated with 35 g/l NaCl solution. Following a zero measurement of the connoted salt concentrations, a 115 g/L glycerine solution was pumped in at a constant rate of 5.6 ml/s to displace the resident NaCl solution. The pair of fluids are chosen so that they have approximately the same density ($\Delta\rho$ = $\rho_{\text{NaCl solution}}$ - $\rho_{\text{glycerine solution}}$ = -1.8 g/L), whereas their viscosity ratio is quite significant (M = $\mu_{\text{NaCl solution}}$ /$\mu_{\text{glycerine solution}}$ = 0.7927).

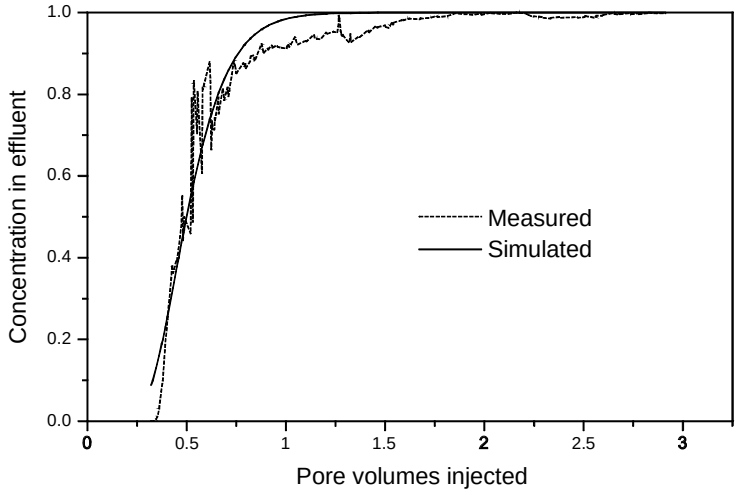

Fig. 5.14: **Measured and simulated concentration breakthrough curves of the first experiment at effluent.**

In this case, NaCl concentrations were directly measured, while glycerine concentrations were calculated. Because the displacing fluid is more viscous and slightly dense than the saturated one, the displacement is stable. As the density difference between the pair of test solutions are so small that its effects on the displacements can be neglected, thus the interface should be vertical instead of slope as those in the first experiment, which has been proved by the fact that all the measured concentration breakthrough curves at locations on a same transverse plane have the same arrival time. And all of the

curves have similar characteristics (Fig. 5.15). For comparison and for convenience only a few measured breakthrough curves and corresponding simulations are shown in Fig. 5.15. The agreement between the experiment observation and simulation in Fig. 5.15 is reasonably well.

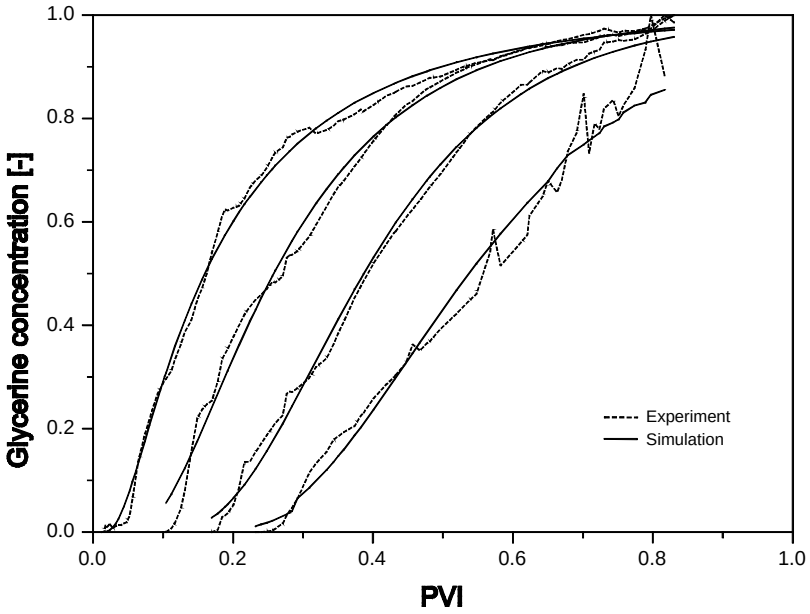

Fig. 5.15: **Glycerine concentration breakthrough curves at locations of row 1, 3, 5 and 7 along the central line on the first measurement plane for the second experiment.**

Both flow rates and glycerine concentrations and temperature in effluent were measured. The measured glycerine concentration as a function of time (breakthrough curves) as shown in Fig. 5.16, is in good agreement with simulation.

5.6 Experiments of unstable miscible displacement

Following the stable cases in section 5.5, more concern is given to two unstable miscible displacement experiments (Exp.3 and Exp.4) in the

present section. In the third experiment, a less viscous NaCl solution was used to displace the connoted more dense glycerine solution. This pair of fluids has small density differences but significant viscosity differences. Such a flow configuration is unstable. In the fouth and last case, a less dense and slightly less viscous fluid (tap water) was introduced into the tank to displace the resident NaCl solution. In such a case, both the density and viscosity differences can result in instability. These two experiments were carried out in order to explain, how the dispersion coefficient depends upon viscous instability and gravitational instability.

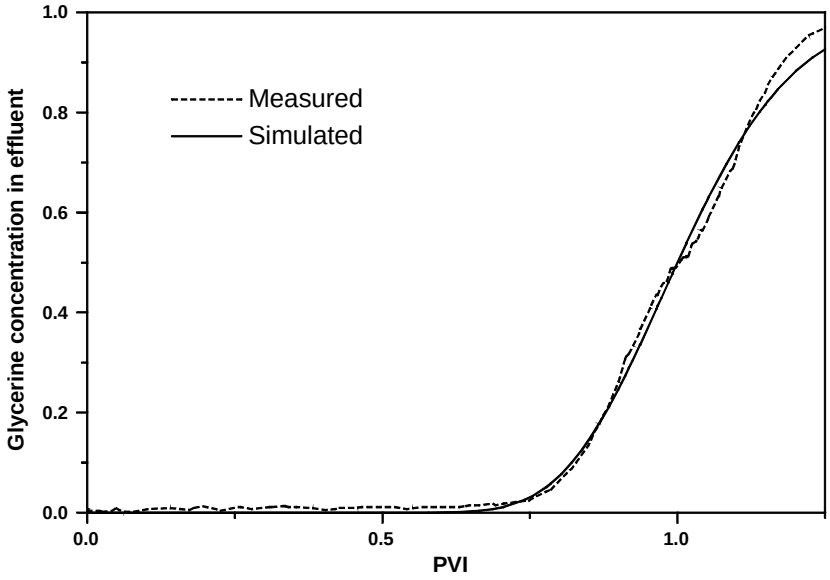

Fig. 5.16: **Measured and simulated concentration breakthrough curves of the second experiment at effluent.**

5.6.1 Small density difference but with significant viscosity difference (Exp. 3: NaCl solution→glycerine solution, viscous instability)

In the last experiment, a NaCl solution had been displaced by a 115 g/L glycerine solution. After the experiment had been finished, the whole

sand tank (porous medium) was saturated with the glycerine solution. At time t = 0, a less viscous but slightly less dense fluid (another 35 g/l NaCl solution) was used to displace the resident glycerine solution. The pair of fluids are chosen so that they have almost the same density ($\Delta\rho$ = $\rho_{\text{glycerine solution}}$ - $\rho_{\text{NaCl solution}}$ = 1.8 g/L), whereas their viscosity ratio is quite significant (M = $\mu_{\text{glycerine solution}}$ /$\mu_{\text{NaCl solution}}$ = 1.262). Since M > 1, the displacement is unstable (viscous instability). Analogue to the viscous instability in the one dimensional case in chapter 4, viscous fingering produces much larger increase of the transition zone with M > 1 than in the case where M < 1.

In this experiment, concentrations of the NaCl solution were directly measured, while glycerine concentrations were calculated.

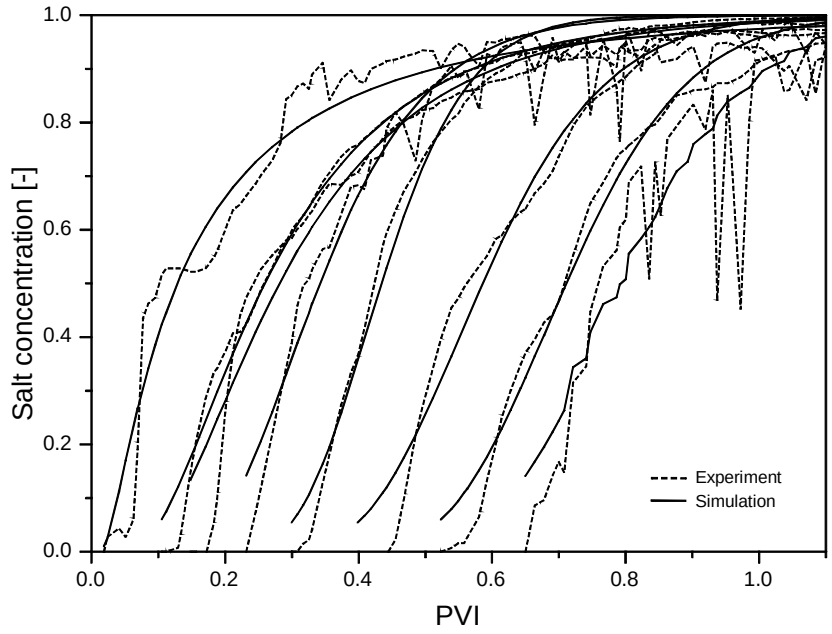

Fig. 5.17: **Measured and simulated concentration breakthrough curves at locations of row 1, 3, 5, 7, 9, 11 and 13 along the central line on the first measurement plane for the third experiment.**

The density difference between the pair of test solutions is so small that its effects on the displacements can be neglected. The interface should be vertical instead of in a slope as those in the first experiment, which has been proved by the fact that all the measured concentration breakthrough curves at locations on a same transverse plane have the same arrival time.

Fig. 5.17 reports a few measured breakthrough curves at some selected locations. For comparison, simulations are also given. All of the curves have similar characteristics (Fig. 5.17). The curves are neither even nor smooth, but with clear zigzag irregularities. The irregularities are more pronounced in the latter stage and all the curves have a long tail. The farther away is from the inflow side, the more uneven are the breakthrough curves and they are more sloping. In spite of this variability, simulation results are acceptable.

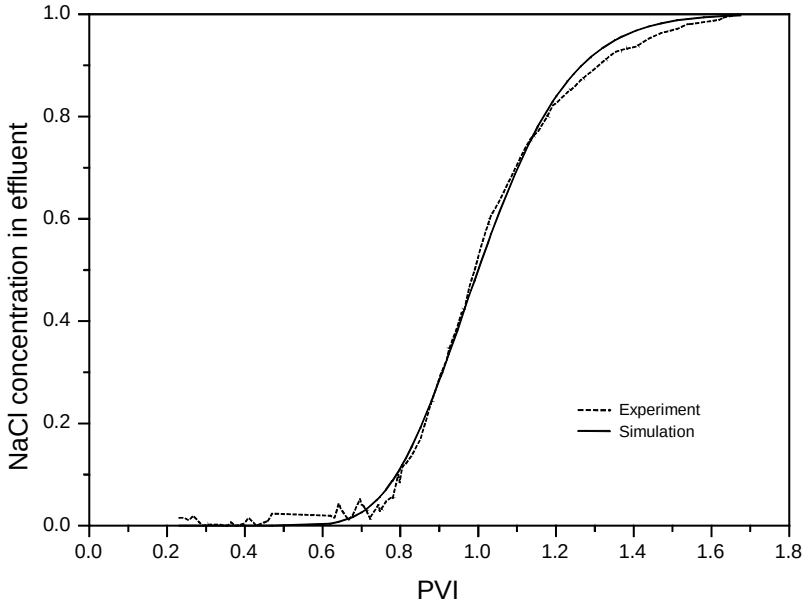

Fig. 5.18: **Measured and simulated concentration breakthrough curves of the third experiment at effluent.**

Both flow rates and NaCl concentrations and temperatures in effluent were measured. The measured NaCl concentration as a function of

time (breakthrough curves), shown in Fig. 5.18, is in good agreement with simulation. Contrary to the zigzag breakthrough curves at measurement location within the sand pack, the concentration breakthrough curve in Fig. 5.18 at the effluent is very smooth, which deserves more discussion.

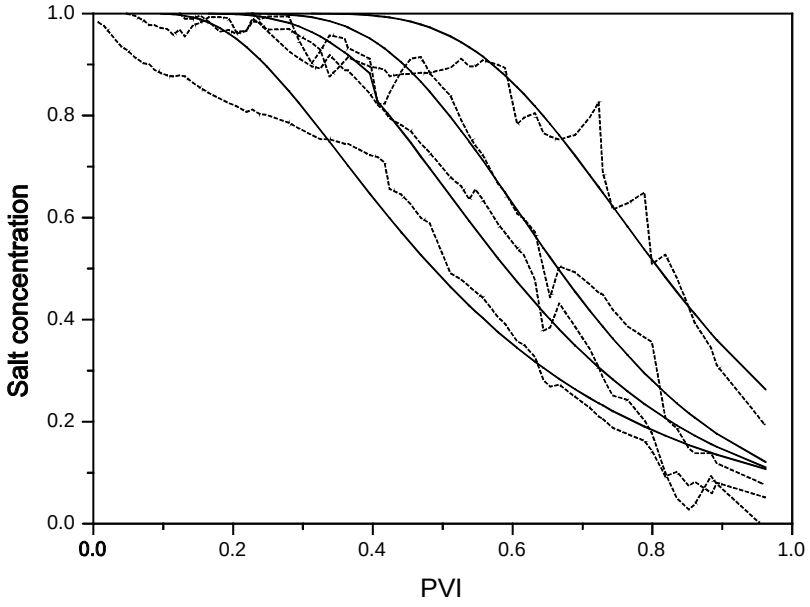

Fig. 5.19: **Salt concentration breakthrough curves at locations of row 1, 9, 11 and 13 along the central line on the first measurement plane for the fourth experiment.**

5.6.2 Small viscosity difference but with significant density difference (Exp. 4: Tap-water→NaCl, gravitational instability)

After completing the third test, the packed porous medium was saturated with the 35 g/l NaCl solution. Following an initial period of pumping with the solution to establish the wanted flow condition in the sand pack and a zero thorough measurement, the displacing source was switched to tap water. The experiment continued for about 8 days.

The pair of fluids is chosen so that they have a quite significant density difference ($\Delta\rho$ = $\rho_{\text{NaCl solution}}$ - $\rho_{\text{tap-water}}$ = 24.4 g/L), whereas their viscosity ratio is also quite significant (M = $\mu_{\text{NaCl solution}}$ / $\mu_{\text{tap-water}}$ = 1.057). Such a flow configuration is both viscously and gravitationally unstable. This instability causes the displacing front to “collapse” and spread more rapidly at depth in both the longitudinal and transverse directions.

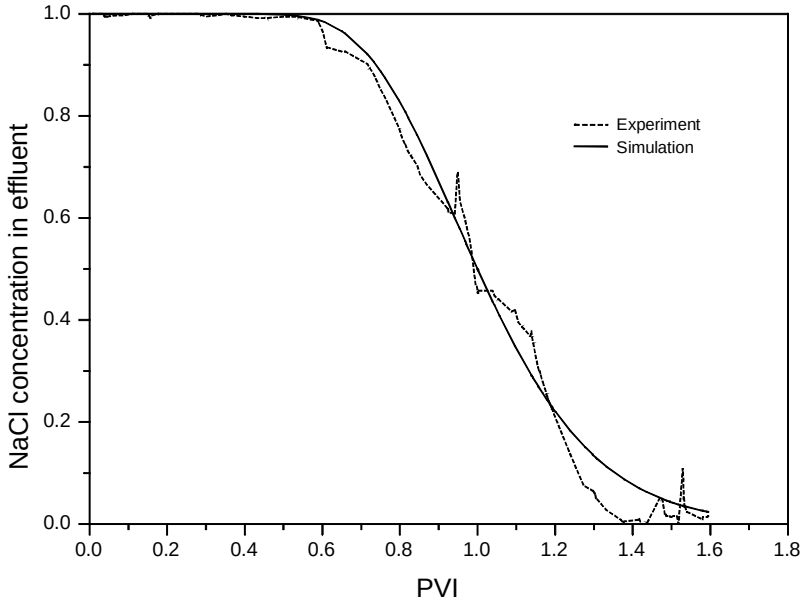

Fig. 5.20: **Salt concentration breakthrough curves of the fourth experiment at effluent.**

Figure 5.19 describes measured concentration breakthrough curves for miscible displacement with significant gravitational instability and slight viscosity instability at some selected locations. For comparison, simulations are also shown in the Fig. 5.19. Comparing Fig. 5.19 and Fig. 5.20 to Fig. 5.17 and Fig. 5.18 in the last section, it is clear that breakthrough curves in both unstable cases have similar characteristics, where more variability and wider transition zone are shown, while the latest displacement exhibits the strongest instability. In spite of this strong instability, both the figures indicate that the

agreement between the experimental observation and simulation is reasonably well.

The flow rates, NaCl concentrations and temperatures in effluent were measured. The measured NaCl concentration as a function of time (breakthrough curves), shown in Fig. 5.20, is in good agreement with simulation. Unlike the smooth breakthrough curves in Fig. 5.16 and Fig. 5.18, the measured breakthrough curves at effluent in Fig. 5.20 shows irregularity. However, compared to those measured within the sand pack (Fig. 5.19), this irregularity is quite small.

Tab. 5.5: **Calculated longitudinal dispersion coefficients D [cm^2/min] and dispersivity α [cm] for layer 1.**

Layer 1	Row	1	2	3	4	5	6	7	8	9	10	11	12	13	14
Section	X [cm]	27.5	52.5	77.5	103	128	153	178	203	253	303	353	403	453	503
	D	.173	.047	.037	.060	.032	.050	.039	.045	.039					
7	α	2.36	.618	.438	.698	.363	.578	.448	.535	.467					
	D	.278	.012	.046	.058	.018	.048	.022	.044	.047	.051	.040	.077	.047	.061
6	α	3.78	.159	.542	.657	.221	.570	.264	.529	.587	.604	.513	.933	.578	.833
	D	.148	.018	.012	.049	.047	.069	.034	.043	.034	.080				
5	α	1.49	.232	.145	.549	.617	.847	.401	.518	.416	.957				
	D	.221	.047	.010	.063	.066	.074	.036	.026	.044	.062	.043	.053	.017	.057
4	α	2.94	.681	.116	.715	.869	.974	.441	.336	.543	.725	.542	.663	.210	.760
	D	.069	.047	.023	.048	.065	.039	.022	.052	.030	.026				
3	α	1.22	.650	.271	.548	.788	.512	.257	.619	.371	.302				
	D	.111	.006	.010	.113	.049	.054	.085	.006	.030	.048	.023	.027	.043	.063
2	α	2.02	.082	.120	1.08	.580	.621	1.06	.064	.363	.596	.285	.329	.520	.835
	D	.077	.035	.043	.040	.019	.017	.036	.030	.058					
1	α	1.36	.438	.514	.417	.221	.228	.431	.338	.689					
	D	.154	.030	.026	.061	.042	.050	.039	.035	.040	.053	.035	.052	.036	.060
Average	α	1.87	.235	.208	.618	.398	.514	.390	.243	.467	.551	.411	.534	.357	.808

5.7 Results and discussion

Experimental observation of miscible displacements in large scale sand pack shows clearly that different pair of test fluids and displacing relationship resulted in distinct concentration breakthrough curves, which has been described qualitatively in the last section. To investigate the displacement quantitatively, dispersivity was determined by using a least-squares fit to the measured data.

Experiment 1

Applying the classical advection-dispersion theory, longitudinal dispersion coefficients and dispersivity at each measurement point were calculated and summarised in Tab. 5.5.

Recall that the connoted fluid above the second measurement plane (35cm above the bottom of the packed sand in Fig. 5.13 and Fig. 5.14) had not been completely displaced even at 2.8 PVI. The flow changed into a quasi-steady state. Without displacing the less dense connoted fluid, the newly injected dense salt solution simply flowed out of the porous medium at effluent. Electrical probes outside the gravity tongue could not sample a complete breakthrough curve. Thus, detail simulation results above the second measurement layer are not given here.

Tab. 5.6: **Calculated longitudinal dispersion coefficients D [cm^2/min] and dispersivity α [cm] for layer 2.**

Layer 2	Row	1	2	3	4	5	6	7	8	9	10	11	12	13	14
Section	X [cm]	27.5	52.5	77.5	103	128	153	178	203	253	303	353	403	453	503
7	D	.001	.004	.007	.006	.006	.024	.023	.011	.014					
	α	.052	.151	.230	.181	.196	.612	.547	.254	.283					
6	D	.001	.003	.004	.006	.015		.014	.010	.013	.017	.024	.023		
	α	.041	.104	.145	.176	.387		.338	.229	.260	.335	.457	.423		
5	D		.009		.008	.013	.011	.019	.009	.012	.018				
	α		.382		.238	.345	.285	.474	.203	.260	.378				
4	D			.007	.010	.014	.009	.011	.015	.015	.021	.028	.021		
	α			.234	.311	.384	.227	.274	.340	.315	.436	.553	.382		
3	D	.001	.002	.006		.012	.008	.010	.014	.018	.023				
	α	.075	.079	.206		.359	.197	.228	.329	.376	.453				
2	D	.001	.003	.004	.009	.011	.007	.024	.017	.014	.034	.013	.020		
	α	.066	.114	.120	.261	.290	.212	.552	.381	.302	.660	.256	.379		
1	D	.001	.001	.005	.007	.019		.020	.017	.013					
	α	.059	.039	.154	.192	.487		.423	.374	.253					
Average	D	.001	.004	.006	.008	.013	.012	.017	.013	.014	.023	.022	.021		
	α	.056	.091	.170	.217	.326	.259	.366	.286	.288	.430	.380	.394		

Fig. 5.21 gives transversely averaged longitudinal dispersivity for the stable miscible displacement with a significant density difference of -24.4 g/L. Comparing to the result of tracer test, Fig. 5.21 shows clearly a reduction in dispersivity within the gravity tongue (below and behind the displacing front, dashed line). Except near the inlet side and in the

area of the displaced tap water, there is little difference among values of the calculated dispersivity.

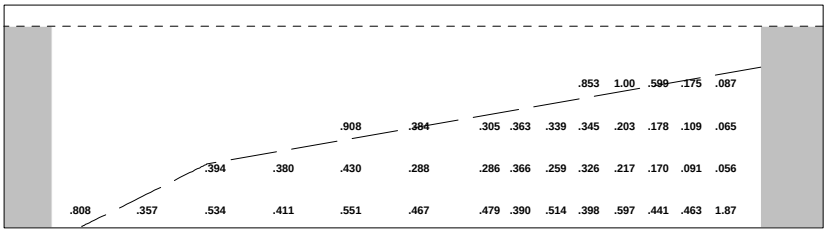

Fig. 5.21: **Transversely averaged dispersivity for the first experiment.**

Experiment 2

Tab. 5.7: **Calculated longitudinal dispersion coefficients D [cm^2/min] and dispersivity α [cm] for the second experiment.**

Layer 1	Row	1	2	3	4	5	6	7	8	9	10	11	12	13	14
Section	**X [cm]**	27.5	52.5	77.5	103	128	153	178	203	253	303	353	403	453	503
	D	.108	.102	.270	.235	.276	.282	.320	.112	.200					
7	**α**	16.2	7.42	15.6	12.2	12.9	13.3	15.8	4.98	6.81					
	D	.108	.178		.205	.230	.284	.391	.287		.173	.130	.100	.092	.065
6	**α**	12.8	16.0		12.0	11.0	13.1	17.5	11.7		5.56	3.91	2.73	2.28	1.46
	D	.104	.151	.263	.300	.268	.194	.339	.204	.147	.152				
5	**α**	13.2	11.3	15.7	17.0	13.4	8.27	14.7	8.53	5.52	4.91				
	D		.140	.178	.250		.120	.152	.423	.183	.124	.105	.145	.136	.091
4	**α**		14.1	11.4	12.7		6.05	6.96	16.5	6.54	4.16	3.24	3.86	3.34	2.03
	D		.145	.169	.392	.120	.127	.148	.391	.207	.120				
3	**α**		12.4	10.6	19.0	6.13	6.14	6.52	17.0	7.68	4.08				
	D			.240		.241	.079	.335	.201	.162	.108	.080	.121	.044	
2	**α**			15.7		12.0	4.60	15.9	8.22	6.06	3.68	2.50	3.31	1.12	
	D				.312	.187	.263	.227	.117	.329					
1	**α**				17.4	11.1	13.3	9.91	4.22	10.2					
	D	.085	.111	.231	.261	.194	.193	.273	.248	.205	.129	.105	.122	.091	.078
Average	**α**	14.1	12.2	13.8	15.1	11.1	9.25	12.5	10.2	7.14	4.48	3.22	3.30	2.25	1.75

Table 5.7 summarizes the calculated dispersion coefficients and dispersivity for the second stable miscible displacement ($\Delta\rho$ = -1.8 g/L,

M = 0.7927). Recall the analysis in section 5.6.2 that there does not indicate much differences between the measured concentration breakthrough curves on different measurement layer. Neither indicate the calculated dispersion coefficients and dispersivity in Table 5.7 any dependence on the measurement section.

Fig. 5.22 compiles transversely averaged longitudinal dispersivity for the stable miscible displacement with a significant viscosity ratio of 0.7927 and a slight density difference of –1.8 g/L. Comparing to the result of tracer test, it is found that the calculated longitudinal dispersivity is in the same order. Thus, it could be concluded that, for the conditions of the experiments, stable miscible displacement is not sensitive to viscosity ratio.

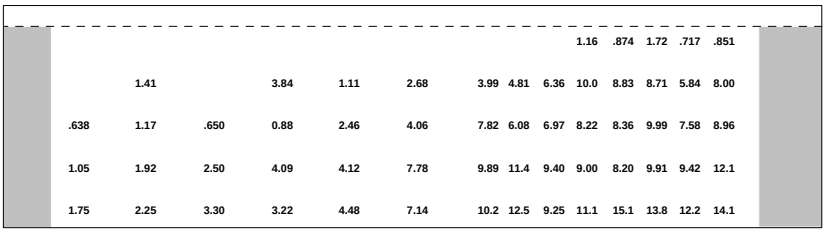

Fig. 5.22: **Transversely averaged dispersivity for the second experiment.**

Experiment 3

Table 5.8 summarizes the calculated dispersion coefficients and dispersivity for the third experiment of unstable miscible displacement with a density difference of 1.8 g/L and a viscosity ratio of 1.262. Because all the measured concentration breakthrough curves on the five-measurement layer exhibit similar characteristics (cf. section 5.6.1), only the results on the first layer are listed in Table 5.8.

Fig. 5.23 gives transversely averaged longitudinal dispersivity for the unstable miscible displacement with a significant viscosity ratio of 1.262 and a slight density difference of 1.8 g/L. Upon comparing, it is found that the results of tracer test, the second stable displacement and the third unstable experiment are surprisingly alike, despite that each single breakthrough curve does exhibit instability in the third

experiment. Thus, it could be concluded that, under the experiment conditions, when $1< M \leq 1.262$, transversely averaged dispersivity does not strongly dependent on viscosity ratio.

Tab. 5.8: **Calculated longitudinal dispersion coefficients D [cm²/min] and dispersivity α [cm] for the third experiment.**

Layer 1	Row	1	2	3	4	5	6	7	8	9	10	11	12	13	14
Section	X [cm]	27.5	52.5	77.5	103	128	153	178	203	253	303	353	403	453	503
	D	.127	.191	.265	.341	.465	.353	.511	.262	.130					
7	α	11.7	13.9	13.0	19.3	16.9	14.6	20.0	6.57	2.71					
	D	.154	.190		.284	.319	.411	.493	.258	.386	.451	.561	.426	.390	.287
6	α	15.0	12.5		8.23	10.3	12.9	14.4	7.63	9.64	11.1	14.9	9.99	8.90	6.62
	D	.157	.192	.288	.332	.655	.393	.425	.221	.199	.340				
5	α	12.8	11.2	12.7	11.6	25.1	12.4	11.9	5.88	4.64	8.23				
	D	.138	.159	.277	.290		.612	.274	.175	.188	.291	.425	.415	.349	.414
4	α	8.12	8.33	16.2	8.21		19.9	6.74	4.17	4.35	7.00	10.3	9.20	7.74	9.59
	D	.182	.185	.302	.376	.337	.285	.271	.210	.183	.260				
3	α	21.6	10.1	15.6	11.9	10.6	12.3	8.04	6.47	4.39	5.80				
	D				.010	.532	.386	.428	.200	.274	.392	.391	.650	.495	.526
2	α				.227	22.1	12.8	14.9	6.15	6.65	10.7	9.97	16.4	11.0	13.2
	D	.145	.140	.228	.420	1.03	.323	.270	.077	.377					
1	α	21.9	7.71	15.2	14.3	40.1	12.5	7.97	2.01	9.47					
	D	.155	.157	.347	.293	.682	.395	.381	.200	.248	.347	.459	.497	.411	.409
Average	α	15.2	10.6	14.5	10.5	20.8	13.9	12.0	5.55	5.98	8.57	11.7	11.9	9.20	9.80

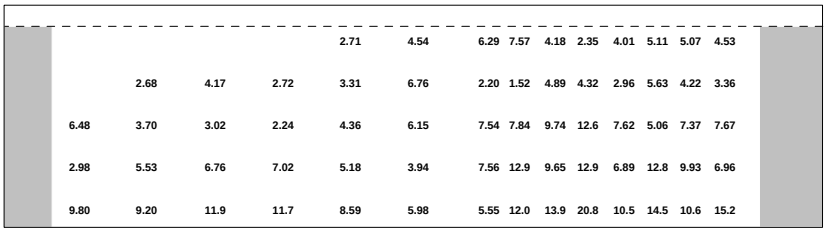

Fig. 5.23: **Transversely averaged dispersivity for the third experiment.**

Experiment 4

Table 5.9 lists the calculated dispersion coefficients and dispersivity for the fourth experiment of unstable miscible displacement with a density

difference of 24.4 g/L and a viscosity ratio of 1.057. As discussed in section 5.6.2, this flow configuration is both gravitational and viscous unstable. Because all the measured concentration breakthrough curves on the five-measurement layers exhibit similar characteristics (cf. section 5.6.1), only the results on the first layer are listed in Table 5.9.

Tab. 5.9: **Calculated longitudinal dispersion coefficients D [cm^2/min] and dispersivity α [cm] for the fourth experiment.**

Layer 1	Row	1	2	3	4	5	6	7	8	9	10	11	12	13	14
Section	X [L]	27.5	52.5	77.5	103	128	153	178	203	253	303	353	403	453	503
	D	.017	.060			.261	.751								
7	α	5.25	13.3			22.2	36.8								
	D	.031	.140			.900						.665	1.14	.191	1.05
6	α	8.70	21.3			79.9						15.0	34.5	4.54	17.9
	D	.017	.092	.067	.030	.329	.694								
5	α	4.52	20.0	8.25	3.08	29.5	50.7								
	D	.009	.102	.136				.835		2.49		.971	1.21	.710	2.24
4	α	2.83	24.0	18.7				43.8		133		28.9	26.4	16.9	40.3
	D	.008	.082	.198	.035	.161		.244		.850					
3	α	2.47	17.5	25.3	3.49	12.9		14.8		30.8					
	D	.021			.005	.132		.610	1.37	.827		1.21	1.03	.693	1.44
2	α	6.27			.523	11.0		42.6	73.4	32.9		29.3	27.0	16.9	25.3
	D	.012	.293	.145	.019	.202	1.00	.582	1.17	.984					
1	α	3.93	73.5	15.2	1.84	14.4	67.9	28.7	49.4	32.0					
	D	.016	.112	.136	.071	.331	.816	.568	1.27	.887		.950	1.13	.531	1.58
Average	α	4.85	19.2	17.4	2.23	28.3	51.8	32.5	61.4	57.1		24.7	29.3	12.8	27.9

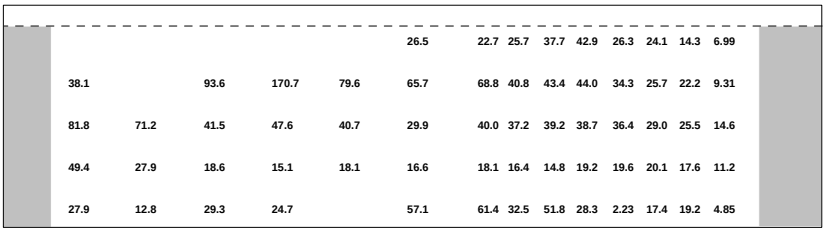

Fig. 5.24: **Transversely averaged dispersivity for the fourth experiment.**

Fig. 5.24 gives transversely averaged longitudinal dispersivity for the unstable miscible displacement with a viscosity ratio of 1.057 and a

density difference of 24.4 g/L. It is found, upon comparing, that the coupling of the two instabilities produces the largest variation and absolute value of transversely averaged dispersivity.

Discussion

Experimental investigations of miscible displacements in a large-scale homogeneous and isotropic sand pack have demonstrated that, depending on the fluid property and displacing relationship, instability can occur. Two types of instability can be classified: the gravitational instability and the viscous instability. The former is due to density differences, while the latter is is the result of unstable viscous ratio. Results of the four experiments and the overall effect of density differences and viscosity ratio on miscible displacements are outlined in Fig. 5.25, where transversely averaged longitudinal dispersivity along the displacing direction is indicated.

There are a few inconsistencies and variability on the curve of the transversely averaged longitudinal dispersivity in Fig. 5.25. These are caused by sampling and testing errors, as a single concentration measurement can have a fairly large effect on computed values. However, in general, the results indicate that the inconsistencies are small, as the calculated dispersivity varies two to three orders of magnitude from experiment to experiment.

Similar to those results from 1-D column test, both stable density difference $\Delta\rho=\rho_{\text{tap-water}} - \rho_{\text{NaCl solution}}$ = -24.4 g/L and stable viscosity ratio $M = \mu_{\text{tap-water}} / \mu_{\text{NaCl solution}}$ = 0.9462 < 1 in the first stable miscible displacements in the large scale 2-D sand tank result in the reduction of dispersion coefficient and dispersivity as well, comparing the results with those from tracer test (Fig. 5.25).

In the second displacement experiment, although it is also stable, there is only a slight density difference between the displacing and the displaced fluid pair. The fluctuations of flow velocity near the displacing source due to technical disturbances, for example, a few times of stop and renew start at the beginning stage, have some influence on the dispersion coefficient. However, the significant stable viscosity ratio between the pair of test solutions alone does not result in much modifications to the dispersion processes (Fig. 5.25).

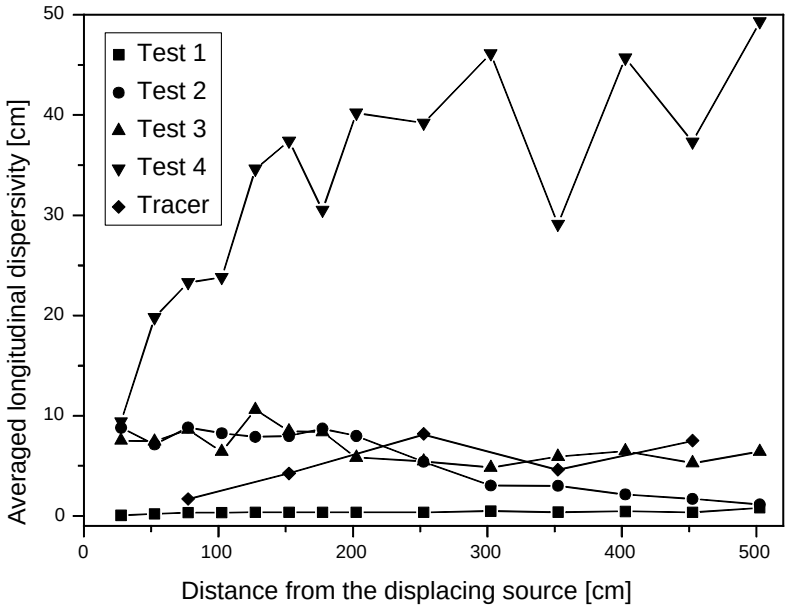

Fig. 5.25: **Transversely averaged longitudinal dispersivity vs. distance from the displacing source.**

Recall that there exists a significant unstable viscosity ratio M = 1.262 > 1 and a slight unstable density difference $\Delta\rho$ = 1.8 g/L between the pair of test solutions in the third miscible displacement test in the sand tank. The flow is unstable. Fig. 5.25 indicates that the instability result in throughout a slightly even modification to the dispersion coefficient.

Since tap-water is used to displace a 35 g/L NaCl solution in the fourth displacement experiment, both unstable density differences $\Delta\rho$ = 24.4 g/L and a slightly unstable viscosity ratio M = 1.057 act together and thus result in still stronger modification to the dispersion coefficients (see Fig. 5.19). This might be also attributed to failure in producing a step-like initial and boundary conditions, which deserves further experimental investigation.

The results of the four displacements seem to suggest that density differences exert much stronger influence over dispersion processes

(e.g., in the first and the fourth experiments) than viscosity ratio does (e.g., in the second and third experiments).

Notable solute concentrations (density differences and viscosity ratio) exert significant modifications to the longitudinal dispersion. In particular, for the present experimental configurations (at relative low PECLET number), miscible displacement is dominated by the effect of density differences. A density difference of 24.4 g/l and opposing displacing relationship can cause two to three orders of change to the longitudinal dispersion coefficients. These results suggest that density effect should not be neglected in horizontal miscible displacement in porous media, especially when the PECLET number is low as in the present experimental configuration. In principle, both stable and unstable miscible displacements in porous media with density and viscosity differences can be simulated using the classical advection-dispersion theory, which gives better results for the former case.

Generalisation of the results

Obviously, dispersion coefficients are not independent parameters. They apply to certain flow configurations. For the purpose of generalisation, results of experimental investigation in porous media can be characterised by some dimensionless numbers as the REYNOLDS number ($Re = u.d_p/\nu$), the SCHMIDT number ($Sc = \nu/D_m$), the PECLET number ($Pe = u.d_p/D_m$) and the RAYLEIGH number (Ra), which are most commonly used in fluid mechanics. The relashionship among the first three numbers are $Pe = (Sc)(\mathrm{Re})$.

RAYLEIGH number in porous medium is the nondimensional ratio between buoyancy forces and the product of viscous forces and solute advection in a porous medium. It is written as:

$$Ra = \frac{d_p{}^2 \cdot g \cdot \Delta\rho}{u \cdot \mu_1} \tag{5.2}$$

where d_p is the characteristic diameter of the packed granular sand grain, g is the gravity acceleration, $\Delta\rho = \rho_2 - \rho_1$ is the density difference between the displaced and the displacing fluid, u is the flow rate, μ_1 is the viscosity of the displacing fluid. The nondimensional RAYLEIGH

number expresses the effects of a density difference in a gravitational field. Besides, another term R_μ that describes the viscosity effect in the presence of solute advection can be defined by:

$$R_\mu = (M-1)\cdot Pe = (\frac{\mu_2}{\mu_1}-1)\cdot\frac{u\cdot d_p}{D_m} \tag{5.3}$$

where $M = \mu_2 / \mu_1$ is the viscosity ratio between the displaced and the displacing fluid, D_m is the molecular diffusion coefficient of the displacing solute. The coupling of these two numbers characterises both the density effect and viscosity effects on dispersion coefficients.

$$R_{\rho\mu} = Ra + R_\mu = \frac{{d_p}^2\cdot g\cdot\Delta\rho}{u\cdot\mu_1} + (\frac{\mu_2}{\mu_1}-1)\cdot\frac{u\cdot d_p}{D_m} \tag{5.4}$$

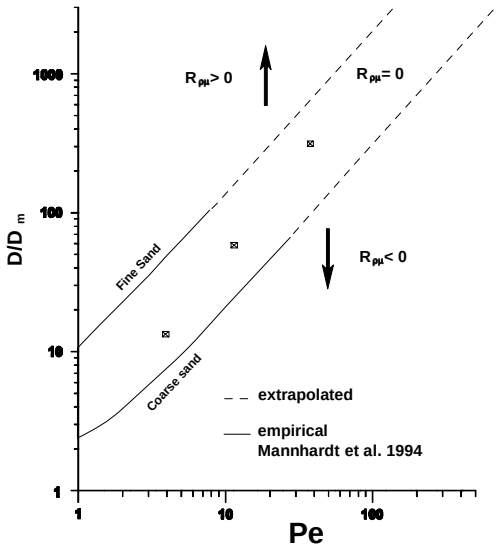

Fig. 5.26: **Schematic representation of density and viscosity effect on dispersion coefficient.**

Dispersion of an ideal tracer is a function only of PECLET number. For describing miscible displacement of non-passive solute, a modification

that relates both the density and viscosity effect to dispersion coefficient is needed.

$$D / D_m = f(R_{\rho\mu}) \cdot f(Pe) \tag{5.5}$$

where:

$$f(R_{\rho\mu}) = \begin{cases} > 1, & R_{\rho\mu} > 0 \\ = 1, & R_{\rho\mu} = 0 \\ < 1, & R_{\rho\mu} < 0 \end{cases} \tag{5.6}$$

The relationship is also shown in Fig. 5.26. Results of tracer tests are included within the two empirical line, where $R_{\rho\mu}$ = 0. If density difference and viscosity ratio between a pair of test solutions are such that the dimensionless number $R_{\rho\mu}$ is positive, a much stronger dispersion is expected. On the other hand, if $R_{\rho\mu}$ < 0, the opposing result is true.

6 SUMMARY AND DISCUSSION

With miscible displacement in a laminar flow system in porous media, significant density differences and viscosity ratio in combination with proper displacing relationship can reseult in hydrodynamic instability, which is closely coupled with other solute transport processes, for example, advection, diffusion and dispersion. Both theoretical and experimental investigations have been performed to examine the density and viscosity effect on the induced unstable flow and further on dispersion processes.

Whenever a dense solute is introduced into a porous material saturated with a static less dense solution, a vertical convection is induced. The solute is then transported downward through a coupling process of advection, hydrodynamic dispersion and molecular diffusion. With proper simplifications, an analytical similarity solution has been deduced. Based on the similarity solution, the descending rate, descending depth and rate of solute transfer have been examined. The theory of similarity regime described in this study has been found to be able to give good approximation to experimental results from literature. However, since a semi-quantitative visual technique was used in both experiments of WOODING (1963) and BACHMAT et al. (1970), only the averaged leading edge was measured. And in both cases, hydrodynamic dispersion and changes in viscosity caused by changes in solute concentration were neglected. These simplifications might have hidden some shortcomings of the present theoretical simulation.

With the help of a self designed and developed electrical technique, which has many significant advantages in comparison with other published traditional sampling method or qualitative (semi- quantitative) visualization technology, measurement of solute concentration can be carried out at any time with any time intervals without any side-effect on the displacement processes. Hence the development of the displacing front in space and time can be monitored in real time. The whole measurement procedure is controlled by a self developed QUICK BASIC programm, which is listed in Appendix II.

In order to examine the direct relationship of dispersion coefficient with fluid density and viscosity, displacing velocity and displacing relationship, salt solutions of different concentrations, which were connated in a Plexiglas column (160 cm long with a diameter of 20 cm)

filled with homogeneous quartz sand, were displaced by fluids of different density and viscosity introduced from the bottom of the column upwardly. Both stable and unstable displacements with large and small density and viscosity differences were performed in the homogeneous sand column. Results show that:

a) The classical advection-dispersion formulation is valid in describing both stable and unstable displacements with dense solution and large density and viscosity differences. For a given porous medium and flow condition, the dispersion coefficient is, however, not a constant.

b) Dependency of dispersion coefficient on density and viscosity differences is given in Fig. 4.7, Fig. 4.9 and Fig. 4.10 respectively. In the stable case, dispersion coefficient drops continually when density variations increase, whereas the dispersion coefficient increases steadily with viscosity ratios.

c) In the case of unstable displacements dispersion is enhanced by the increase of both the density and viscosity differences.

Based on the results and experience obtained, four further displacement experiments were carried out in a large Plexiglas tank (with a dimension of 600 cm long, 200 cm wide and 150 cm high) filled also with homogeneous quartz sand in a horizontal uniform flow field:

1. A 35 g/l NaCl solution displaced tap water filled in the porous medium (35 g/l NaCl solution → tap-water);
2. The 35 g/l NaCl solution was displaced by a 115 g/l glycerine solution (115 g/l glycerine solution → 35 g/l NaCl solution);
3. The third displacement was performed conversely (35 g/l NaCl solution →115 g/l glycerine solution);
4. To displace the saturated salt solution, tap water was applied (tap-water → 35 g/l NaCl solution).

Similar to those results from the 1-D column test, both stable density difference $\Delta\rho=\rho_{\text{tap-water}} - \rho_{\text{NaCl solution}}$ = -24.4 g/L and stable viscosity ratio $M = \mu_{\text{tap-water}} / \mu_{\text{NaCl solution}}$ = 0.9462 <1 in the first stable miscible displacements in the large scale 2-D sand tank result in the reduction of dispersion coefficient and dispersivity as well.

In the second displacement experiment in the sand tank, though it is also stable, there is only a slight density difference between the displacing and the displaced fluid pair. Except that fluctuations of flow velocity near the displacing source due to technical disturbances, for example, a few times of stop and renew start at the beginning stage, cause additional influence to the dispersion coefficient, the significant stable viscosity ratio between the test solutions alone, however, does not result in much modification to the dispersion processes.

A significant unstable viscosity ratio M = 1.262 > 1 and a small unstable density difference $\Delta\rho$ = 1.8 g/L between the pair of test solutions in the third miscible displacement test in the sand tank results in throughout a slightly even modification to the dispersion coefficient.

Since tap-water is used to displace a 35 g/L NaCl solution in the fourth displacement experiment in the sand tank, both unstable density differences $\Delta\rho$ = 24.4 g/L and a small unstable viscosity ratio M = 1.057 act together and thus result in still stronger modification to the dispersion coefficients (see Fig. 5.19). The enlargement of the dispersion coefficient stops, however, at certain distance from the inlet side of the tank (downstream from the displacing source).

For the conditions of these experiments (low PECLET number), it appears that density differences result in much stronger modification to dispersion than viscosity ratios do.

Note that, however, the presence of large-scale heterogeneity, which is absent in the present investigation, may create sufficiently large variations in flow rate to completely mask the present density and viscosity effect. Therefore, not only the density and viscosity effect, but also the effect of heterogeneity on miscible displacements in porous media and their interactions should be included in the future study. The case in which unstable miscible displacements are at extremely low flow velocity at the beginning stage would be of great interest as well.

In future experimental investigations on miscible displacement with significant density and viscosity differences in porous medium, the following items should be taken into consideration:

- Try best to produce a step-like initial and boundary condition, because artificial disturbance could totally overshadow the hydrodynamic instability due to density and viscosity

differences. A precise and unlimited adaptable pump would be helpful.

- Miscible displacements with fluid pair having very large density differences and viscosity ratios at the same time.

- Variable fluid velocities.

- Other measurement method, such as NMR (Nuclear Magnetic Resonance) or MRI in combination with certain fluid pairs (Dimethylsulphoxid $C_2H_6O_2S$ (DMSO), Gadolinium-complex Gd, Glycerine $C_3H_8O_3$, ^3H_2O), which seems to be a promised technique in examining miscible displacements in porous media, although high expense and difficulty for measuring large size samples have prevented it from being the standard tool at present.

7 REFERENCES

ADAMS, E. W. (1987): Adding Buoyancy Effects and Particle Settling to Vest and Teach, I: Program Verification and Sample Results. - In: Sonderforschungsbereich 210 „ Strömungsmechanische Bemessungsgrundlagen für Bauwerke“, Universität Karlsruhe.

AKHMATSKAYA, E., TODD, B. D., DAVIS, P. J., EVANS, D. J., GUBBINS, K. E., POZHAR, L. A. (1997): A Study of Viscosity Inhomogeneity in Porous Media. - Journal of Chemical Physics, 106(11): 4684-4695.

ALAHYARI, A., LONGMIRE, E. K. (1994): Particle Image Velocimetry in a Variable Density flow: Application to a Dynamically Evolving Microburst. - Experiments in Fluids, 17(6): 434-440.

AL-NAAFA, M. A., SELIM, M. S.(1994): Measurement of Diffusion Coefficients by TAYLOR's Method of Hydrodynamic Stability. – AIChE Journal, 40(8): 1412-1417.

AMIN, I. E., CAMPANA, M. E. (1996): A General Lumped Parameter Model for the Interpretation of Tracer Data and Transit Time Calculation in Hydrologic Systems. - Journal of Hydrology, 179: 1-21.

ANDERSON, M. P., WOESSNER, W. W.(1992): APPLIED GROUNDWATER MODELING: Simulation of Flow and Advective Transport, 381pp, Academic Press, Inc., San Diego, California.

ARYA, A., HEWETT, T. A., LARSON, R. G., GUPTA, V. G. (1988): Dispersion and Reservoir Heterogeneity. - SEP Reservoir Eng., 3: 139-148.

ASIF, M., NARAYAN, K. A. (1990): Stability of miscible fluid displacement in a porous medium. - Ingenieur-Archiv 60: 345-349.

BACHMAT, Y., ELRICK, D. E. (1970): Hydodynamic Instability of Miscible Fluids in a Vertical Porous Column. - Water Resources Research, 6(1): 156-171.

BACRI, J. –C., RAKOTOMALALA, N., SALIN, D. (1987): Stable and unstable miscible flows through porous media. - Physics and Chemistry of Porous Media (AIP, New York), 116-128.

BACRI, J. –C., HOYOS, M., RAKOTOMALALA, N., SALIN, D., BOURLION, M., LENORMAND, R., SOUCEMARIANADIN, A. (1991): Ultrasonic diagnostic in porous media and suspensions. - J. Phys. III France 1: 1455-1466.

BACRI, J. –C., RAKOTOMALALA, N., SALIN, D., WOUMENI, R. (1992): Miscible viscous fingering: Experiments versus continuum approach. - Phys. Fluids A4(8): 1611-1619.

BAKR, A. A., GELHAR, L. W., GUTJAHR, A. L., MACMILLAN, J. R. (1978): Stochastic Analysis of Spatial Variability in Subsurface Flows, 1. Comparison of One- and Three-Dimensional Flows. - Water Resources Research, 14(2): 263-271.

BARRY, D. A., SPOSITO, G. (1990): Three-dimensional Statistical Moment Analysis of the Stanford/Waterloo Borden Tracer Data. - Water Resources Research, 26(8): 1735-1747.

BEAR, J., TODD, D. K. (1960): The Transition Zone between Fresh and Salt Waters in Coastal Aquifers. - Water Resources Center Contribution No. 29, Hydraulic Laboratory, University of California, Berkeley.

BEAR, J. (1961a): Some Experiments in Dispersion. - Journal of Geophysical Research, 66(8): 2455-2467.

BEAR, J. (1961b): On the Tensor Form of Dispersion in Porous Media. - Journal of Geophysical Research, 66(4): 1185-1197.

BEAR, J. (1972): Dynamics of Fluids in Porous Media, 764pp., Elsevier Scientific, New York.

BEAR, J. (1979): Hydraulics of Groundwater, McGRAW-HILL INTERNATIONAL BOOK COMPANY, 567pp.

BEAR, J., VERRUIJT, A.(1987): Modeling Groundwater Flow and Pollution. D. Reidel Publishing Company, Boston, MA.

BEIMS, U.(1983): Planung, Durchführung und Auswertung von Gütepumpversuchen. - Zeitschrift für angewandte Geologie, 29(10): 482-490.

BEJAN, A. (1980): Natural Convection in a Vertical Cylindrical Well Filled with Porous Medium. - Int. J. Heat Mass Transfer, 23: 726-729.

BIGGAR, J. W., NIELSEN, D. R.(1964): Chloride-36 Diffusion during Stable and Unstable Flow through Glass Beads. - Soil Sci. Soc. Am. Proc..28:591-594.

BJERG, P. L., AMMENTORP, H. C., CHRISTENSEN, T. H.(1993): Model Simulations of a Field Experiment on Cation Exchange-Affected Multicomponent Solute Transport in a Sandy Aquifer. - Journal of Contaminant Hydrology, 12: 291-311, Elsevier Science Publishers B.V., Amsterdam.

BOGGS, J. M., YOUNG, S. C., BEARD, L. M., GELHAR, L. W., REHFELDT, K. R., ADAMS, E. E.(1992): Field Study of Dispersion in a Heterogeneous Aquifer, 1. Overview and Site Description. - Water Resources Research, 28(12): 3281-3291.

BOUHROUM, A.(1985): Beitrag zur Verdrängung mischbarer Flüssigkeiten in porösen Medien unter Berücksichtigung der Dichte - und Viskositäts - Unterschiede. Genehmigte Dissertation von der Fakultät für Bergbau, Hüttenwesen und Maschinenwesen der Technischen Universität Clausthal.

BREIER, J., GATZMANGA, H., KATHE, H.(1971): Betriebliches Dichtemessgerät. - Mess. Steuern Regeln, Beil. Automatisierung, 8(3), 56.

BREIER, J.(1980): Automatisierungstechnik, Praxis Aufgaben Lösungen. 380S., VEB Verlag Technik Berlin.

BROOKER, A. M. H., TOWNLEY, L. R.(1994): Flow and Solute Transport through a Leeve Separating Fluids with Different Densities. - Water Resources Research, 30(6): 1847-1856.

BRUSSEAU, M. L.(1964): Transport of Reactive Contaminants in Heterogeneous Porous Media. - Rev. Geophys., 32: 285-313.

BUES, M. A., AACHIB, M.(1991): Influence of the Heterogeneity of the Parameters of Miscible Displacement in a Saturated Porous Medium. - Exp. Fluids, 11: 25-32.

BUSCHECK, T. A., DOUGHTY, C., TSANG, C. F.(1983): Prediction and Analysis of a Field Experiment on a Multi-layered Aquifer Thermal Energy Storage System with Strong Buoyancy Flow. - Water Resources Research, 19(5): 1307-1316.

CALA, M. A., GREENKORN, R. A.(1986): Velocity Effects on Dispersion in Porous Media, With a single Heterogeneity. - Water Resources Research, 22(6): 919-926.

CHAMBERS, L. W., BAHR, J. M.(1992): Tracer Test Evaluation of a Drainage Ditch Capture Zone. - Ground Water, 30(5): 667-675.

CHANG, S.-H., SLATTERY, J. C. (1986): A linear stability analysis for miscible displacement. - Transport in Porous Media 1: 179-199.

CHANG, S.-H., SLATTERY, J. C. (1988a): Stability of vertical miscible displacements with developing density and viscosity gradients. - Transport in Porous Media 3: 277-297.

CHANG, S.-H., SLATTERY, J. C. (1988b): A new description for dispersion. - Transport in Porous Media 3: 515-527.

CHANG, S.-H., SLATTERY, J. C. (1989): The effect of dispersion model on the linear stability of miscible displacement in porous media. - Transport in Porous Media 4: 85-96.

CHRISTIE, M. A., JONES, A. D. W., MUGGERIDGE, A. H.(1990): Comparison between Laboratory Experiments and Detailed Simulations of Unstable Miscible Displacement Influenced by Gravity. – North Sea Oil and Gas Reservoirs-II, The Norwegian Institute of Technology (Graham & Trotman Eds.), 244-250.

CLARKE, A. L.(1967): Dichtebestimmungen an geringen Flüssigkeitsmengen. - J. Sci. Instrum., 44(5): 382-384.

CORAPCIOGLU, M. Y., HOSSAIN, M. A.(1990): Ground-Water Contamination by High-Density Immiscible Hydrocarbon Slugs in Gravity-Driven Gravel Aquifers. - Ground Water, 28(3): 403-412.

COSKUNER, G., BENSTEN, R. G.(1987): Prediction of Instability for Miscible Displacements in a Hele-Shaw Cell. - Rev. Inst. Fr. Pet., 42(2): 151-162.

DAGAN, G.(1986): Statistical Theory of Groundwater Flow and Transport: Pore to Laboratory, Laboratory to Formation, Formation to Regional Scale. - Water Resources Research, 22: 120-135.

DANE et al. (1991): Stability and mixing of dense aqueous phase plumes in porous media. - EOS Trans. Amer. Geophysics Union, 72, 126.

DAUS, A. D., FRIND, E. O., SUDICKY, E. A.(1985): Comparative Error Analysis in Finite Element Formulations of the Advection-Dispersion Equation. - Adv. Water Resour., 8: 86-95.

de JOSSELIN de JONG, G.(1960): Singularity Distributions for the Analysis of Multiple Fluid Flow through Porous Media. J. Geophys. Res., 65(11): 3739-3758.

de MARSILY, G.(1986): Quantitative Hydrogeology, 440pp., Academic, San Diego, Calif..

DELHOMME, J. P.(1979): Spatial Variability and Uncertainty in Groundwater Flow Parameters: A Geostatistical Approach. - Water Resources Research, 15(2): 269-280.

DOMENICO, P. A., ROBBINS, G. A.(1984): A Dispersion Scale Effect in Model Calibrations and Field Tracer Experiments. - J. Hydrol., 7: 123-132.

DOMENICO, P. A., SCHWARTZ, F. W.(1990): Physical and Chemical Hydrogeology, 824pp., John Wiley & Sons, Inc.

DORGARTEN, H. -W.(1989): Das Verhalten hydrophober Stoffe in Boden und Grundwasser. -Diss., 125S.; Aachen.

DORGARTEN, H.-W., TSANG, C.-F.(1991): Modeling the Density-Driven Movement of Liquid Wastes in Deep Sloping Aquifers. - Ground Water, 29(5): 655-662.

DUDGEON, C.R.(1967): Wall Effects in Permeameters. - Journal of the Hydraulics Division, ASCE, Vol. 93, No. HY5, Seite 137 -148.

ELDER, J. W.(1967): Transient Convection in a Porous Medium. - J. Fluid Mech., 27(3): 609-623.

ELRICK, D. E., ERH, K. T., KRUPP, H. K.(1966): Application of Miscible Displacement Techniques to Soils. - Water Resources Research, 2(4): 717-727.

EVANS, D. G., NUNN, J. A., HANOR, J. S.(1991): Mechanisms Driving Groundwater Flow near Salt Domes. - Geophs. Res. Lett., 18(5): 927-930.

EVANS, D. G., RAFFENSPERGER, J. P.(1992): On the Stream Function for Variable-Density Groundwater Flow. - Water Resources Research, 28(8): 2141-2145.

FAN, Y., KAHAWITA, R.(1994): A Numerical Study of Variable Density Flow and Mixing in Porous Media. - Water Resources Research, 30(10): 2707-2716.

FISCHER, H. B., LIST, E. J., KOH, R. C. Y., IMBERGER, J., BROOKS, N. H.(1979): Mixing in Inland and Coastal Waters. ACADEMIC PRESS, 483S.

FOGG, G. E., SENGER, R. K.(1985): Automatic Generation of Flow Nets with Conventional Ground-water Modeling Algorithms. - Ground Water, 23(3): 336-344.

FREEZE, R. A.(1975): A Stochastic-Conceptual Analysis of One-Dimensional Groundwater Flow in Nonuniform Homogeneous Media. - Water Resources Research, 11(5): 725-741.

FREEZE, R. A., CHERRY, J. A.(1979): Groundwater, Printice-Hall, Englewood Cliffs, N. J..

FREYBERG, D. L.(1986): A Natural Gradient Experiment on Solute Transport in a Sand Aquifer, 2. Spatial Moments and the Advection and Dispersion of Nonreactive Tracers. - Water Resources Research, 22(13): 2031-2046.

FRIED, J. J.(1975): Groundwater Pollution, 330pp, American Elsevier Publishing Company, INC., New York.

FRIND, E. O.(1982): Simulation of Long-Term Transient Density-Dependent Transport in Groundwater. - Adv. Water Resour., 5: 73-97.

FRIND, E. O., MATANGA, G. B.(1985): The Dual Formulation of Flow of Contaminant Transport Modeling, 1, Review of Theory and Accuracy Aspects. - Water Resources Research, 21: 159-169.

GARABEDIAN, S. P., LEBLANC, D. R., GELHAR, L.W., CELIA, M.A.(1991): Large-scale Natural Gradient Tracer Test in Sand and Gravel, Cape Cod, Massachusetts. 2. Analysis of Spatial Moments for a nonreactive Tracer. - Water Resources Research, 27(5): 911-924.

GARVEN, G., FREEZE, R. A.(1984): Theoretical Analysis of the Role of Ground-water Flow in the Genesis of Stratabound ore Deposits, 1, Mathematical and Numerical Model. - Am. J. Sci., 284:1085-1124.

GARVEN, G.(1986): The Role of Regional Fluid Flow in the Genesis of the Pine Point Deposit, Western Canada Sedimentary Basin—A Reply. - Econ. Geol., 81(4): 1015-1020.

GEBHART, B., JALURIA, Y., MAHAJAN, R. L., SAMMAKIA, B.(1988): Buoyancy-Induced Flows and Transport, 1001pp, Hemisphere Publishing Corporation, Washington

GELHAR, L. W., GUTJAHR, A. L., NAFF, R. L.(1979): Stochastic Analysis of Macrodispersion in a Stratified Aquifer. - Water Resources Research, 15(6): 1387-1397.

GELHAR, L. W.(1986): Stochastic Subsurface Hydrology from Theory to Application. - Water Resources Research, 22(1): 135-145.

GELHAR, L. W.(1993): Stochastic Subsurface Hydrology, 390pp., Printice Hall, Englewood Cliffs, NJ.

GERMANN, P. F.(1991): Length scales of convection - dispersion approaches to flow and transport in porous media. - Journal of Contaminant Hydrology, Vol.7, Seite 39 - 49.

GLASS, R. J., PARLANGER, J.-Y., STEENHUIS, T. S.(1989a): Wetting Front Instability, 1, Theoratical Discussion and Dimensional Analysis. - Water Resources Research, 25(6): 1187-1194.

GLASS, R. J., STEENHUIS, T. S., PARLANGER, J.-Y.(1989b): Wetting Front Instability, 2, Experimental Determination of Relationships between System Parameters and Two-Dimensional Unstable Flow Field Behavior in Initially Dry Media. - Water Resources Research, 25(6): 1195-1207.

GOMIS, V., BOLUDA, N., RUIZ, F.(1996): Application of a Model for Simulating Transport of Reactive Multispecies Components to the Study of the Hydrochemistry of Salt Water Intrusions. - Journal of Contaminant Hydrology, 22: 67-81, Elsevier Science Publishers B.V., Amsterdam.

GUILLOT, G., KASSAB, G., HULIN, P., RIGORD, P. (1991): - Monitoring of tracer dispersion in porous media by NMR imaging. - J. Phys. D: Appl. Phys., 24: 763-773.

GUTJAHR, A. L., GELHAR, L. W., BAKR, A. A., MACMILLAN, J. R.(1978): Stochastic Analysis of Spatial Variability in Subsurface Flow, 2, Evaluation and Application. - Water Resources Research, 14(5): 953-959.

GÜVEN, O. R., FALTA, R. W., MOLTZ, F. J., MELVILLE, J. G.(1986): A Simplified Analysis of Two Well Tracer Tests in Stratified Aquifers. - Ground Water, 24(1): 63-71.

HASSANIZADEH, M., GARY, W. G.(1979a): General conservation equations for multi phase systems: 1. Averaging procedure. Advances in Water Resources, Vol.2, 131-144.

HASSANIZADEH, M., GARY, W. G.(1979b): General conservation equations for multi phase systems: 2. Mass, energy and

entropy equations. Advances in Water Resources, Vol.2, 191-203.

HASSANIZADEH, M., GARY, W. G.(1980): General conservation equations for multi phase systems: 3. Constitutive theory for porous media. Advances in Water Resources, Vol.3, 25-40.

HASSANIZADEH, M.((1986a): Derivation of basic equations of mass transport in porous media, Part 1. Macroscopic balance laws. Advances in Water Resources, Vol. 9, 196-206.

HASSANIZADEH, S. M.(1986b): Derivation of basic equations of mass transport in porous media, Part 2. Generalized DARCY's and Fick's laws. Advances in Water Resources, Vol. 9, 207-222.

HASSANIZADEH, S. J., LEIJNSE, T.(1988): On the Modeling of Brine Transport in Porous Media. Water Resources Research, 24(2): 321-330.

HAYWORTH et al. (1991): Experimental studies of dense solute plumes in porous media. - EOS trans. Amer. Geophys. Union, 72, 130.

HELLER, J. P. (1965): Onset of instability patterns between miscible fluids in porous media. - J. Appl. Phys. 37: 1566-1579.

HERBERT, A. W., JACKSON, C. P., LEVER, D. A.(1988): Coupled Groundwater Flow and Solute Transport with Fluid Density Strongly Dependent upon Concentration. Water Resources Research, 24(10): 1781-1795.

HICKERNELL, F. J., YORTSOS, Y. C. (1986): Linear stability of miscible displacement processes in porous media in the absence of dispersion. - Studies in Applied Mathematics, 74: 93-115.

HICKEY, J. J.(1989): Circular Convection during Subsurface Injection of Liquid Waste, St. Petersburg, Florida. - Water Resources Research, 25(7): 1481-1494.

HILL, S. (1952): Channelling in packed columns. - Chemical Engineering Science, 1(6): 247-253.

HOLM, L.W.(1986): Miscibility and Miscible Displacement. – Journal of petroleum Technology, 8: 817-818.

HOLZBECHER, E.(1998): Modeling Density -Driven Flow in Porous Media, 284pp., Springer Verlag.

HOMSY G. M., SHERWOOD, A. E. (1976): Convective instabilities in porous media with through flow. - AIChE Journal, 22(1): 168-174.

HOPMANS, J. W., DANE, J. H.(1986): Calibration and Use of a Dual-Energy Gamma Radiation System for Multiple Point Measurements in a Soil. - Water Resources Research, 22(??): 1109-1114.

HU, Q., BRUSSEAU, M. L.(1995): Dispersive-Diffusive Transport of Non-sorbed Solute in Multicomponent Solutions. - Journal of Contaminant Hydrology, 19: 261-267.

HUYAKORN, P. S., ANDERSON, P. F., MERCER, J. W., WHITE, H. O.,Jr.(1987): Saltwater Intrusion in Aquifers: Development and Testing of a Three-Dimensional Finite Element Model. - Water Resources Research, 23(2): 293-312.

HYDROCOIN- The international HYDROCOIN Project, Level 1: code verification, OECD, Paris, 198p, 1988.

HYDROCOIN- The international HYDROCOIN Project, Level 2: model validation, OECD, Paris, 194p, 1990.

INTRAVAL (1992) -The international INTRAVAL project, Phase 1, Test case 13, Experimental Study of Brine Transport in Porous Media (Edited by P. GLASBERGEN).

ISAACS, L. T., HUNT, B.(1986): A Simple Approximation for a Moving Interface in a Coastal Aquifer. - Journal of Hydrology, 83: 29-43, Elsevier Science Publishers B.V., Amsterdam.

ISTOK, J. D., HUMPHREY, M. D. (1995): Laboratory Investigation of Buoyancy-Induced Flow (Plume Sinking) During Two-Well Tracer Tests. - Ground Water, 33(4): 597-604.

JIAO, C. (2000) : Free convection and hydrodynamic instability of miscible fluids in a vertical porous column. – in: Proceedings of the Fourth Engineering Mechanics Conference (EM2000) of the American Society of Civil Engineers, May 21-24, 2000, Department of Civil Engineering, The University of Texas at Austin.

JOHNS, R. T., RIVERA, A.(1996): Comment on „Dispersive Transport Dynamics in a Strongly Coupled Groundwater-Brine Flow System“ by Curtis M. Oldenburg and Karsten Preuss. - Water Resources Research, 32(11): 3405-3410.

KÄSS, W.(1992): Geohydrologische Markierungstechnik, Lehrbuch der Hydrogeologie, 9. Berlin - Stuttgart (Bornträger), S.519.

KESTIN, J., KHSLIFA, H. E., CORREIA, R. J.(1981): Tables of the Dynamic and Kinematic Viscosity of Aqueous NaCl Solutions in the Temperature Range 20-150^{o}C and the Pressure Range 0.1-35 Mpa. - J. Phys. Chem. Ref. Data, 10: 71-87.

KIMMEL, A. E., BRAIDS, O. C.(1980): Leachate Plumes in Ground Water from Babylon and Islip Landfill, Long Island, New York. - U.S. Geol. Surv. Prof. Pap., 1085.

KINZELBACH, W.(1987): Numerische Methoden zur Modelliering des Transports von Schadstoffen im Grundwasser. R. Oldenbourg Verlag München Wien.

KINZELBACH, W.(1992): Numerische Methoden zur Modellierung des Transports von Schadstoffen im Grundwasser. – Aufl., Schriftenreihe gwf Wasser, Abwasser, Nr. 21: 343 S., Oldenbourg, München, Wien.

KINZELBACH, W. & RAUSCH, R. (1995): Grundwassermodellierung. – 283 S., Bornträger, Berlin, Stuttgart.

KIRKNER, D. J., REEVES, H.(1988): Multi-component Mass Transport with Homogeneous and Heterogeneous Chemical Reactions: Effect of the Chemistry on the Choice of Numerical Algorithm, 1, Theory. - Water Resources Research, 24: 1719-1729.

KNOPMAN, D. S., VOSS, C. I., GARABEDIAN S. P.(1991): Sampling Design for Groundwater Solute Transport: Tests of Methods and Analysis of Cape Cod Tracer Test Data. - Water Resources Research, 27(5): 925-949.

KOCH, D. L., BRADY, J. F.(1986): The Effective Diffusivity of Fibrous Media. – AIChe Journal, 32(4): 575-591.

KOCH, D. L., BRADY, J. F.(1987a): Nonlocal dispersion in porous media: nonmechanical effects. – Chemical Engineering Science, 42(6): 1377-1392.

KOCH, D. L., BRADY, J. F.(1987b): The symmetry properties of the effective diffusivity tensor in anisotropic porous media. – Phys. Fluids, 30(3): 642-650.

KOCH, D. L., BRADY, J. F.(1988): Anomalous diffusion in heterogeneous porous media. – Phys. Fluids, 31(5): 965-973.

KOCH, D. L., BRADY, J. F.(1989a): Anomalous diffusion due to long - range velocity fluctuations in the absence of a mean flow. – Phys. Fluids, **A 1** (1): 47-51.

KOCH, D. L., BRADY, J. F.(1989b): The effect of order on dispersion in porous media. – Journal of Fluid Mechanics, 200: 173-188.

KOCH, M., ZHANG, G.(1992): Numerical Simulation of the Effects of Variable Density in a Contaminant Plume. - Ground Water, 30(5): 731-742.

KONG, D., HARMON, T. C.(1996): Using the Multiple Cell Balance Method to Solve the Problem of Two-dimensional Groundwater Flow and Contaminant Transport with Nonequilibrium Sorption. - Journal of Contaminant Hydrology, 23: 285-301.

KRUPP, H. K., ELRICK, D. E.(1969): Density Effects in Miscible Displacement Experiments. - Soil Sci., 107(5): 372-380.

KUIPER, L. K.(1983): A Numerical Procedure for the Solution of Steady State Variable Density Groundwater Flow Equation. - Water Resources Research, 19(1): 234-240.

LARKIN, R. G., CLARK, J. E., PAPADEAS, P. W.(1994): Comparison of Modeled Disposal Well Plumes Using Average and Variable Injectate Densities. - Ground Water, 32(1): 35-40.

LEBLANC, D. R., GARABEDIAN, S. P., HESS, K. M., GELHAR, L. W., QUADRI, R. D., STOLLENWER, K. G., WOOD, W. W.(1991): Large-scale Natural Gradient Tracer Test in Sand and Gravel, Cape Cod, Massachusetts, 1. Experimental Design and Observed Tracer Movement. - Water Resources Research, 27(5): 895-910.

LEBON, L., LEBLOND, J., HULIN, J. P. (1997): Experimental-Measurement of Dispersion Processes at short Times Using a Pulsed-Field Gradient NMR Technique. – Physics of Fluids, 9(3): 481-490.

LEE, C.-H., CHENG, R. T.-S.(1974): On Seawater Encroachment in Coastal Aquifers. - Water Resources Research, 10(5): 1039-1043.

LENHARD, R. J., OOSTROM, M., SIMMONS, C. S., WHITE, M. D.(1995): Investigation of Density-Dependent Gas Advection of Trichloroethylene: Experiment and a Model Validation Exercise. - Journal of Contaminant Hydrology, 19: 47-67.

LEROY, C., HULIN, P., LENORMAND, R. (1992): Tracer dispersion in stratified porous media: influence of transverse dispersion and gravity. - J. of Contaminant Hydrology, 11: 51-68.

LIST, E. J.(1965): The stability and mixing of a density-stratified horizontal flow in a saturated porous medium, 164pp, W. M. Keck Laboratory of Hydraulics and Water Resources, Division of Engineering and Applied Science, California Institute of Technology, Pasadena, California.

LIU, H. H., DANE, J. H.(1996): An Interpolation-corrected Modified Method of Characteristics to Solve Advection- Dispersion Equations, Adv. Water Res., 19: 359-368.

LIU, H. H., DANE, J. H.(1997): A Numerical Study on Gravitational Instabilities of Dense Aqueous Phase Plumes in Three-

dimensional Porous Media. - Journal of Hydrology, 194: 126-142.

LIU, P. L-F., CHENG, A. H-D., LIGGETT, J. A.(1981): Boundary Integral Equation Solutions to Moving Interface between Two Fluids in Porous Media. - Water Resources Research, 17(5): 1445-1452.

MACFARLANE, D. S., CHERRY, J. A., GILLHAM, R. W., SUDICKY, E. A.(1983): Migration of Contaminants in Groundwater at a Landfill: A Case Study, 1, Groundwater Flow and Plume Delineation. - Journal of Hydrology, 63: 1-29.

MANNHARDT, K., NASR-EL-DIN, H. A. (1994): A Review of One-Dimensional Convection-Dispersion Models and Their Applications to Miscible Displacement in Porous Media. – In Situ, 18(3): 277-345.

MANICKAM, O., HOMSY, G. M. (1993): Stability of miscible displacements in porous media with nonmonotonic viscosity profiles. - Phys. Fluids A 5(6): 1356-1367.

MANICKAM, O., HOMSY, G. M. (1994): Simulation of viscous fingering in miscible displacements with nonmonotonic viscosity profiles. - Phys. Fluids 6(1): 95-107.

MANICKAM, O., HOMSY, G. M. (1995): Fingering instabilities in vertical miscible displacement flows in porous media. - J. Fluid Mech., 288: 75-102.

MARLE, C. M.(1981): Multiphase Flow in Porous Media, 257pp., Gulf, Houston, Texas.

MAS-PLA, J., YEH, T.-C. J., MCCARTHY, J. F., WILLIAMS, T. M.(1992): A Forced Gradient Tracer Experiment in a Coastal Sandy Aquifer, Georgetown Site, South Carolina. - Ground Water, 30(6): 958-964.

MATHERON, G., MARSILY, G. DE(1980): Is Transport in Porous Media Always Diffusive? A Counterexample. - Water Resources Research, 16(5): 901-917.

MATTHEß, G.(1990): Die Beschaffenheit des Grundwassers, Lehrbuch der Hydrogeologie, 2, Berlin - Stuttgart (Bornträger), S. 498.

MATTHEß, G., UBELL, K.(1983): Allgemeine Hydrogeologie Grundwasserhaushalt, Lehrbuch der Hydrogeologie, 1, Berlin - Stuttgart (Bornträger), S. 438.

MENDOZA, C. A., FRIND, E. O.(1990a): Advective-dispersive Transport of Dense Organic Vapors in the Unsaturated Zone, 1, Model Development. - Water Resources Research, 26(3):379-387.

MENDOZA, C. A., FRIND, E. O.(1990b): Advective-dispersive Transport of Dense Organic Vapors in the Unsaturated Zone, 2, Sensitivity Analysis. - Water Resources Research, 26(3):388-398.

MILLER, D. G., TING, A. W., RARD, J. A., EPPSTEIN, L. B.(1986): Ternary Diffusion Coefficients of the Brine Systems NaCl (0.5M)-Na_2SO_4(0.5M)-H_2O and NaCl (0.489M)-$MgCl_2$ (0.051M)-H_2O (Seawater Composition) at 25°C. - Geochimica et Cosmochimica Acta, 50: 2397-2403

MOLTYANER, G. L., KILLEY, R. W. D.(1988): Twin Lake Tracer Tests: Longitudinal Dispersion. - Water Resources Research, 24(10): 1613-1627.

MORGENSTERN, R.(1974): Verschiedene Dichtemessungsarten mit Praxisbeispielen vorgestellt. - Maschinenmarkt, 80(78): 1519-1522.

MOSER, H.(1995): Einfluß der Salzkonzentration auf die hydrodynamische Dispersion im porösen Medium. Techn. Univ. Berlin, Inst. für Wasserbau und Wasserwirtschaft, Mitteilung 128, 95p.

MOTZ, L. H.(1995): Discussion of „A Density-dependent Flow and Transport Analysis of the Effects of Groundwater Development in a Freshwater Lens of Limited Areal Extent: The Geneva Area (Florida, U.S.A.) Case Study“, by Panday et al. (1993). - Journal of Contaminant Hydrology, 18: 321-326.

MOURSI, A. M., MCCORQUODALE, J. A., EL-SEBAKHY, I. S.(1995): Experimantal Studies of Heavy Radial Density Currents. - Journal of Environmental Engineering, 121(12): 920-929.

MULQUEEN, J., KIRKHAM, D.(1972): Leaching of a Surface Layer of Sodium Chloride into tile Drains in a Sand-tank Model. - J. Soil Sci. Soc. Amer, 36: 3-9.

NELSON, R. W.(1978): Evaluating the Environmental Consequences of Groundwater Contamination, 2, Obtaining Location/Arrival Time and Location/Outflow Quantity Distributions for Steady Flow Systems. - Water Resources Research, 14(3): 416-428.

NEUMAN, S. P., WITHERSPOON, P. A.(1970): Finite Element Method of Analyzing Steady Seepage with a Free Surface. - Water Resources Research, 6(3): 889-897.

NEUMAN, P. S.(1990): Universal Scaling of Hydraulic Conductivities and Dispersivities in Geological Media. - Water Resources Research, 26(8): 1749-1758.

NIELD, D. A., BEJAN, A. (1992): Convection in Porous Media, 408 pp., Springer-Verlag, Berlin.

NIELSEN, D. R., BIGGAR, J. W.(1961): Miscible Displacement in Soils, I. Experimantal Information. Soil Sci. Soc. Am. Proc., 25: 1-5

OGATA, A.(1970): Theory of Dispersion in a Granular Medium. -in: Geological Survey Professional Paper, 411-I: Fluid Movement in Earth Materials, 33pp; United States Government Printing Office; Washington.

OHLENBUSCH, R.(2001): Numerische Modellrechnung zur Ausbreitung von Inhaltsstoffen aus Weichgelinjektionssohlen – Schr. Angew. Geol., Nr. 60, Univ. Karlsruhe, Karlsruhe.

OLDENBURG, C. M., PRUESS, K.(1995): Dispersive Transport Dynamics in a Strongly Coupled Groundwater-Brine Flow System. - Water Resources Research, 31(2): 289-302.

OOSTROM, M., HAYWORTH, J. S., DANE, J. H., GÜVEN, O.(1992a): Behavoir of Dense Aqueous Phase Leachate Plumes in

Homogeneous Porous Media. - Water Resources Research, 28(8): 2123-2134.

OOSTROM, M., DANE, J. H., GÜVEN, O., HAYWORTH, J. S.(1992b): Experimental Investigation of Dense Solute Plumes in an Unconfined Aquifer Model. - Water Resources Research, 28(9): 2315-2326.

OPHORI, D. U. (1998): The significance of viscosity in density dependent flow of groundwater. - J. of Hydrology 204: 261-270.

OSTERCAMP, W. R., WOOD, W. W. (1987): Playa-lake basins on the southern high plains of Texas and New Mexico, I. Hydrologic, geometric, and geological evidence for their development. – Geol. Soc. Am. Bull., 99: 215-223.

OSWALD, S., SCHWARZ, C., KINZELBACH, W. (1996): Benchmarking in numerical modeling of density driven flow. – in: Proc. Of 14th Salt Water Intrusion Meeting SWIM 96, report No. 87, Geological Survey of Sweden, Uppsala, Sweden, 32-40.

PARK, N.(1996): Closed-Form Solutions for Steady State Density-Dependent Flow and Transport in a Vertical Soil Column. - Water Resources Research, 32(5): 1317-1322.

PARKER, J. C.(1989): Multiphase Flow and Transport in Porous Media. - Rev. Geophys., 27(2): 311-328.

PASCHKE, N. W., HOOPES, J. A.(1984): Buoyant Contaminant Plumes in Groundwater. - Water Resources Research, 20(9): 1183-1192.

PASSINIEMI, P.(1982): THEORY AND MEASUREMENT OF TRACER DIFFUSION IN ELECTROLYTES. Tracer Diffusion Coefficient of ^{22}NaCl and Na^{36}Cl in Aqueous Sodium Chloride at 298.15 K Measured with Closed Cappillary Method. Thesis for the degree of Doctor of Technology, Helsinki University of Technology Laboratory of Physical Chemistry, Espoo, Finland.

PATANKAR, S. V.(1980): Numerical Heat Transfer and Fluid Flow. - in: series in computational methods in mechanics and thermal sciences, MINKOWYCZ, W. J., SPARROW, E. M., editors, HEMISPHERE PUBLISHING CORPORATION

PETERSON, F. L., WILLIAMS, J. A., WHEATCRAFT, S. W.(1978): Waste Injection into a Two-Phase Flowfield: Sand Box and Hele-Shaw Models Study. - Ground Water, 16: 410-416.

PETITJEANS, P., MAXWORTHY, T.(1996): Miscible displacements in a capillary tubes. Part 1. Experiments. – Journal of Fluid Mechanics, 326: 37-56.

PHILLIPS, O. M.(1991): Flow and Reactions in Permeable Rocks, 285pp., Cambridge University Press, New York.

PICKENS, J. F., GRISAK, G. E.(1981): Scale-Dependent Dispersion in a Stratified Granular Aquifer. - Water Resources Research, 17(4): 1191-1211.

PINDER, G. F., COOPER, JR., H. H.(1970): A Numerical Technique for Calculating the Transient Position of the Saltwater Front. - Water Resources Research, 6(3): 875-882.

PINDER, G. F., FRIND, O. E.(1972): Application of Galerkin's Procedure to Aquifer Analysis. - Water Resources Research, 8(1): 108-120.

QUINLAN, J. F.(1986): Ground-water Tracers (119 References). - Ground Water, 24(3): 396-397.

QUINTARD, M., BERTIN, H., PROUVOST, L. (1987): Criteria for the stability of miscible displacement through porous columns. - Chem.-Ing.-Tech., 59: 354-355.

RANGANATHAN, V., HANOR, J. S.(1988): Density-driven Groundwater Flow near Salt Domes. - Chemical Geology, 74: 173-188, Elsevier Science Publishers B.V., Amsterdam.

RAJARAM, H., GELHAR, L. W.(1991): Three-dimensional Spatial Moments Analysis of the Borden Tracer Test. - Water Resources Research, 27(6): 1239-1251.

REILLY, T. E., GOODMAN, A. S.(1987): Analysis of Saltwater Upconing beneath a Pumping Well. - Journal of Hydrology, 89: 169-204; Amsterdam.

RIGORD, P., Leroy, C., CHARLAIX, E., BAUDET, C., GUYON, E., HULIN, J. P. (1990): Reversible and irreversible tracer dispersion in porous media. - J. Phys.: Condens. Matter 2, SA437-SA442.

ROGERSON, A., MEIBURG, E. (1993a): Shear stabilization of miscible displacement processes in porous media. - Phys. Fluids A 5 (6): 1344-1355.

ROGERSON, A., MEIBURG, E. (1993b): Numerical simulation of miscible displacement processes in porous media flow under gravity. - Phys. Fluids A 5 (11): 2644-2660.

RONEN, D., YECHIELI, Y., KRIBUS, A.(1995): Buoyancy-induced Flow of a Tracer in Vertical Conduits. - Water Resources Research, 31(5): 1167-1173.

ROSE, D. A., PASSIOURA, J. B.(1971): Gravity Segregation during Miscible Displacement. - Soil Sci., 111: 258-265.

RUBIN, H., ROTH, C.(1979): On the Growth of Instabilities in Groundwater due to Temperature and Salinity Gradients. - Advances in Water Resources, 2(6): 69-76.

RUBIN, J.(1983): Transport of Reacting Solutes in Porous Media: Relation between Mathematical Nature of Problem Formulation and Chemical Nature of Reactions. - Water Resources Research, 19(5): 1231-1252.

SAFFMAN P. G., Taylor, G. I. (1959): The penetration of a fluid into a porous medium or Hele-Shaw cell containing a more viscous liquid. - Proc. R. Soc. London Ser. A24: 312-329.

SCHACKE, W.(1970): Kontinuierliches Dichtemessgerät für Flüssigkeiten. - Mess. Steuern Regeln, Beil. Automatisierung, 7(10): 188.

SCHEIDEGGER, A. E.(1954): Statistical Hydrodynamics in Porous Media. - J. Appl. Phys., 25(8): 994-1000.

SCHEIDEGGER, A. E.(1960): The Physics of flow through Porous Media. Revised edtion, University of Toronto Press, 313pp.

SCHINCARIOL, R. A., SCHWARTZ, F. W. (1990): An Experimental Investigation of Variable Density Flow and Mixing in Homogeneous and Heterogeneous Media. - Water Resources Research, 26(10): 2317-2329.

SCHINCARIOL, R. A., SCHWARTZ, F. W., MENDOZA, C. A.(1994): On the Generation of Instabilities in Variable Density Flow. - Water Resources Research, 30(4): 913-927.

SCHINCARIOL, R. E., HERDERICK, E. A., SCHWARTZ, F. W.(1993): On the Application of Image Analysis to Determine Concentration Distributions in Laboratory Experiments. - J. Contam. Hydrol., 12(3): 197-215.

SCHMITT, R. W.(1995): The Salt Finger Experiments of Jevons(1857) and RAYLEIGH(1880). - Journal of Physical Oceanography, 25(1): 8-17.

SCHNELL, K.(2001): Hydrogeochemische Prozesse bei Weichgelinjektionen im Grundwasser – Stoffbilanzierung und potentielle Langzeitfolgen – Schr. Angew. Geol., Nr. 62, Univ. Karlsruhe, Karlsruhe.

SCHOWALTER, W. R. (1965): Stability criterion for miscible displacement of fluids from a porous medium. - A.I.Ch.E. Journal, 11(1): 99-105.

SCHRÖDER, E.(1993): Numerische und experimentelle Untersuchung der dreidimensionalen gemischten Konvektion in quaderförmigen Behältern und im Rechteckkanal.

SCHWARTZ, F. W.(1977): Macroscopic Dispersion in Porous Media: The Controlling Factors. - Water Resources Research, 13(4): 743-752.

SCHWILLE, F., WEBER, D.(1991): Modellversuche zur Schwerkraftausbreitung schwerer organischer Dämpfe in der lufthaltigen Zone (engl.). - Schr. Angew. Geol. Karlsruhe, 12: 59S.; Karlsruhe.

SEGOL, G., PINDER, G. F., GRAY, W. G.(1975): A Galerkin Element Technique for Calculating the Transient Position of the Saltwater Front. - Water Resources Research, 11(2): 343-347.

SEGOL, G., PINDER, G. F.(1976): Transient Simulation of Saltwater Intrusion in Southeastern Florida. - Water Resources Research, 12(1): 65-70.

SENGER, R. K., FOGG, G. E.(1990a): Stream Functions and Equivalent Freshwater Heads for Modeling Regional Flow of Variable-Density Groundwater, 1, Review of Theory and Verification. - Water Resources Research, 26(9): 2089-2096.

SENGER, R. K., FOGG, G. E.(1990b): Stream Functions and Equivalent Freshwater Heads for Modeling Regional Flow of Variable-Density Groundwater, 2, Application and Implications for Modeling Strategy. - Water Resources Research, 26(9): 2097-2106.

SIMMONS, C. T., NARAYAN, K. A. (1997): Mixed convection processes below a saline disposal basin. - J. of Hydrology 194: 263-285.

SMITH, L., SCHWARTZ, F. W.(1980): Mass Transport, 1. A Stochastic Analysis of Macroscopic Dispersion. - Water Resources Research, 16(2): 303-313.

SOUZA, W. R., VOSS, C. I.(1987): Analysis of an Anisotropic Coastal Aquifer System Using Variable-Density Flow and Solute Transport Simulation. - Journal of Hydrology, 92: 17-41, Elsevier Science Publishers B.V., Amsterdam.

SPOSITO, G., GUPTA, V. K., BHATTACHARYA, R. N.(1979): Foundation theories of Solute Transport in Porous Media: A Critical Review. - Advan. Water Resour., 2(2): 59-68.

STILLWATER, R., KLUTE, A.(1988): Improved Methodology for a Collinear Dual-Energy Gamma Radiation System. - Water Resources Research, 24(8): 1411-1422.

STRACK, O. D. L.(1976): A single-Potential Solution for Regional Interface Problems in Coastal Aquifers. - Water Resources Research, 12(6):1165-1174.

STRACK, O. D. L.(1995): A Dupuit-Forchheimer Model for Three-dimensional Flow with Variable Density. - Water Resources Research, 31(12): 3007-3017.

SUDICKY, E. A., CHERRY, J. A., FRIND, E. O.(1983): Migration of Contaminants in Groundwater at a Landfill: A Case Study, 4. A Natural-gradient Dispersion Test. - Journal of Hydrology, 63: 81-108.

SUDICKY, E. A.(1986): A Natural Gradient Experiment of Solute Transport in a Sand Aquifer, 1. Spatial Variability of Hydraulic Conductivity, and Ist Role in the Dispersion Process. Water Resources Research, 22(13): 2069-2082.

TAIGBENU, A., LIGGETT, J. A.(1986): A Integral Formulation Applied to the Diffusion and Boussinesq Equations. - International Journal for Numerical Methods in Engineering, 23: 1057-1079.

TAN, C. T., HOMSY, G. M. (1986): Stability of miscible displacements in porous media: Rectilinear flow. - Phys. Fluids 29(11): 3549-3556.

TAN, C. T., HOMSY, G. M. (1988): Simulation of nonlinear viscous fingering in miscible displacement. - Phys. Fluids 31(6): 1330-1338.

TAYLOR, G. I. (1953): Dispersion of soluble matter in solvent flowing slowly through a tube. - Proc. R. Soc. London Ser. A 219, 186.

TCHELEPI, H. A., ORR, Jr., F. M., RAKOTOMALALA, N., SALIN, D., WOUMENI, R. (1993): Dispersion, permeability heterogeneity, and viscous fingering: Acoustic experimental observations and particle-tracking simulations. - Phys. Fluids A 5(7): 1558-1574.

THELIANDER, H., GREN, U.(1989): Simple Algorithm for the Estimation of the Density of Aqueous Solutions Containing Two or More Different Salts. - Computers & Chemical Engineering, 13(4-5): 419-424.

TOMPSON, A. F. B.(1993): Numerical Simulation of Chemical Migration in Physically and Chemically Heterogeneous Porous Media. - Water Resources Research, 29(11): 3709-3726.

TURNER, J. S.(1973): Buoyancy Effects in Fluids. - Cambridge Monographs on Mechanics & Applied Mathematics, 367 S., Cambridge University Press, London.

VAN der MOLEN, W. H., VAN OMMEN, H. C.(1988): Transport of Solutes in Soils and Aquifers. - Journal of Hydrology, 100: 433-451.

VOSS, C. I., SOUZA, W. R.(1987): Variable Density Flow and Solute Transport Simulation of Regional Aquifers Containing a Narrow Freshwater-Saltwater Transition Zone. - Water Resources Research, 23(10): 1851-1866.

WEAST, R. C.(1989) CRC Handbook of Chemistry and Physics, CRC Press, Boca Raton, Florida.

WELTY, C., GELHAR, L. W.(1991): Stochastic Analysis of the Effects of Fluid Density and Viscosity Variability on Macrodispersion in Heterogeneous Porous Media. - Water Resources Research, 27(8): 2061-2075.

WEXLER, E. J.(1989): Analytical Solutions for One, Two, and Three-dimensional Solute Transport in Ground-water Systems with Uniform Flow. - U.S. Geol. Surv. Open File Rep., 89-56.

WICKS, C. M., HERMAN, J. S.(1996): Regional Hydrogeochemistry of a Modern Coastal Mixing Zone. - Water Resources Research, 32(2): 401-407.

WIEST, Roger, J. M. De (1969): Flow through Porous Media. ACADEMIC PRESS, New York and London.

WILLIAMS, A. E.(1997): Fluid density distribution in a high temperature, stratified thermohaline system: implications for saline hydrothermal circulation. - Earth and Planetary Science Letters., 146: 121-136.

WOOD, W. W., OSTERCAMP, W. R. (1987) : Playa-lake basins on the southern high plains of Texas and New Mexico, II, A hydrologic model and mass-balance arguments for their development. – Geol. Soc. Am. Bull., 99: 224-230.

WOODING, R. A.(1963): Free Convection of Fluid in a Vertical Tube Filled with Porous Material. - J. Fluid Mech., 13: 129-144.

WOODING, R. A.(1969): Growth of Fingers at an Unstable Diffusing Interface in a Porous Medium or Hele-Shaw Cell. - J. Fluid Mech., 39: 477-495.

YEH, G. T.(1981): On the Computation of Darcian Velocity and Mass Balance in the Finite Element Modeling of Groundwater Flow. - Water Resources Research, 17:1529-1534.

YIH, C. S.(1961): Flow on a nonhomogeneous Fluid in a Porous Medium. - J. Fluid Mech., 10: 133-140.

YIH, C.-S., ZHU, S.(1996): Selective Withdrawal from Stratified Streams. - Journal of the Australian Mathematical Society, Series B, Applied Mathematics, 38(1): 26-40.

YORTSOS, Y. C.(1987): Stability of a certain class of miscible displacement processes in porous media. - IMA Journal of Applied Mathematics, 38, 167-179.

YORTSOS, Y. C., ZEYBEK, M.(1988): Dispersion driven instability in miscible displacement in porous media. – Phys. Fluids, 31, 3511.

YORTSOS, Y. C.(1990): Instabilities in displacement processes in porous media. - J. Phys. Condensed Matter, 2, SA 443.

ZHANG, H., SCHWARTZ, F. W.(1995): Multispecies Contaminant Plumes in Variable Density Flow Systems. - Water Resources Research, 31(4): 837-847.

ZHANG, H., SCHWARTZ, F. W., SUDICKY, E. A.(1994): On the Vectorization of Finite Element Codes for High Performance Computers. - Water Resources Research, 30(12): 3553-3559.

ZHANG, H., SCHWARTZ, F. W.(1995): Multispecies Contaminant Plumes in Variable Density Flow Systems. - Water Resources Research, 31(4): 837-847.

ZIMMERMAN, W. B., HOMSY, G. M. (1991): Nonlinear viscous fingering in miscible displacement with anisotropic dispersion. - Phys. Fluids A 3(8): 1859-1872.

APPENDICES

Appendix I Technical data of RLC 100 meter

Specification

Measuring parameters:	R, L, C, Q(D), Δ, δ
Equivalent connection:	series or parallel connection
Connection of the measuring object:	four-wire line with Kelvin terminal
Measuring frequencies:	1 kHz±3%
Measuring voltages:	<2V
Selection of measuring range:	automatically or within fixed range
Polarization of the measuring object:	internal voltage source, approx. 2V
Measuring time:	max. 400 ms for R, L, C, Δ, δ

Measuring range of parameters

Measuring parameters	**Measuring range from**		**to**
R	1 mΩ	-	1.999 MΩ
L	0.1 µH	-	199.9 H
C	0.1 pF	-	1.999 mF

Measuring tolerances of R measurement

Equivalent connection	Series connection					Parallel connection		
Measuring range R(Ω)	0 -	1 2	2 20	3 200	4 2 k	5 20 k	6 200 k	7 2 M
Measuring error R	-	±%2 ± 3 dig	± %1 ± 3 dig	± %0.5 ± 2 dig			± %1 ± 2 dig	± %2 ± 3 dig

Remote control

The RLC 100 can be fully controlled and read out via the serial interface RS-232C.

Data transmission rate:	1,200 to 9,600 Bd
Length of data character:	8 bit
Numbers of STOP bits:	1
Parity:	none
Protocol:	RTS/CTS, without(NONE)
End characters on receiving:	LF(10 dec.)
End characters on transmission:	CR + LF (13 dec. + 10 dec.)
Length of input buffer:	64 characters
Length of output buffer:	256 characters

Appendix II Data acquisition program

```
10   REM ************************************************************************
12   REM *         A COMPUTER CONTROLLED DATA ACQUISITION SYSTEM                  *
14   REM ************************************************************************
16   REM * 400 electric probes are connected to 34 switches, which, in turn, are connected to *
17   REM * a measuring instrument RLC 100 through 34 switch channels (channel 101-120) *
18   REM * and (201-214) of  a DATA ACQUISITION/SWITCH UNIT (HP34970A). The      *
19   REM * switch unit and measuring instrument are controlled by a 486 computer. In this    *
20   REM * way, measured data are queried automatically and saved in a disk.     *
100  REM ************************************************************************
106  REM * NE(KK)-------------Indicator(1=measured; 0=to be measured);          *
120  REM * Nummer(I,J,K)-----Codifying of the probes(Row, Section, Level);      *
122  REM * Kanalnumber(60)--Channel number of HP34970A;                         *
123  REM * replyString$--------Queried character(measured data);               *
124  REM * scanList$------------Channel list to be scanned;                     *
125  REM * LANG----------------Character length of measured data;              *
130  REM * NSTRING$---------List of measuring probes;                          *
131  REM * NELEK(34,12)-----Probe number (channel, switch);                     *
132  REM * NR--------------------Row to be measured.                           *
190  REM ************************************************************************
200  DIM NE, LANG, Kanalnumber(60), Nummer(14, 7, 5) AS INTEGER
220  DIM Ohm#(5500), NELEK(34, 12), NE(5500)
230  DIM replyString$, scanList$, NSTRING$
300  REM ************************************************************************
302  REM *               SET BEGINNING DATE AND TIME                            *
304  REM ************************************************************************
350  II1 = INT(TIMER / 3600)
360  II2 = INT((TIMER - II1 * 3600) / 60)
370  II3 = TIMER - II1 * 3600 - II2 * 60
380  CLS
400  PRINT , "*********************************************************************"
402  PRINT , "* It begins on "; DATE$; " at "; II1; ":"; II2; ":"; II3; " .                    *"
404  PRINT , "*********************************************************************"
406  PRINT , "*                    Correct (Y/N) ?                                 *"
408  PRINT , "*        'Y' = End !!!   Input new date and time !!!                 *"
410  PRINT , "*            'N' or other key = Continue !!!                         *"
412  PRINT , "*********************************************************************"
450  INPUT A$
460  IF A$ = "y" OR A$ = "Y" THEN
470  END
480  END IF
500  CLS
510  PRINT , "*********************************************************************"
512  PRINT , "*             GIVE A NAME FOR OUTPUT DATA FILE                      *"
519  PRINT , "*********************************************************************"
520  INPUT DNAME$
521  REM ************************************************************************
523  REM * SET CHANNEL NUMBER FOR HP34970A(101~120, 201~220, 301~320)   *
525  REM ************************************************************************
```

```
526   FOR I = 1 TO 20
527   Kanalnumber(I) = 100 + I
528   NEXT I
529   FOR I = 21 TO 40
530   Kanalnumber(I) = 180 + I
531   NEXT I
532   FOR I = 41 TO 60
533   Kanalnumber(I) = 260 + I
534   NEXT I
540   REM ************************************************************************
542   REM *                      INPUT PROBE CODE                                  *
544   REM ************************************************************************
546   REM * Each probe is codified after its Level(1~5), Row(01~14) and Section (1~7).  *
549   REM ************************************************************************
550   OPEN "COD.DAT" FOR INPUT AS #7
551   FOR I = 1 TO 14
552   FOR K = 5 TO 1 STEP -1
553   FOR J = 1 TO 7
554   INPUT #7, Nummer(I, J, K)
555   NEXT J: NEXT K: NEXT I
600   REM ************************************************************************
602   REM *              ACTIVATE INTERFACE OF RLC100                              *
604   REM ************************************************************************
610   IDCL$ = CHR$(20): IREN$ = CHR$(9)
620   ILLO$ = CHR$(25): IGTL$ = CHR$(1)
700   REM ************************************************************************
702   REM *                CONFIGURE COMPUTER INTERFACE                            *
704   REM ************************************************************************
750   OPEN "com2:9600,n,8,1,CS30000,LF" FOR RANDOM AS #1
760   OPEN "com1:2400,n,8,1,CS30000,LF" FOR RANDOM AS #2
770   OPEN DNAME$ + ".DAT" FOR APPEND AS #4
780   OPEN "LPT1:" FOR OUTPUT AS #3
790   WIDTH #3, 132
800   REM ************************************************************************
802   REM *                    CONFIGURE HP34970A                                  *
804   REM ************************************************************************
810   PRINT #2, "*CLS"
820   PRINT #2, "SYSTem:REM"
900   REM ************************************************************************
902   REM *    OUTPUT THE BEGINNING DATE AND TIME IN THE OUTPUT FILE      *
904   REM ************************************************************************
930   PRINT #4, "It begins on "; DATE$; " at "; II1; ":"; II2; ":"; II3; " ."
940   PRINT #4,
950   PRINT #4,
1000  REM ************************************************************************
1002  REM *                    ACTIVATE RLC100                                     *
1004  REM ************************************************************************
1010  PRINT #1, IDCL$; IREN$; ILLO$; "*RST;*CLS"
1020  REM ************************************************************************
1022  REM *       SET OPERATING PARAMETERS FOR RLC100(RESISTANCE)          *
```

```
1024  REM ************************************************************************
1030  PRINT #1, "MODE_R"
1040  REM ************************************************************************
1042  REM *    SET OPERATING PARAMETERS (HP34970A) AND WAITING TIME       *
1044  REM ************************************************************************
1052  REM * The DMM of HP 34970A is deactivated. Waiting for  0.6 seconds.          *
1057  REM ************************************************************************
1060  PRINT #2, "INST:DMM?"
1070  INPUT #2, replyString$
1080  IF VAL(replyString$) = 1 THEN
1090  PRINT #2, "INST:DMM OFF"
1100  END IF
1110  PRINT #2, "*RST"
1120  Anfangszeit = TIMER
1121  IF Anfangszeit < (86400 - .6) THEN
1122  DO
1123  Zeit1 = TIMER - Anfangszeit
1124  LOOP UNTIL Zeit1 >= .6
1125  ELSEIF Anfangszeit = (86400 - .6) THEN
1126  DO
1127  Zeit1 = TIMER - Anfangszeit
1128  LOOP UNTIL ABS(Zeit1) >= .6
1129  ELSEIF Anfangszeit <= 86400 THEN
1130  DO
1131  Zeit1 = TIMER - Anfangszeit
1132  LOOP UNTIL Zeit1 < 0!
1133  DO
1134  Zeit1 = Anfangszeit - 86400 + .6
1135  LOOP UNTIL TIMER >= Zeit1
1136  END IF
1200  REM ************************************************************************
1202  REM *                  INPUT PROBE NUMBER                                  *
1205  REM ************************************************************************
1210  OPEN "NELEK.DAT" FOR INPUT AS #6
1220  FOR I = 1 TO 34
1230  FOR J = 1 TO 12
1240  INPUT #6, NELEK(I, J)
1250  NEXT J : NEXT I
1270  REM ************************************************************************
1272  REM *              SET INITIAL VALUE FOR VARIABLES                         *
1275  REM ************************************************************************
1300  FOR I = 1 TO 34
1310  FOR J = 1 TO 12
1320  Ohm#(NELEK(I, J)) = 0!
1330  NEXT J : NEXT I
1557  CLS
1559  PRINT , "*****************************************************************"
1561  PRINT , "*               The Row to be measured NR =?                    *"
1563  PRINT , "*****************************************************************"
1570  INPUT NR
```

```
1600   FOR IE = 1 TO 5500
1610   NE(IE) = 0
1620   NEXT IE
1700   FOR I = 1 TO 34
1710   FOR J = 1 TO 12
1711   KKK = NELEK(I, J)
1712   IF KKK = 0 GOTO 1780
1715   IF NE(KKK) = 1 GOTO 1780
1720   NSTRING$ = STR$(NELEK(I, J))
1730   K = INT(VAL(RIGHT$(NSTRING$, 1)))
1740   L = INT(VAL(NSTRING$) / 1000)
1750   M = INT((INT(VAL(NSTRING$)) - L * 1000 - K) / 10)
1760   IF M = NR GOTO 2000
1780   NEXT J
1790   GOTO 3430
2000   CLS
2200   REM ************************************************************************
2202   REM *                CLOSE A CHANNEL IN HP34970A                           *
2204   REM ************************************************************************
2310   PRINT #2, "*RST"
2324   PRINT #2, "ROUT:CLOS (@", STR$(Kanalnumber(I)), ")"
2340   REM ************************************************************************
2346   REM * To reduce contact resistance, wait for 0.6 seconds after a switch has been on.  *
2349   REM ************************************************************************
2350   DO
2351   Anfangszeit = TIMER
2352   IF Anfangszeit < (86400 - .6) THEN
2353   DO
2354   Zeit1 = TIMER - Anfangszeit
2355   LOOP UNTIL Zeit1 >= .6
2356   ELSEIF Anfangszeit = (86400 - .6) THEN
2357   DO
2358   Zeit1 = TIMER - Anfangszeit
2359   LOOP UNTIL ABS(Zeit1) >= .6
2360   ELSEIF Anfangszeit <= 86400 THEN
2361   DO
2362   Zeit1 = TIMER - Anfangszeit
2363   LOOP UNTIL Zeit1 < 0!
2364   DO
2365   Zeit1 = Anfangszeit - 86400 + .6
2366   LOOP UNTIL TIMER >= Zeit1
2367   END IF
2400   CLS
2500   FOR J = 1 TO 12
2501   KKK = NELEK(I, J)
2504   IF KKK = 0 GOTO 3385
2509   IF NE(KKK) = 1 GOTO 3385
2510   BEEP:
2520   REM ************************************************************************
2526   REM * Measurement is activated just when the key "ESC" has been tasted.     *
```

```
2529  REM ************************************************************************
2530  PRINT , "*  *  *  *  *  *  *  *  *  *  *  *  *  *  *  *  *"
2533  PRINT , "  Switch"; Kanalnumber(I); "is on ! "
2534  PRINT , " ------------------------------------------------------------"
2538  PRINT , NELEK(I, J); " is to be measured (Esc) !!!!!! "
2540  PRINT , "*  *  *  *  *  *  *  *  *  *  *  *  *  *  *  *  *"
2700  DO
2710  LOOP UNTIL INKEY$ = CHR$(27)
2720  BEEP:
3180  REM ************************************************************************
3182  REM *                  STARTING OF MEASUREMENT                             *
3184  REM ************************************************************************
3200  PRINT #1, "*WAI;MEAS?;*WAI"
3205  REM ************************************************************************
3211  REM * Measured data is to be queried by Computer through the digital channel #1.  *
3212  REM * 0 < Measuring range < 2000000 ohm, otherwise 'Overflow'                     *
3213  REM * Some bad probes as 2061, 4083 will be erased.                               *
3216  REM ************************************************************************
3220  DO
3225  INPUT #1, replyString$
3230  LANG = LEN(replyString$)
3240  LOOP UNTIL LANG > 0
3250  PRINT , "R"; NELEK(I, J); " = "; replyString$
3260  Ohm#(NELEK(I, J)) = VAL(RIGHT$(replyString$, LANG - 3))
3261  IF KKK = 2061 OR KKK = 4083 GOTO 3384
3262  IF Ohm#(NELEK(I, J)) > 2000000 THEN
3263  PRINT #1, "*RST"
3269  CLS
3270  PRINT , "R"; NELEK(I, J); " > "; "2000000 !!!"
3271  PRINT , "*       Acceptable(Y/N)?              *"
3272  PRINT , "*     *     *     *     *     *     *"
3273  BEEP
3274  INPUT a$
3275  IF a$ = "n" OR a$ = "N" GOTO 2510
3276  END IF
3384  NE(KKK) = 1
3385  NEXT J
3386  BEEP: BEEP
3390  REM ************************************************************************
3392  REM *           OPEN THE CLOSED CHANNEL IN HP34970A                          *
3394  REM ************************************************************************
3400  PRINT #2, "ROUT:OPEN (@", STR$(Kanalnumber(I)), ")"
3420  PRINT #2, "*RST"
3430  NEXT I
4000  REM ************************************************************************
4007  REM *       Measured data is saved in Row sequence (1~14).                   *
4009  REM ************************************************************************
4530  FOR K = 5 TO 1 STEP -1
4540  FOR J = 1 TO 7
4560  IF Nummer(NR, J, K) = 1000 THEN
```

```
4570  PRINT #4, "   1E-6   ";
4580  ELSEIF ABS(Ohm#(Nummer(NR, J, K))) > 2000000# THEN
4590  PRINT #4, " Overflow ";
4600  ELSE
4610  PRINT #4, " "; Ohm#(Nummer(NR, J, K)); " ";
4620  END IF
4630  NEXT J
4640  PRINT #4,
4650  NEXT K
4660  PRINT #4,
4670  PRINT #4,
4680  BEEP: BEEP: BEEP: BEEP
4700  REM ************************************************************************
4702  REM *         A Row of probes has been successfully measured.                *
4704  REM ************************************************************************
4710  II1 = INT(TIMER / 3600)
4720  II2 = INT((TIMER - II1 * 3600) / 60)
4730  II3 = TIMER - II1 * 3600 - II2 * 60
4750  PRINT #4, "Row"; NR; "starts on"; DATE$; "at"; II1; ":"; II2; ":"; II3
4760  PRINT #4,
4770  PRINT #4,
5000  IF NR > 14 OR NR = 14 THEN
5001  CLS
5010  PRINT , "************************************************************"
5012  PRINT , "*           Row "; NR; " is completely measured.                *"
5014  PRINT , "************************************************************"
5020  GOTO 6000
5030  ELSEIF NR = 13 THEN
5040  NR = NR + 1
5050  GOTO 1700
5060  ELSE
5500  PRINT , "************************************************************"
5503  PRINT , "*           Row "; NR; " is completely measured.                *"
5507  PRINT , "*       Further measurement of Row (NR+1) (y, Y/Other)?         *"
5510  PRINT , "*      'Y' or 'y' = continue !!!   Other key = Stop !!!         *"
5512  PRINT , "************************************************************"
5550  INPUT a$
5560  IF a$ = "y" OR a$ = "Y" THEN
5565  NR = NR + 1
5570  GOTO 1700
5580  ELSE
5590  GOTO 6000
5600  END IF
5602  GOTO 6000
5608  END IF
6000  CLS
7000  REM ************************************************************************
7006  REM *  Transition to local control. Entrance (data channel #1, #2) to the measuring      *
7007  REM *  instrument RLC 100 meter and the Switch unit HP 34970A will be closed.       *
7009  REM ************************************************************************
```

```
7010   PRINT #1, "*RST"
7015   PRINT #1, "*OPC?"
7020   INPUT #1, AA$
7030   PRINT #1, IGTL$
7100   PRINT #2, "*OPC"
7110   PRINT #2, "SYSTem:LOCal"
7120   CLOSE #1: CLOSE #2 :CLOSE #3: CLOSE #4
8900   REM ************************************************************
8930   CLS: BEEP: END
8990   REM ************************************************************
9000   REM _____________________________PROGRAMM END_____________________________
```

Appendix III Table of normal probability function

z	0	1	2	3	4	5	6	7	8	9
0.0	.0000	.0040	.0080	.0120	.0160	.0199	.0239	.0279	.0319	.0359
0.1	.0398	.0438	.0478	.0517	.0557	.0596	.0636	.0675	.0714	.0754
0.2	.0793	.0832	.0871	.0910	.0948	.0987	.1026	.1064	.1103	.1141
0.3	.1179	.1217	.1255	.1293	.1331	.1368	.1406	.1443	.1480	.1517
0.4	.1554	.1591	.1628	.1664	.1700	.1736	.1772	.1808	.1844	.1879
0.5	.1915	.1950	.1985	.2019	.2054	.2088	.2123	.2157	.2190	.2224
0.6	.2258	.2291	.2324	.2357	.2389	.2422	.2454	.2486	.2518	.2549
0.7	.2580	.2612	.2652	.2673	.2704	.2734	.2764	.2794	.2823	.2852
0.8	.2881	.2910	.2939	.2967	.2996	.3023	.3051	.3078	.3106	.3133
0.9	.3159	.3186	.3212	.3238	.3264	.3289	.3315	.3340	.3365	.3389
1.0	.3413	.3438	.3461	.3485	.3508	.3531	.3554	.3577	.3599	.3621
1.1	.3643	.3665	.3686	.3708	.3729	.3749	.3770	.3790	.3810	.3830
1.2	.3849	.3869	.3888	.3907	.3925	.3944	.3962	.3980	.3997	.4015
1.3	.4032	.4049	.4066	.4082	.4099	.4115	.4131	.4147	.4162	.4177
1.4	.4192	.4207	.4222	.4236	.4251	.4265	.4279	.4292	.4306	.4319
1.5	.4332	.4345	.4357	.4370	.4382	.4394	.4406	.4418	.4429	.4441
1.6	.4452	.4463	.4474	.4484	.4495	.4505	.4515	.4525	.4535	.4545
1.7	.4554	.4564	.4573	.4582	.4591	.4599	.4608	.4616	.4625	.4633
1.8	.4641	.4649	.4656	.4664	.4671	.4678	.4686	.4693	.4699	.4706
1.9	.4713	.4719	.4726	.4732	.4738	.4744	.4750	.4756	.4761	.4767
2.0	.4772	.4778	.4783	.4788	.4793	.4798	.4803	.4808	.4812	.4817
2.1	.4821	.4826	.4830	.4834	.4838	.4842	.4846	.4850	.4854	.4857
2.2	.4861	.4864	.4868	.4871	.4875	.4878	.4881	.4884	.4887	.4890
2.3	.4893	.4896	.4898	.4901	.4904	.4906	.4909	.4911	.4913	.4916
2.4	.4918	.4920	.4922	.4925	.4927	.4929	.4931	.4932	.4934	.4936
2.5	.4938	.4940	.4941	.4943	.4945	.4946	.4948	.4949	.4951	.4952
2.6	.4953	.4955	.4956	.4957	.4959	.4960	.4961	.4962	.4963	.4964
2.7	.4965	.4966	.4967	.4968	.4969	.4970	.4971	.4972	.4973	.4974
2.8	.4974	.4975	.4976	.4977	.4977	.4978	.4979	.4979	.4980	.4981
2.9	.4981	.4982	.4982	.4983	.4984	.4984	.4985	.4985	.4986	.4986
3.0	.4987	.4987	.4987	.4988	.4988	.4989	.4989	.4989	.4990	.4990
3.1	.4990	.4991	.4991	.4991	.4992	.4992	.4992	.4992	.4993	.4993
3.2	.4993	.4993	.4994	.4994	.4994	.4994	.4994	.4995	.4995	.4995
3.3	.4995	.4995	.4995	.4996	.4996	.4996	.4996	.4996	.4996	.4997
3.4	.4997	.4997	.4997	.4997	.4997	.4997	.4997	.4997	.4997	.4998
3.5	.4998	.4998	.4998	.4998	.4998	.4998	.4998	.4998	.4998	.4998
3.6	.4998	.4998	.4999	.4999	.4999	.4999	.4999	.4999	.4999	.4999
3.7	.4999	.4999	.4999	.4999	.4999	.4999	.4999	.4999	.4999	.4999
3.8	.4999	.4999	.4999	.4999	.4999	.4999	.4999	.4999	.4999	.4999
3.9	.5000	.5000	.5000	.5000	.5000	.5000	.5000	.5000	.5000	.5000